DESIGN OF HYDRAULIC VALVELESS CONTROL ACTUATION SYSTEM

A THESIS SUBMITTED TO
THE GRADUATE SCHOOL OF NATURAL AND APPLIED SCIENCES
OF
MIDDLE EAST TECHNICAL UNIVERSITY

BY

MEHMET CAN KARABULUT

IN PARTIAL FULFILLMENT OF THE REQUIREMENTS
FOR
THE DEGREE OF MASTER OF SCIENCE
IN
MECHANICAL ENGINEERING

APRIL 2016

Approval of the thesis:

DESIGN OF HYDRAULIC VALVELESS CONTROL ACTUATION SYSTEM

submitted by **MEHMET CAN KARABULUT** in partial fulfillment of the requirements for the degree of **Master of Science in Mechanical Engineering, Middle East Technical University** by,

Prof. Dr. Gülbin Dural Ünver _____
Dean, Graduate School of **Natural and Applied Sciences**

Prof. Dr. Tuna Balkan _____
Head of Department, **Mechanical Engineering**

Prof. Dr. Tuna Balkan _____
Supervisor, **Mechanical Engineering Dept., METU**

Examining Committee Members

Prof. Dr. Y. Samim Ünlüsoy _____
Mechanical Engineering Dept., METU

Prof. Dr. Tuna Balkan _____
Mechanical Engineering Dept., METU

Prof. Dr. Metin Akkök _____
Mechanical Engineering Dept., METU

Assoc. Prof. Dr. Yiğit Yazıcıoğlu _____
Mechanical Engineering Dept., METU

Assoc. Prof. Dr. S. Çağlar Başlamışlı _____
Mechanical Engineering Dept., Hacettepe University

Date: 27.04.2016

I hereby declare that all information in this document has been obtained and presented in accordance with academic rules and ethical conduct. I also declare that, as required by these rules and conduct, I have fully cited and referenced all material and results that are not original to this work.

Name, Last name : Mehmet Can KARABULUT

Signature :

ABSTRACT

DESIGN OF HYDRAULIC VALVELESS CONTROL ACTUATION SYSTEM

Karabulut, Mehmet Can

M.S., Department of Mechanical Engineering

Supervisor: Prof. Dr. Tuna Balkan

April 2016, 147 Pages

In this thesis study, a pump controlled hydraulic control actuation system is investigated and a system is designed by using the performance criteria of the available conventional valve controlled hydraulic control actuator. A prototype actuator and load system is manufactured and tested.

In order to understand dynamic behavior of the system, a simulation is performed in MATLAB Simulink® environment. Sub-systems and components of the system are tested to identify their parameters which are not supplied by manufacturer data sheets as well as friction characteristics of the actuator.

By conducting open loop and closed loop step response and closed loop frequency response tests, the dynamic performance of the system is examined. Furthermore, to observe performance of the system under operational conditions, an inertia is

attached to the system and tests are repeated under inertial load. Then, with an auxiliary electric motor, an external load scenario is applied and performance of the system is evaluated.

Real time tests and data acquisition are carried out by using the LabVIEW® software.

Keywords: Fluid Power Control, Control Actuation System, Electro-Hydrostatic Actuator

ÖZ

HİDROLİK VALFSİZ KONTROL TAHRİK SİSTEMİ TASARIMI

Karabulut, Mehmet Can

Yüksek Lisans, Makina Mühendisliği Bölümü

Tez Yöneticisi: Prof. Dr. Tuna Balkan

Nisan 2016, 147 Sayfa

Bu tez çalışması kapsamında pompa denetimli hidrolik kontrol eyleyici sistemi incelenmiş ve geleneksel valf denetimli bir hidrolik kontrol eyleyicisinin performans isterleri temel alınarak sistem tasarımı yapılmıştır. Prototip olarak bir eyleyici ve yükleme sistemi üretilmiş ve test edilmiştir.

Sistemin dinamik davranışlarını anlamak üzere MATLAB Simulink® ortamında benzetim çalışması yapılmıştır. Ürün bilgi kataloglarında sunulmayan parametreleri elde etmek için kompleyi oluşturan alt parçalar seviyesinde testler gerçekleştirilmiştir. Eyleyici komplesi seviyesinde gerçekleştirilen sistem tanılama testleriyle de kompleye ait sürtünme karakteristiği çıkartılmıştır.

Sistemin dinamik başarımını görmek üzere açık döngü ve kapalı döngü basamak girdi ve kapalı döngü frekans tepkisi testleri yapılarak incelenmiştir. Bunlara ilave olarak, sistemin çalışma koşullarındaki başarımını görmek adına sisteme bir atalet

yükü eklenmiş ve testler tekrarlanmıştır. Harici bir sistem ile yükleme test senaryosu gerçekleştirilmiş ve sistem performansı değerlendirilmiştir.

Gerçek zamanlı testler ve veri toplama çalışmaları LabVIEW® yazılımı kullanılarak gerçekleştirilmiştir.

Anahtar Kelimeler: Akışkan Gücü Kontrolü, Kontrol Tahrik Sistemi, Elektro-Hidrostatik Eyleyici

to my family…

ACKNOWLEDGMENTS

I would like to express my sincere gratitude to my supervisor Prof. Tuna Balkan for his supervision, guidance, advice and help he provided throughout this study.

I would like to thank to my manager, my colleagues and friends who contributed this thesis by their understanding, patience and encouragement. I also thank to Okan Eyyüpoğlu who is always ready to help. I wish to express my appreciation to ROKETSAN Inc. for all facilities provided.

Mostly, I am grateful to my parents Hayriye and Erol and my dear sister Dilsun for their love, confidence and encouragement they provided me not only throughout this thesis but throughout my life.

Finally, I would like to present my deepest thanks to my lovely Nesli, for her love, invaluable support and understanding.

TABLE OF CONTENTS

LIST OF TABLES

TABLES

LIST OF FIGURES

FIGURES

LIST OF SYMBOLS

SYMBOLS

A	Active area of hydraulic cylinder
d	Pipe diameter
D	Displacement of pump
F_{bk}	Breakaway (static) friction force of actuator
F_{ex}	External load
F_{mx}	Maximum force output of actuator
i	Current
J_{mp}	Inertia of motor-pump couple
k	Polytropic exponent of gas
k_{cv}	Flow resistance in check valve
K_{elp}	External leakage coefficient of pump
K_{ilc}	Internal leakage coefficient of cylinder
K_{ilp}	Internal leakage coefficient of pump
K_{leak}	Overall leakage coefficient of pump

K_p	Position controller of system
K_s	Speed controller of the motor
K_t	Torque constant of motor
K_v	Voltage loop of motor driver
K_{vp}	Viscous friction coefficient of actuator
K_{vm}	Viscous friction of motor
K_w	Speed constant of motor
L	Inductance of motor
M	Total mass of piston and load
n_{safe}	Safety factor
p_1	Outlet pressure of pump
p_2	Inlet pressure of pump
p_a	Pressure at actuator chamber A
p_{ac}	Current pressure of accumulator
p_{ac0}	Initial pressure of accumulator
p_b	Pressure at actuator chamber B
p_{cdr}	Case Drain Pressure

p_{cv}	Check valve cracking pressure
P_{em}	Electric motor power
P_h	Hydraulic power
Q_a	Flow to/from chamber A
Q_{ac}	Flow to/from accumulator
Q_{ac1}	Flow from accumulator to chamber A
Q_{ac2}	Flow from accumulator to chamber B
Q_b	Flow to/from chamber B
Q_{in}	Inlet flow to pump
Q_{mx}	Maximum flow in system
Q_{out}	Outlet flow from pump
R	Resistance of motor
Re	Reynolds Number
S_y	Yield strength of material
T_{em}	Electric motor torque
T_l	Load torque on motor
T_m	Motor torque

V	Fluid Velocity
V_1	Volume of fluid at pump outlet port
V_2	Volume of fluid at pump inlet port
V_{g0}	Initial volume of gas
V_m	Input voltage of motor
x	Position of actuator
x_0	Initial position of actuator
β_e	Bulk modulus of hydraulic fluid
η_e	Electrical efficiency of motor
η_{mech}	Mechanical efficiency of pump
v	Kinetic viscosity
ω	Rotational speed of motor
ω_{em}	Rotational speed of motor
ω_p	Rotational speed of pump

CHAPTER 1

INTRODUCTION

1.1 Background and Motivation

Fluid power has an important role in the development of mankind while it is a basic power source such as wind mills, water wheels for daily needs like production of food, wood grinding for papermaking, iron hammering, fiber pounding for clothes. In 1648, Blaise Pascal discovered that pressure exerted anywhere in a confined incompressible fluid is transmitted equally in all directions throughout the fluid such that the pressure variations (initial differences) remain the same [1]. Then, the fluid behavior under different conditions was explained with mathematical formulas by Daniel Bernoulli in 1738 which was later turned into idea of high pressurized water network for energy distribution up to finding more convenient way of energy distribution, electricity. Industrial revolution was escalated the demand for fluid power and at 20^{th} century improvement in control mechanisms, feedback systems; servo systems with involvement of electronic, mechanic and hydraulic discipline were shown up. During period of Pre and Post World War II, electrohydraulic servomechanisms became more crucial technology for control actuation systems of aircrafts and missiles.

Nowadays, not only heavy duty operations like presses, agricultural and earthmoving machines, industrial robots that are used, but also precision operations; such as, humanlike robot actuators and limb prosthesis actuators. The

reasons why hydraulic systems are widely used in every type of applications are these [2]:

- Comparatively small final actuator size.
- High torque/force output to mass ratio.
- The capability of high load applications.
- Thanks to fluid medium, hydraulic oil, transfer, system is self-lubricating and heat dissipative.

As well as the advantages, there are some weaknesses those need to be considered:

- Bulky centralized power system requirement with large oil reservoir.
- Low energy efficiency; to have a constant supply pressure, pump is in a continuous run mode.
- Leakage and noise.

The conventional hydraulic actuator utilizes a control valve to adjust amount of fluid into the hydraulic cylinder chambers. These kinds of systems are generally called as "Valve Controlled Systems". When the pressurized fluid passes the control valve due to throttling losses, it loses big portion of its energy. Although these control valves make the system response fast and precise, orifice throttling causes hydraulic energy loss by heat dissipation which increases oil temperature and varies bulk modulus. To eliminate valve losses completely, a technic called "Valveless Controlled System" or "Pump Controlled System" was derived. In such system, the flow rate in hydraulic cylinder chambers is directly controlled by pump and motor couple instead of control valves. This hydrostatic technic is used for a long time in agricultural and earthmoving vehicles for power transmission in between equipment and auxiliary components.

A hydrostatic system has two main methods to control flow rate of a pump. The first and traditional one, a variable displacement pump and a constant speed

electric motor is used. The flow rate is adjusted by changing the pump displacement. The second one is using fixed displacement pump and a variable speed electric motor. Drive speed of the pump is changed by the electric motor then the flow rate is regulated implicitly. Moreover, the combination of variable displacement pump and variable speed electric motor can be another option, but it brings more variables to control and overall system will be more complex.

The focus of this thesis work is design and testing of an Electro-Hydrostatic Actuator (EHA) which is the special name for the hydrostatic circuit that has fixed displacement pump and speed controllable servomotor.

1.2 Objective of the Thesis

The objective of this thesis is to design an Electro-Hydrostatic Actuator for a control actuation system which satisfies performance characteristics of an available servo valve controlled electro-hydraulic actuator. It is aimed that the EHA has a similar dynamic performance with the servo valve controlled system and to present it as alternative for Electro-Hydraulic and Electro-Mechanical Actuators.

At the end of the design process, a lumped, integrated prototype is developed and a control actuation system that can replace the servo valve controlled actuator is provided.

The mathematical model for the EHA is developed to simulate the actuator behavior and estimate performance characteristics before real time tests and design a control system to fulfill performance requirements. Main physical parameters such as leakage and friction of the system are determined by identification tests and the mathematical model is verified after finding these parameters.

In equipment based sub-system identification tests, variation of the dead band with pump load and shaft speed are examined and the servomotor performance is determined.

Performance tests of the prototype system with and without external load are conducted and a controller that satisfies the performance criteria is designed in parallel to the system performance tests.

1.3 Thesis Outline

The thesis is organized as five chapters and their contents are summarized as follows.

In Chapter 2, conventional concepts of flight control actuation systems namely Electro-Hydraulic and Electro-Mechanical Actuators are discussed. Servo valve controlled and servomotor controlled control actuation systems are introduced as literature review of flight control actuation systems. Moreover, detailed information of the hydrostatic actuation techniques and their types are presented. Examples of EHAs for different applications are shown and their hydraulic circuits are illustrated. A brief comparison is made and strengths and weaknesses of EHA according to conventional control actuation methods are mentioned.

In Chapter 3, an EHA system design which satisfies the design parameters and performance criteria of the available servo valve controlled hydraulic control actuator is given. A nonlinear mathematical model is obtained and a nonlinear simulation model is developed in MATLAB Simulink® environment. Also, according to system architecture defined in Section 3.3.2, a detailed description of mechanical design process of the prototype is given and selection of the prototype components is explained. According to the system performance criteria, hydraulic actuator speed under a specified load and system bandwidth are important requirements. Therefore, a controller is designed in time domain to satisfy the

actuator speed as well as a controller in frequency domain to satisfy the system bandwidth.

Chapter 4 investigates the unknown system parameters which are experimentally identified and the mathematical model is validated with test results. Step and frequency response tests are performed to make a comparison between simulation results. The EHA prototype is tested under inertial load and external load defined in system performance criteria. The test results are compared with simulation results.

In Chapter 5, the complete study is summarized. The conclusions of this study and outcomes of thesis work are declared. Besides, recommendations for future work and similar applications are discussed.

CHAPTER 2

CONVENTIONAL AND HYDROSTATIC CONTROL ACTUATION SYSTEMS

In this chapter, an introduction to control actuation systems is given. The conventional control actuation systems such as mechanical and hydraulic actuators are discussed in basis. The innovative control actuation system concept of hydrostatic actuation is introduced and forms of hydrostatic actuation are detailed. The main focus of this research, Electro-Hydrostatic Actuator (EHA) is presented and compared with the conventional actuation systems in the end of this chapter.

2.1 Electro-Hydraulic Actuation Systems

Among control actuation systems, hydraulic actuation systems are a very mature technology due to vast utilization in earthmovers, agricultural machinery, ships and aircrafts.

According to operating principle, electro hydraulic actuation systems are composed of two parts basically, i.e. hydraulic power source and servo mechanism. Servo mechanism is responsible to drive a control surface to deflect via a transmission mechanism according to a control command from a controller. The function of the hydraulic power source is to supply sufficient hydraulic flow to the servo mechanism as its power. There are oil supply channel and oil return channel from the power source to the servo mechanism. High-pressure oil from

the hydraulic power source is supplied to the servo mechanism through the oil supply channel, and low-pressure oil from the servo mechanism returns to the hydraulic power source through the oil return channel to achieve oil circulation. A block diagram and a hydraulic circuit of the Electro-Hydraulic Actuator are shown in Figure 1 and Figure 2 respectively.

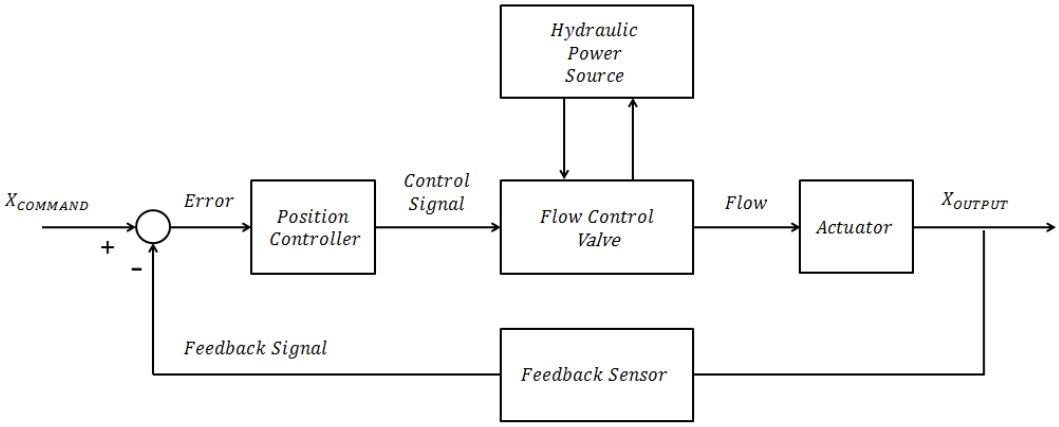

Figure 1: Block Diagram of an Electro-Hydraulic Actuator

The hydraulic power source is mainly consisting of an electromotor, a hydraulic pump, a relief valve, an oil filter and an accumulator. The electric motor driven pump transfers hydraulic oil from a reservoir and supplies high-pressure hydraulic oil. The high-pressurized hydraulic oil flows into servo mechanism through oil supply channel by passing the oil filter. There are auxiliary elements connected to high pressure channel such as, pressure relief valve and accumulator is for regulate pressure output at the pump outlet. The hydraulic pump is a variable displacement one. Owing to the auxiliary elements, operating pressure of the control actuator's hydraulic system keeps approximately constant, while output flow rate of the hydraulic pump changes with load flow.

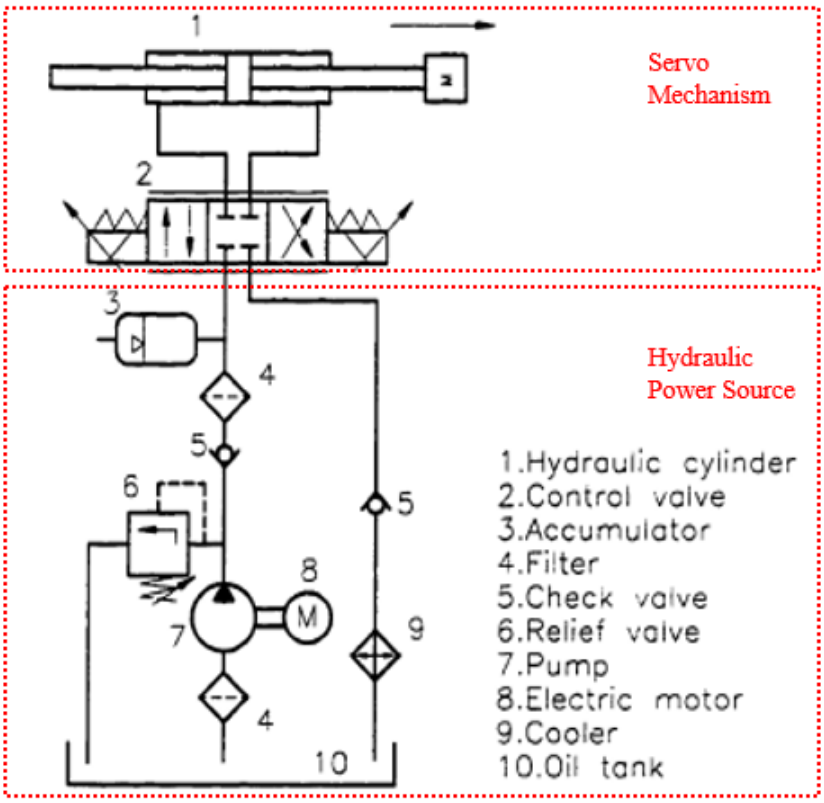

Figure 2: Typical Hydraulic Circuit of an Electro-Hydraulic Actuator [31]

The essential part of this actuation system is the servo mechanism which is composed of a servo valve, a hydraulic cylinder. The key instrument is the servo valve whose duty is to convert a controller's command signal to flow regulation to the hydraulic cylinder.

A schematic diagram of the flight control actuator's movement of an aircraft is shown in Figure 3. When a positive signal is sent to the servo valve, the valve takes the position 2 and the hydraulic oil flows out from the servo valve's opening 2. Moreover, the control actuator's piston connecting rod retracts; the control actuator moves forward stroke, which corresponds to a definite aileron deflection angle regarding to the command signal. When a negative signal is sent to the

servo valve, the hydraulic oil flows out from the servo valve's opening 1, the hydraulic cylinder stretches out; the aileron deflect to an angle to the other side.

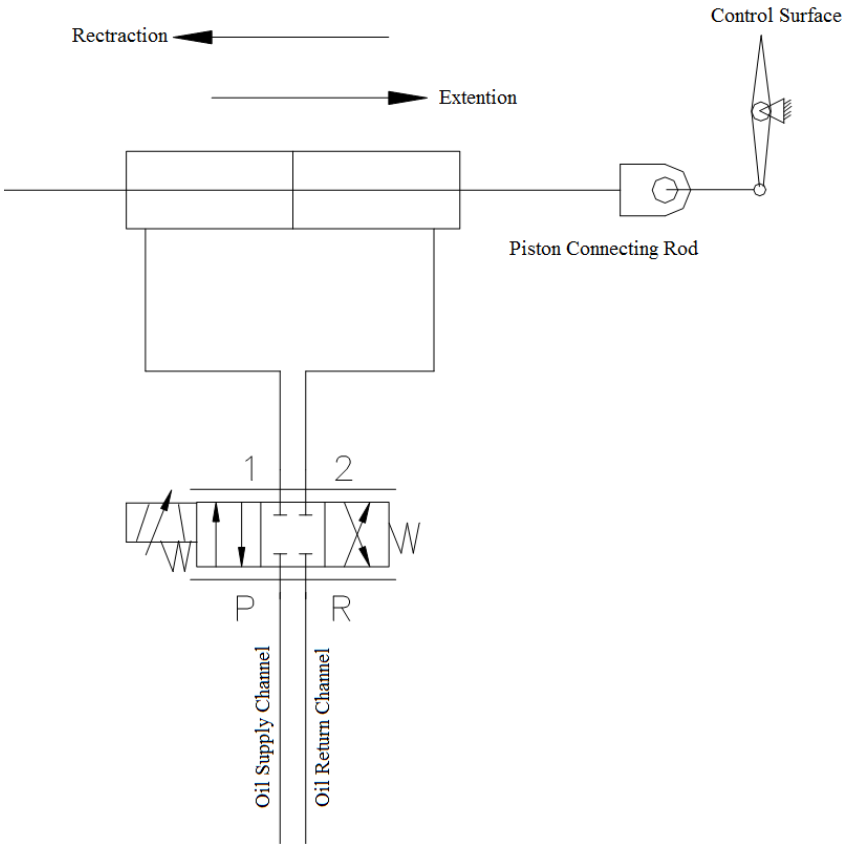

Figure 3: Schematic Diagram of the Servo Mechanism

As shown in Figure 3, a control actuator can be dedicated to manipulate a flight control surface; therefore, number of control actuator equals to number of necessary control surface. However, it is possible to have a hydraulic power source and necessary quantity of servo mechanism to control more than one flight control surfaces. In distributed hydraulic architecture, a hydraulic power source is shared by all servo mechanisms. Oil supply channels and return channels of all the actuators are connected to the same centralized hydraulic power source.

2.2 Electro-Mechanical Actuation Systems

Electro-mechanical actuator raises prominence due to improvements in servomotor technology and demand of energy saver systems and modular design in comparison with an electro-hydraulic actuator.

A typical electro-mechanical actuation system is comprised of an electro servomotor, a transmission mechanism and a mechanical linkage between transmission and a control element. Power is generated at the servomotor shaft is transferred with a gear box and a transmission mechanism like lead and ball screw to satisfy required torque and speed output at the control element. However, in some cases the gear assembly is not utilized, lead screw or ball screw is sufficient for power transformation from the servomotor to the control element.

A typical electro-mechanical actuator for flight surface control diagram is illustrated at Figure 4. Its operating principle can be explained like that, according to control command to the servomotor, it rotates in a direction. Owing to gearing and ball-screw mechanism the rod is retracted or stretched out. Rotational motion of the gears is converted to linear motion of the ball screw and finally transformed to the flight surface via mechanical linkages. Via sensor feedbacks the position of the flight surface is controlled by a control system computer.

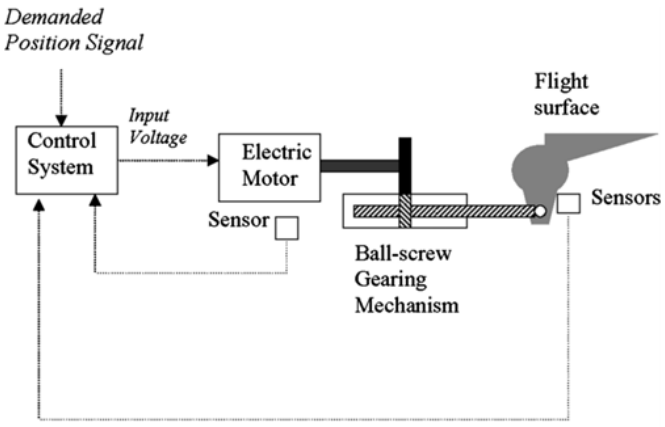

Figure 4: Typical Electro-Mechanical Actuator [32]

For a position controlled Electro-Mechanical Actuator, a basic block diagram demonstration is given in Figure 5.

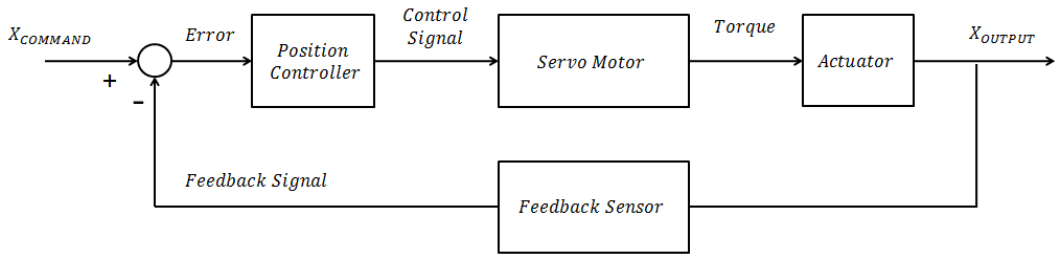

Figure 5: Block Diagram of the Electro-Mechanical Actuator

2.3 Electro-Hydrostatic Actuation Systems

This part provides detailed information about hydrostatic actuation which is a form of hydrostatic transformation that has been using for a long time in the industry. According to components used in hydraulic circuits, hydrostatic actuation methods differ and are classified in categories.

Hydrostatic actuation systems basically alter from conventional hydraulic actuation system in this manner; flow in hydraulic circuit is directly controlled by pump-electric motor couple and it is the final control element in the circuit.

2.3.1 Types of Hydrostatic Actuation

Hydrostatic actuation systems can be basically classified according to type of pump-electric motor couple and hydraulic cylinder in the hydraulic circuit. Firstly, there are three possible types of hydrostatic actuation systems for categorizing pump-electric motor couple. They can be configured as fixed or variable speed electric motor and fixed or variable displacement pump. Secondly, hydraulic cylinder can be chosen symmetric or asymmetric; these different options lead different hydraulic circuit variations in basis.

2.3.2 Types of Pump - Electric Motor Couple

There are three options for pump and electric motor mating. They are given in detail in the following sections.

2.3.2.1 Variable Displacement Pump – Fixed Speed Electric Motor Hydrostatic Actuation Systems

In this type of systems, an electric motor that drives a pump has a constant rotational speed. Flow rate and its direction are regulated by arranging displacement amount of the pump as seen from Figure 6. The pump displacement can be controlled via a valve at the figure; however, it can be controllable with electronic or hydraulic hardware according to the type of the pump.

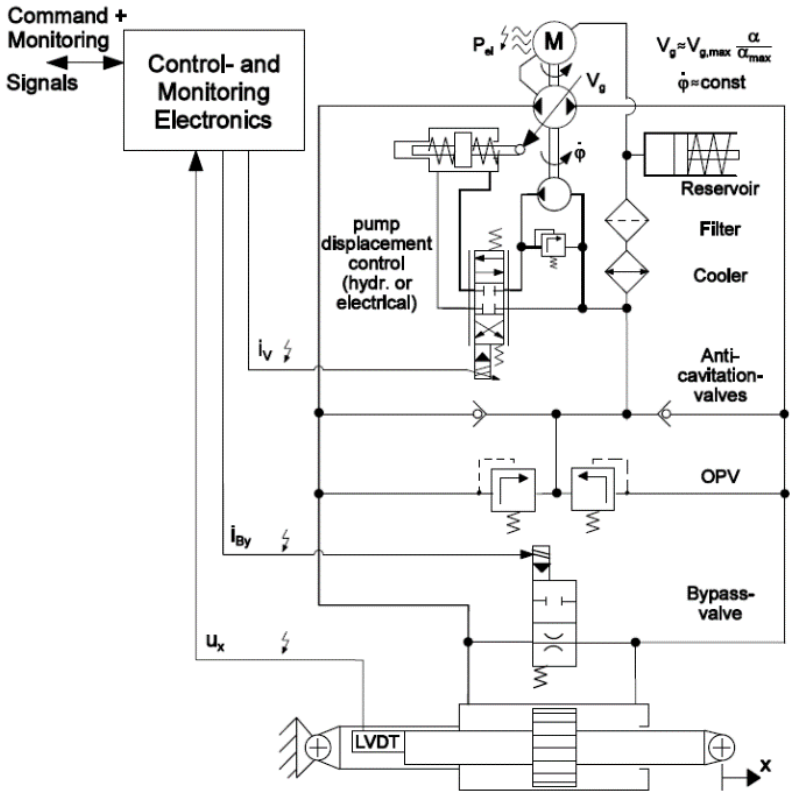

Figure 6: Variable Displacement Pump – Fixed Speed Electric Motor EHA [25]

Main kinds of variable displacement pumps are rotary vane pump and axial piston pump. To begin with, a vane pump has vanes on its body and they contact with casing during rotation of body. In Figure 7, the vanes are usually compressed into their channels with utilization of springs in order to provide contact with casing surfaces and these springs get shorter or longer during rotation. Due to eccentricity between rotor and casing, the fluid between vanes is compressed from inlet to outlet of the pump and as conclusion, the fluid become pressurized. By changing eccentricity amount between rotor and casing, pumps can be arranged to give different flow rates. However, they do not preferred as much as axial piston pumps in this type of actuation system due to lower pressure ratings.

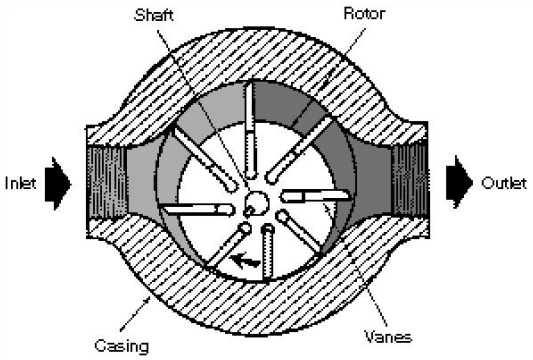

Figure 7: A Vane Pump [26]

Widely used variable displacement pump is axial piston pump which is composed of a series of pistons attached a swash plate as in Figure 8. In relation to change in angle of the swash plate, stroke length of the piston in one revolution varies and amount of the fluid that supplied by the piston changes. Additionally, some feedback and control mechanisms are employed to alter the swash plate angle such as pressure control by substituting a valve controlled hydraulic sub-circuit. They are capable of working under high flow rates and pressures compared to vane pumps. Therefore, they are significantly preferred in hydraulic applications from the past.

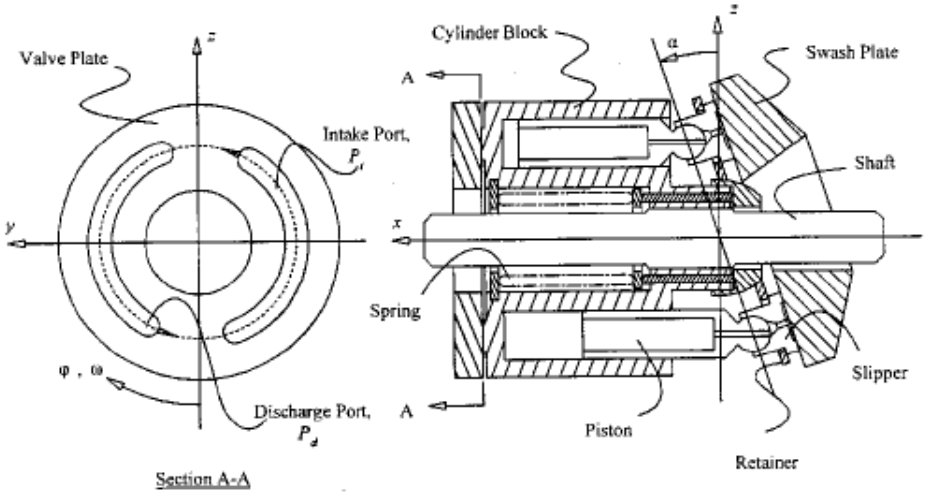

Figure 8: An Axial Piston Pump [27]

Although, axial piston pumps are used from very beginning of the hydrostatic actuation, there are some points that need to be considered while using these in designs. One of them is the “Ripple Effect” which can be seen in other types of pumps but it is very significant drawback for piston pumps because of their working principle and structure [5]. There are some methods for minimizing this pulsing effect in the flow such as adding damping holes, orifices between piston chamber and pump discharge port [6]. Another solution is increasing odd number of pistons in the pump so the oscillations in flow are reduced [7]. For high precision applications like control actuation systems, it is a problem that required to be solved. One of the solutions for this kind of problems is using higher speed pump and motor couple; so, pulsation frequency of flow gets much higher than actuator working frequency. Consequently, it does not affect the dynamics of the actuation system.

Additional drawback is energy inefficiency. It is caused by fixed speed motor, because of rotating continuously during idle mode of operation. Helduser completed a work to compare the energy efficiency of speed controlled and displacement controlled pump system [8]. A plastic injection machine in which

can be driven both of two pumps was operated with a specific duty cycle and total power consumptions were compared. It was concluded that displacement controlled pump spends more energy due to constant speed rotation of the electric motor.

2.3.2.2 Fixed Displacement Pump – Variable Speed Electric Motor Hydrostatic Actuation Systems

In these systems, pump displacement is fixed, which means a pump supplies a specific amount of fluid in one revolution. In order to change the flow rate into the hydraulic cylinder, the motor speed needs to be adjusted. As Figure 9, the system controller regulates the motor speed by measuring angular velocity of the electric motor and giving corrective speed command.

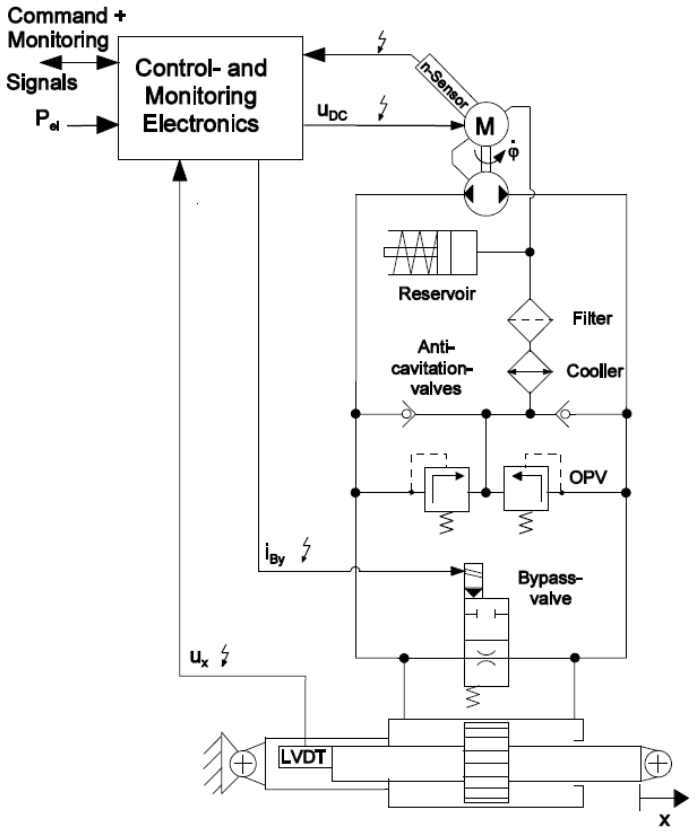

Figure 9: Fixed Displacement Pump – Variable Speed Electric Motor EHA [25]

In a variable displacement pump-fixed speed electric motor system, the electric motor is simple and the pump is more complicated structurally due to displacement change ability. In contrast, at these systems, pumps do not have complex structure and electric motors get complicated by its servo drivers. The main types of fixed displacement pumps are gerator, internal gear, external gear and screw pump.

Gerator pump is similar type of internal gear pump, and different in ways of design, performance and applications. As illustrated in Figure 10, they have an internal gear which is driven, an idler female gear rotor and does not have a crescent like as in internal gear pumps. A gerator pump needs least machining and least number of components compared to other kinds of pumps. However, they are more suitable for medium pressure applications.

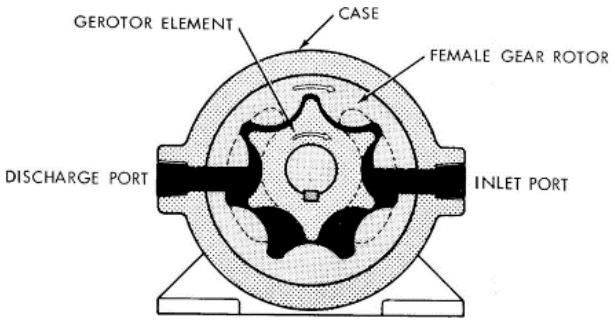

Figure 10: A Gerator Pump [28]

Gear pumps shown in Figure 11 are a popular and well-known option among fixed displacement pumps; since, they are greatly suitable to work under high pressures with high viscosity fluid, especially internal gear pumps.

An important point when using such a fixed displacement pump in a control actuation application is that, while there is a control command in the system, pump is supposed to be provide flow when rotation speed is very close to zero to compensate the error. It is necessary to have a small dead band when the direction

of rotation changes and at speeds which are close to zero. In standard and industrial applications, these pumps are not expected to operate under these circumstances. Additionally, these pumps have low efficiencies at low speeds and high pressures. Because, it is not considered in pump design. However, there are some pumps designed for such purposes. They have fairly good machining tolerances; furthermore, their internal fluid dynamics is designed in such way, flow resistances in both directions of rotation is equal. Thanks to these, it is capable of supplying flow at low speeds with a small range of dead band when the pump direction of rotation alters.

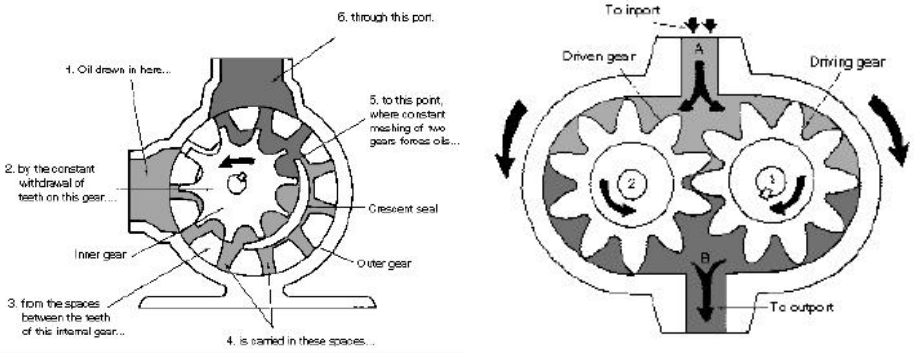

Figure 11: An Internal and an External Gear Pump [29]

For the problem of dead band and improvement to bi-directional performance of pumps, screw pumps were researched for better performance characteristics [9]. The idea behind this research is minimizing mechanical interaction between pump parts so that mechanical friction is lower. The screw pump which demonstrated in Figure 12 eliminates gear mesh mechanical contacts. Non-linear characteristics like static, contact frictions are reduced. Another plus of the screw pumps is that pumping operation has no discontinuity which removes the pulsations in both flow rate and pressure. In the research, the designed screw pump was tested to compare with a similar capacity internal gear pump and it was shown that,

necessary torque value to change direction of rotation and pulsation amount of the screw pump was smaller nearly 30% than the internal gear pump.

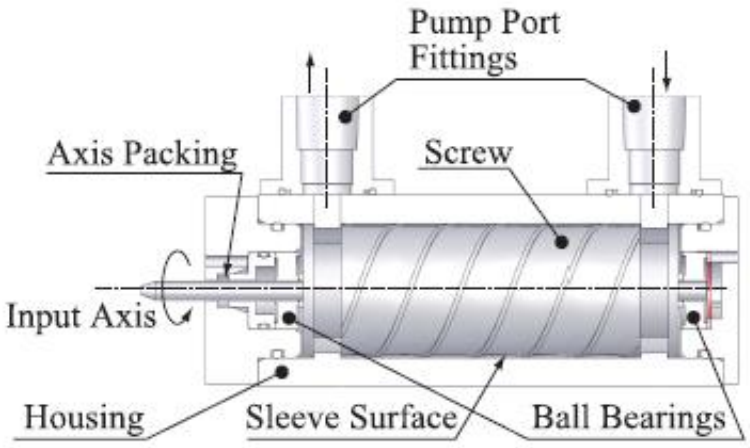

Figure 12: A Screw Pump [9]

2.3.2.3 Variable Displacement Pump – Variable Speed Electric Motor Hydrostatic Actuation Systems

The last option for pump-electric motor couple is variable displacement pumps and variable speed electric motor combination. It combines the benefits of two other options in Section 2.3.2.1 and 2.3.2.2. The main contribution of this system is that, system performance can be adjusted to meet different requirements of dynamic response and energy loss, since it lets control more parameters [10]. In a closed loop system, two variable namely electric motor speed and pump displacement are controlled for an output, piston position e.g. Obviously, although multiple input bring extra complexity to the control system, it also provides extra flexibility to the system due to controlling more degree of freedom. Besides, it offers a chance to satisfy different dynamic performance and energy consumption criteria by changing weighting coefficients of two control variables.

2.3.3 Types of Hydraulic Cylinder

In hydraulic literature, linear hydraulic cylinders are categorized with respect to effective areas of hydraulic cylinder in pressure chambers. Moreover, if effective areas of cylinder in two pressure chambers are equal each other; it is defined as "symmetrical hydraulic cylinder". If effective areas in pressure chambers are unequal to each other, it is called as "asymmetric hydraulic cylinder".

Another way of grouping hydraulic cylinders is done by describing if cylinder rod has mechanical interface to outside; in other words, they named accordingly if they give an output to outside or not. If the cylinder has a rod at the both side of it, it is named as "double rod". If there is only one rod, it is titled as "single rod". According to different type of categories, hydraulic cylinders can be diversified.

The type of hydraulic cylinder such as symmetric or asymmetric has a direct effect on pressure and flow rate which are controlled in the hydraulic circuit. In a valve controlled system, asymmetric flow rate, different flow rate between inlet and outlet of the cylinder due to different chamber volumes does not cause problem. It is because of the fact that the return flow is directed to a reservoir and the pump takes the necessary amount of fluid from the reservoir. In a pump controlled system, if internal and external leakage in the pump is ignored, flow rate at inlet and outlet of the pump needs to be equal. However, asymmetric hydraulic cylinders have different inlet and outlet flow rates and the pump is directly connected to the actuator in pump controlled systems. Therefore, the flow rate which is excess or lack in relation to direction of the cylinder motion is supposed to be provided in some way. In the following, hydraulic circuit solutions for this problem will be discussed.

2.3.3.1 Asymmetric Hydraulic Cylinder Circuits

Variation of flow rate with different working direction due to cylinder area difference is compensated by using additional pumps, hydraulic valves,

accumulators. In Figure 13, some open and closed hydraulic circuit solutions are offered for varying number of pumps and pump drives. Also, for minimum pump and driver utilization some circuit alternatives are given in which switching valves are used to regulate inlet and outlet flow rate.

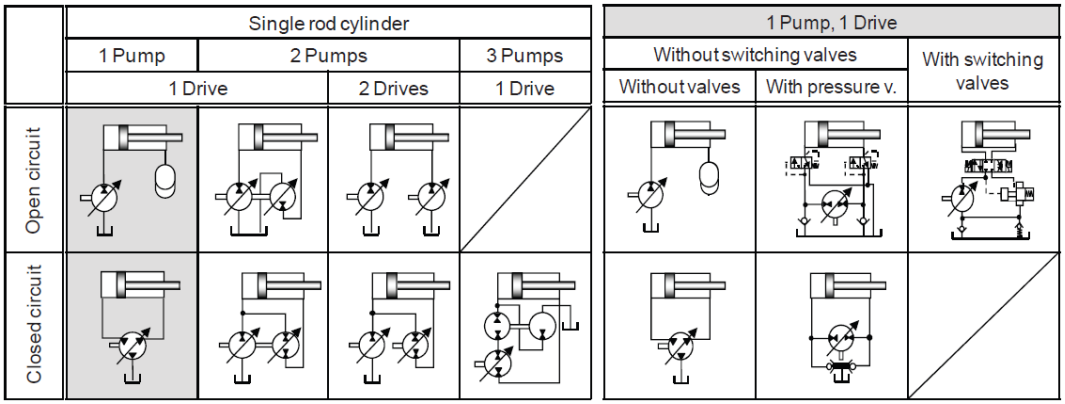

Figure 13: Alternative Solution Matrix for Asymmetric Cylinder [37]

Fluid reservoirs in open loop hydraulic circuits increase total volume due to re-routing fluid in the circuit; nevertheless, in closed circuit, it is only needed as much as fluid volume difference of cylinder for reservoir volume. It is also supposed to be considered for more than one driver solution, additional drive unit costs are added to overall cost. Also, solutions which contain tandem pumps with one drive are capable to be used with variable displacement pumps. Fixed displacement pumps fails to work like this, such that they require turning opposite direction when the hydraulic cylinder is kept steady and rotated same direction with a ratio relation between the pump displacement and the cylinder area difference when moving the cylinder. For applications, one drive attended to each pump, both variable and fixed displacement pump can be used.

Hydraulic circuits in which more than one pump/hydraulic motor used are usually designed as one of the pumps is responsible for delivering main flow rate to move

a hydraulic cylinder in desired direction and another pump's/hydraulic motor's duty is to provide deficient flow in the hydraulic actuator.

Another solution to compensate flow rate varieties at inlet and outlet of the hydraulic cylinder due to area difference in the hydraulic cylinder is utilization of hydraulic transformer [11]. They are devices that can alter inlet flow and pressure to another flow and pressure level by preserving hydraulic power which is product of pressure and flow rate. To make an analogy with mechanical and electrical systems, they are respectively like gear sets and electrical transformers. In basic, they are a mechanically coupled pump and hydraulic motor. As illustrated in Figure 14, a switch or shuttle valve in imposed to the system to drive the system in two modes, namely, load stroke and rapid stroke. When the switch valve is at the position (1), the system acts like a symmetrical cylinder with bigger area. Therefore, it can give high force output. When the switch valve is at other position, it again acts like symmetrical cylinder. However, for this time, effective cylinder area is the smaller one which makes the output force lower and more rapid. Using such an additional part increases the hydraulic circuit complexity and cost.

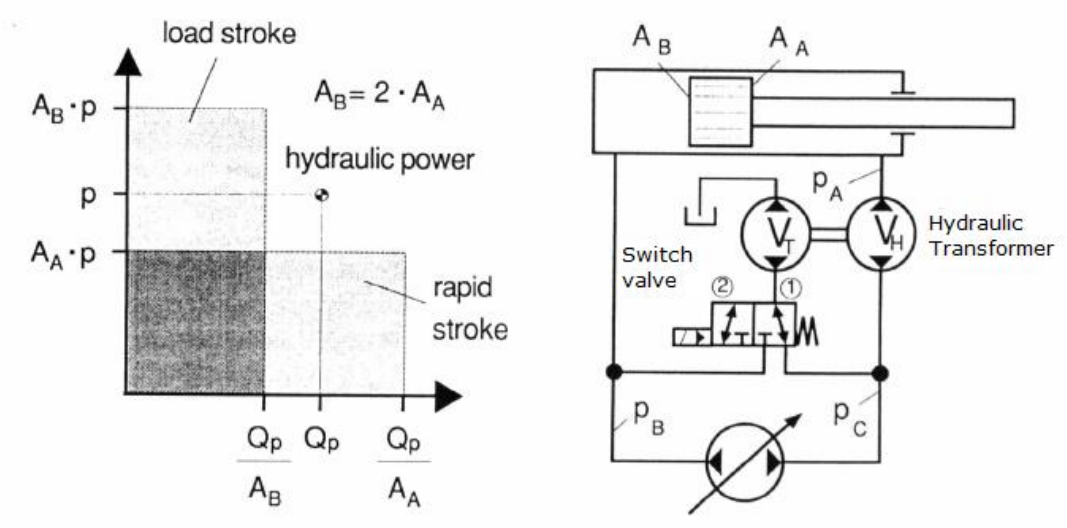

Figure 14: Hydrostatic Transmission with Switch Valve to Choose Between Rapid and Load Stroke [11]

Another solution for flow compensation with using a shuttle valve was proposed by Hewett [33]. It was used a 2/3 shuttle valve and two check valves for inner supplementary hydraulic circuit. Çalışkan offered an improved version of Hewett's solution by means of system stability. It is reported that undesirable pressure oscillations happen when the system switches between pump and motor mode in these kinds of hydraulic circuit solutions. Undesirable and uncontrollable system behavior during switching operations is called as instability [34]. Underlapped shuttle valve is utilized as a solution to that problem. The hydraulic circuit proposed is demonstrated in Figure 15 with respect to mode of the operations and the hydraulic circuit has different configurations according to spool position of the shuttle valve. Moreover, flow compensation due to the asymmetric hydraulic cylinder is managed by the shuttle valve which connects the cylinder chambers to an accumulator according to pilot pressure supplied by the chamber pressures.

Ivantsysnova and Rahmfeld recommended a solution for controlling an asymmetric hydraulic cylinder [12]. A bi-directional variable displacement pump is the main pump, the final control element, which is attached directly to a hydraulic actuator. A secondary variable displacement pump, namely charge pump, has tandem drive with the main pump and is responsible for keeping an accumulator line at a constant pressure value. Two pilot operated check valves are used to keep low pressure side of the hydraulic cylinder connected to the accumulator line. It is aimed that when the cylinder moves in "+x direction", the main pump tries to deliver more fluid then it sucks and the lack amount of fluid is provided by the accumulator. Furthermore, when the cylinder moves in "–x direction", the excess amount of fluid is taken by the accumulator. By this way, the accumulator behaves as an energy storage element in the system; besides, it is the side which makes their work different from conventional hydrostatic systems.

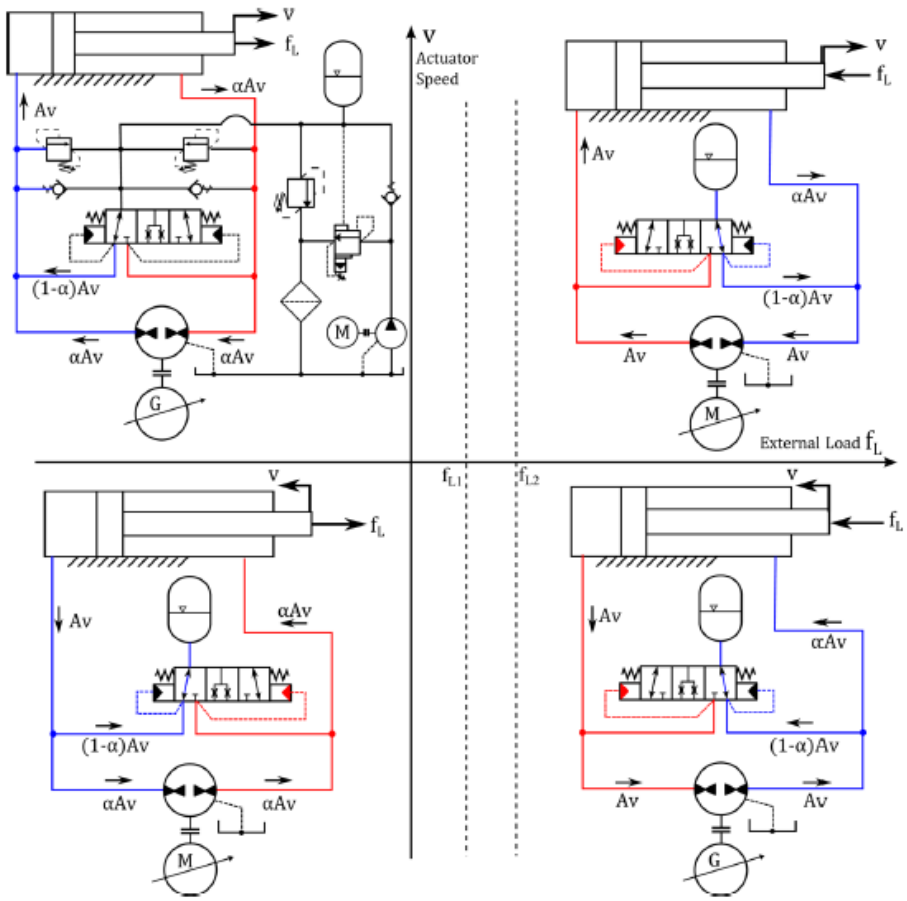

Figure 15: Working Principle of the Hydraulic Circuit with Shuttle Valve [34]

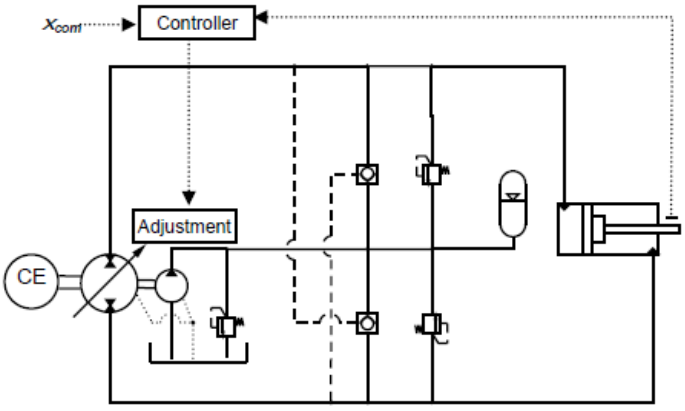

Figure 16: Ivantsysnova and Rahmfeld's Hydraulic Circuit [12]

To clarify how the complete system operates, simplified version of the system is illustrated on force-velocity graph at Figure 17. The charge pump is not shown on the graph and accumulator is assumed as a constant pressure source. In first and third quadrant of the graph, forces on the system and cylinder velocity are at the same direction; therefore, the hydraulic unit operates as a pump and delivers hydraulic energy into the cylinder. In second and fourth quadrant, forces on the system and the cylinder velocity are at opposite direction; therefore, the hydraulic unit operates in hydraulic motor mode. In other words, it converts the hydraulic energy to the mechanical energy and then transmits to drive element of the hydraulic unit [30].

At first quadrant, the cylinder moves forward direction; so, the fluid in the pressure chamber B of the cylinder, the rod side, is sucked by the pump and directed to the pressure chamber A. "γ" is devoted for the hydraulic cylinder area ratio and it is bigger than one as a value. Due to the area ratio, if the flow rate from the rod side is "Q", the flow rate that transmitted to the chamber A is equal to "γ.Q" by neglecting effects of system leakage and fluid compressibility. Therefore, the flow at inlet of the pump is lack as much as "(γ-1)*Q". The lacking flow rate is supplied by the accumulator. High pressure at pilot line of the check valve number 2 helps to open the valve and low pressure accumulator line is connected to rod side of the cylinder.

At second quadrant, velocity direction of the cylinder does not change. Thus, flow requirement of pressure chambers are same with first quadrant. The lacking flow rate is supplied again by the accumulator; nevertheless, the accumulator directly provides flow to the cylinder at this time. It is because of the force direction which is opposed according to first quadrant and high pressure line changes and the check valve number 1 is opened.

At third quadrant, the hydraulic unit operates as a pump like in first quadrant. The pump sucks the fluid from the chamber A and transmits it to the chamber B.

Additionally, due to cylinder area difference, when the chamber B needs flow rate of “Q”, the chamber A supplies flow rate of “γ.Q” which means that there is excess flow rate of “(γ-1)*Q”. This excess amount of fluid is taken by the accumulator when pilot line of the check valve number 1 is at high pressure and so opened.

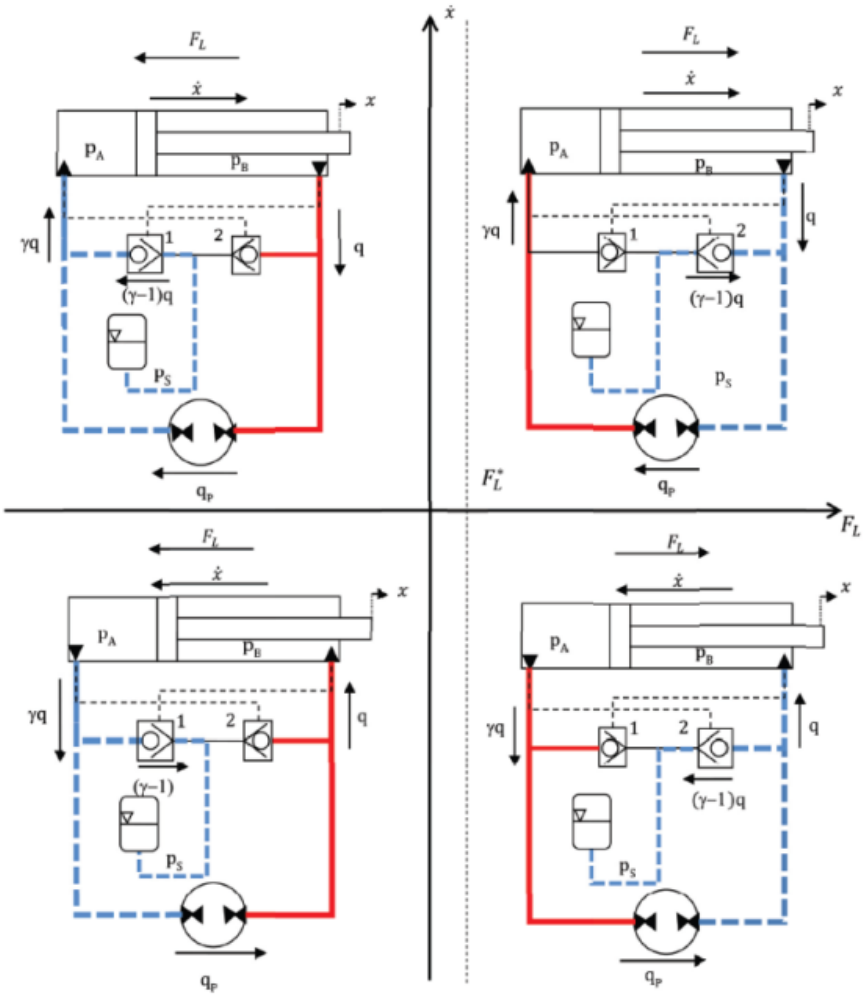

Figure 17: Four Quadrant Operation of EHA [30]

At fourth quadrant, the hydraulic unit operates as a motor like in second quadrant. The hydraulic cylinder is retracted and load force performs an action on the system [30].

2.3.3.2 Symmetric Hydraulic Cylinder Circuits

Employment of symmetric hydraulic cylinders in hydrostatic circuit decreases system complexity; since, it has some flow rates at inlet and outlet of cylinders. Therefore, there is no necessity of elements for lacking flow in ideal case. Nevertheless, in real operations there is still required to have an inner or re-feeding hydraulic circuit to compensate lacking flow because of external leakage in the elements in hydraulic circuit. Also, external leakages in bi-directional pumps cannot be directed to inlet of pumps as in single direction pumps. Additionally, external leakage in the pump must be moved away for proper operation of pump; if not, preventing excessive pressure can built up and it damages the pump. Thus, for supplementing lacking flow due to internal and external leakage, inner hydraulic circuit is used. Another reason is preventing cavitation at pump inlet which is caused by pump suction. It creates low pressure close to vacuum pressure and air dissolved in fluid media gets expend and forms air bubbles. These air bubbles travel into pump and during pressure increase from inlet to outlet of pump, they get implode and damage gears, housing and seals. The inner hydraulic circuit keeps pressure of pump inlet at above of vacuum pressure; minimizes risk of cavitation.

If a comparison made with hydraulic circuits in symmetrical and asymmetrical cylinder used, in asymmetric ones, inner hydraulic circuit flow capacity should be higher than the symmetrical one. They both have common leakage issues. However, inner hydraulic circuit is supposed to compensate the flow rate difference due to different cylinder areas and responsible for supplying backup flow. It means that inner hydraulic circuit flow source element like pump or accumulator which need to be bigger in size. Furthermore, direction valves in asymmetric cylinder used circuits make systems more complex. Pilot operated check valves need to be employed in asymmetric ones to be piloted to open the correct check valve and connect the inner hydraulic circuit to add or deduct flow

to main circuit. Conversely, in symmetric ones, ordinary check valves are enough for connecting the inner hydraulic circuit to the main circuit.

The single rod asymmetric cylinder is the most popular type of actuator in hydraulic industry for reasons cost, simplicity and smaller space requirements. Symmetrical cylinders are disadvantageous in these manners, they are more costly and do not use one of their rod efficiently. Goldenberg and Habibi offered a solution for a symmetrical single rod actuator [2]. It is designed to have equal effective areas (namely, A1, A2) as presented at Figure 18.

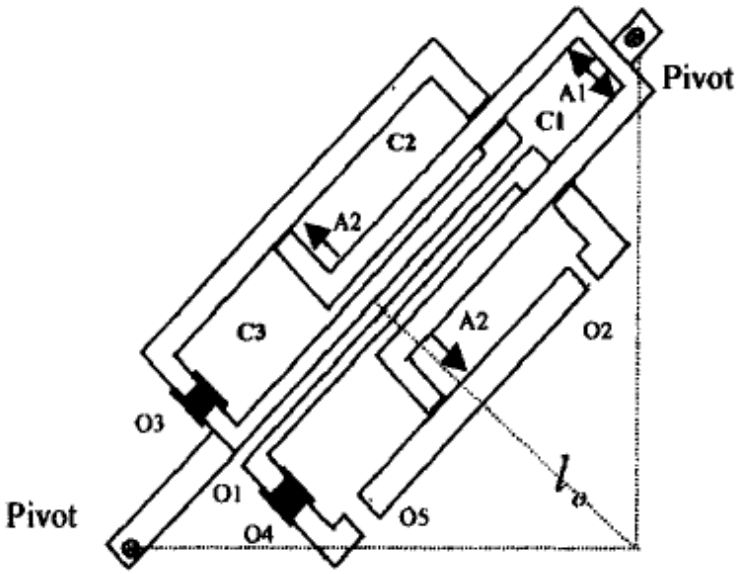

Figure 18: Single Rod Symmetric Linear Actuator [2]

The idea of Goldberg and Habibi gives a sight to designers to develop more functional symmetrical single rod actuators. In Figure 19, there is an example of practical utilization of dead space in a hydraulic cylinder by integrating a reservoir inside of the cylinder rod. It is designed for a plane landing gear and according the study, it leads an improvement in total weight of the landing gear about 6% percent [13].

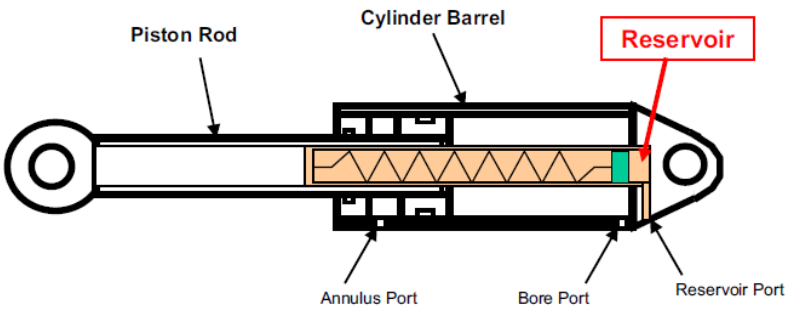

Figure 19: Reservoir Integrated Symmetrical Single Rod Actuator [13]

2.3.4 Hydrostatic Circuit for Alternative Applications

Being robust and reliable is an asset in aerospace and defense industry. Moreover, it is demanded from systems to tolerate potential faults during operations. Therefore, to make designs fault tolerant and have a proactive approach, hydraulic circuits are modified according to system requirements.

Systems that have redundant and backup structures are preferred commonly due to more fault tolerant requirements of aerospace and defense industry. Some control actuation producers are developed conventional servo valve controlled hydraulic actuator with EHA backup. It is a kind of system that they are share a common hydraulic cylinder and the hydraulic system with the servo valve is the prime controller of the system. In case of a fault occurs, a switch valve change the control of the hydraulic cylinder from to conventional servo valve system to electro-hydrostatic system as illustrated in Figure 20**.**

Dual EHA is another option to increase the safety of the overall system. In dual EHA, two EHA is connected to each other in a way of parallel or series. In a parallel system, two independent EHA is linked to the same control surface as seen in Figure 21 (a). When one of the actuator is failed, its cylinder is decoupled by by-pass valves from its pump to move freely. Afterward, the other actuator

takes the control. When the system is in series as seen in Figure 21 (b), two EHA is attached in series to each other by two hydraulic cylinders or one common cylinder which has four pressure chambers for two independent pump – motor couples. According to power request, two EHA can work together while the overall force output is doubled or one can be a redundant actuator. With respect to parallel, series option increases the power provided; however, decreases reliability of the overall system.

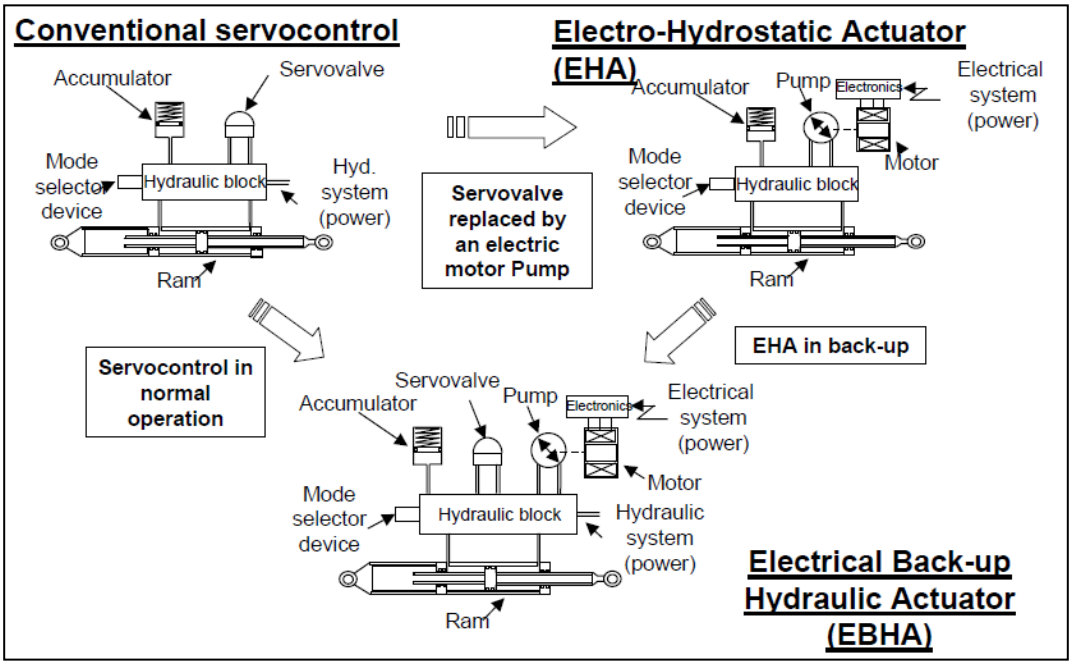

Figure 20: Electro-Hydrostatic Backup Hydraulic Actuator [38]

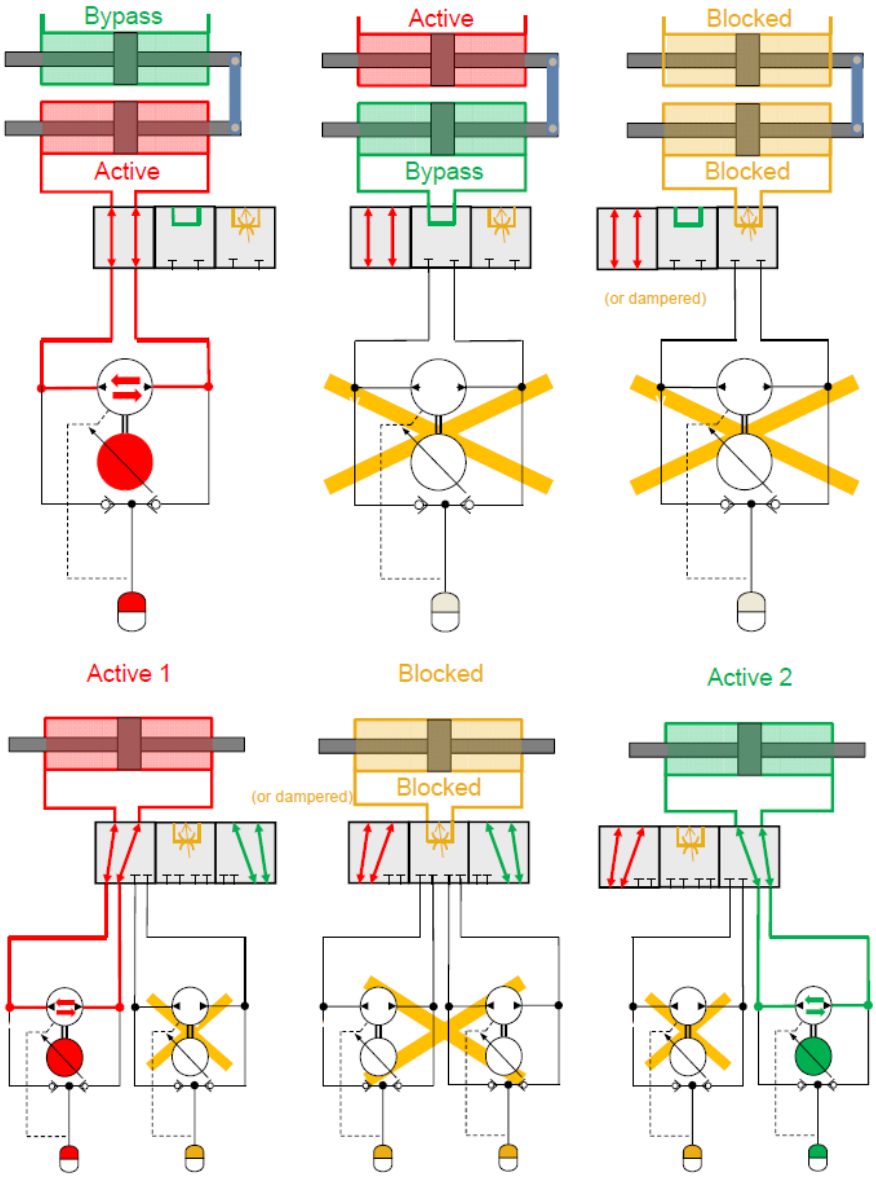

Figure 21: Parallel (a) and Series (b) Options in a Dual EHA [3]

2.3.5 Comparison between EHA and Conventional Control Actuation Systems

Conventional control actuation methods and EHA can be compared with each other as follows [3, 24]:

Table 1: Comparison between EHA and Conventional Control Actuation Systems

Electro-Mechanical **EMA**	**Electro-Hydraulic** **EH**	**Electro-Hydrostatic** **EHA**
Advantages		
Lower cost than EH for low power request	Mature technology	Higher tolerance to fluid cleanliness
High energy efficiency	High frequency operation	Good energy efficiency
Powered by wire	Compact size	Powered by wire
Easy installation	Light weight	Easy installation
Environmental cleanliness	High robustness and reliability	High robustness and reliability
Well suited for rotary actuation	Fail-safe options	Fail-safe options
High stiffness	Easy redundancy (2+ actuators)	Easy redundancy (2+ actuators)
	No backlash	No backlash

	Ideal for high & static forces	Good for high & static forces
		Unlimited hydraulic gear ratio
Disadvantages		
Heavy weight	Low energy efficiency	Weight
No fail-safe option (gearbox can block)	Requires hydraulic power unit (motor, pump, filtering, cooling)	Complexity
No redundancy (single actuator)	Environment contamination	Electrical noise
Backlash		Limited stiffness
High power consumption to hold static load		Power consumption to hold static load
Electrical noise		

CHAPTER 3

SYSTEM DESIGN AND MODELING OF EHA

In this chapter, detailed design of the Electro-Hydrostatic Actuator is described. At first, the design consideration and performance criteria of the valve controlled actuator are defined and the EHA system architecture that substitutes the valve controlled actuator is clarified. According to the system architecture, mechanical design of the parts, hydraulic and electrical equipment selections are reported.

3.1 Design Considerations and Performance Criteria

The control actuation system performance criteria are defined in Table 2 below.

Table 2: Flight Control Actuator Specifications

Stroke	±20 mm
Maximum Force Output	9500 N
No-Load Velocity	300 mm/s
Loaded Velocity	265 mm/s at 2000 N
Power Output	1100 W

The design criteria are listed as follows:

- The actuator can operate with inertia of 0.32 kgm^2 which is connected to the actuator via a mechanism shown in Figure 22. Also, it should satisfy the specifications specified at the control actuation system performance criteria defined in Table 2.
- Table 2 represents the actuator performance under inertial loading condition.

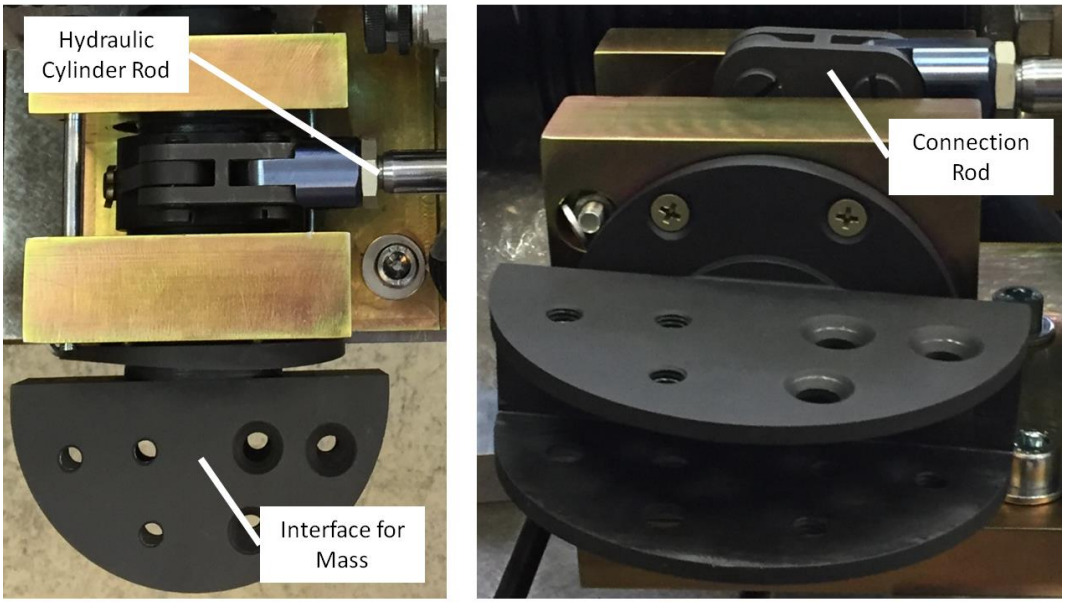

Figure 22: The Transmission Mechanism

- According to electrical circuit considerations, electric motor supply voltage should be 56 VDC (Voltage Direct Current) and command input to the actuator should be analog ±10 V.
- A closed loop position control of the hydraulic cylinder is required and controller performance is described with the criterion that is tabulated at Table 3.

The specification of the control actuation system is defined in this part and design process of an EHA to fulfill the performance measurements is the focus of this research. Therefore, overall design of the actuator is handled relating mechanical, hydraulic and electrical perspective which is explained in the next chapter.

Table 3: Desired Step and Frequency Response Characteristics

Rise Time	0.120 s
Settling Time	0.240 s
Settling Percentage	1 %
Overshoot Percentage	10 %
Undershoot Percentage	1 %
Frequency Response	10 Hz at -3 dB or 90 deg

3.2 System Design of EHA

The Electro-Hydrostatic Actuator (EHA) is composed of mainly, a variable speed servomotor, a fixed displacement pump and a symmetrical hydraulic cylinder as shown in Figure 23. One revolution of the pump gives a specific amount of fluid and due to symmetry in cylinder piston cross sectional areas. Motion speed of the cylinder is proportional to the pump rotational speed; so, the electric motor speed. The motion is controlled with regulating electric motor speed by controlling speed commands that are sent by servomotor controller. Since it is a symmetric actuator,

there is no need for a supplementary flow source. Thus, the pump can be connected directly to the cylinder chambers. The inner hydraulic circuit is used for feeding the main hydraulic circuit to compensate leakages and prevent pump cavitation. An accumulator is employed for reserve pressurized fluid source and check valves are used to direct the flow to necessary line between the pump and the cylinder. Case drain of the pump is connected to the inner hydraulic circuit and a check valve is used for providing one directional flow.

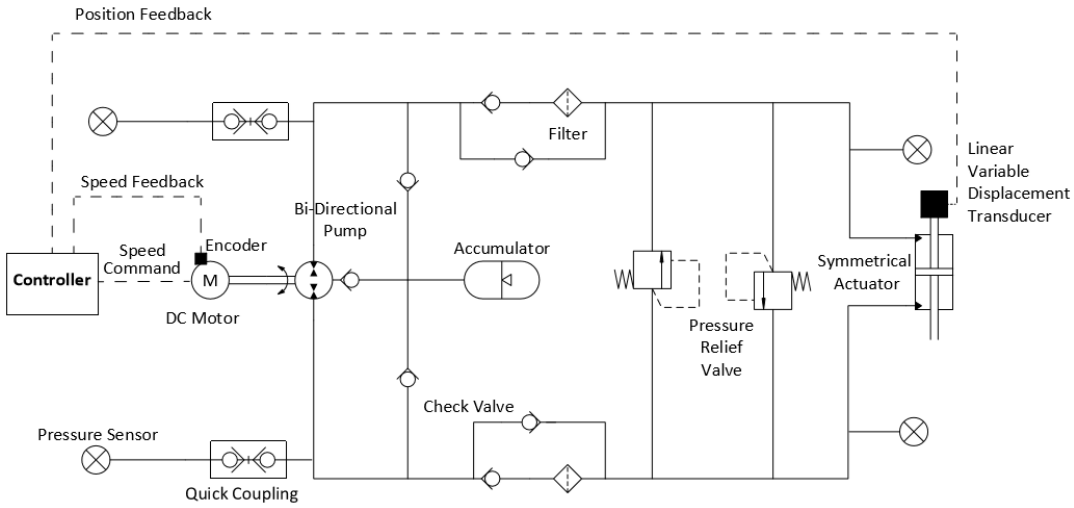

Figure 23: Schematic of Electro-Hydrostatic Actuator Prototype

Pressure relief valves are used in order to prevent the risk of excess pressure built up in the system due to stuck of hydraulic components during operation such as the hydraulic cylinder and check valves.

Filtering sub-circuits are used to protect the system from the contamination in the hydraulic fluid and check valve are used to direct fluid whether flow will pass the filter or not. Additionally, filtering is not essential in this system; because of the fact that, the system is not as sensitive as in the valve controlled system. Since, the hydraulic component used in the system does not have very small orifices or nozzles which make parts vulnerable to contamination of hydraulic media.

It can be noticeable that EHA configuration has less complexity, theoretically same dynamic response in both working direction, and more reliability, it is chosen among hydrostatic transmission options for the control actuation system. Actuator design parameters is derived from the given performance parameters and design consideration from the valve controlled actuator. Mechanical part design, hydraulic and electrical equipment selection is made in the aspect of the performance and design limitations.

3.3 Mathematical Model of EHA

The EHA system is mainly consist of the following parts:

- Hydraulic pump
- Hydraulic cylinder
- Servomotor
- Inner hydraulic circuit

In this section, the mathematical models of these parts are explained in detail.

3.3.1 Pump Equations

While modeling the pump, some assumptions are made. To begin with, orifices of the hydraulic pump in which internal and external leakage occur is small with respect to the flow sections. Therefore, the leak flow is assumed to be laminar and leakages are modeled as the linear functions of pressure difference across the ports. The pump flow is modeled according to the theoretical flow, leakage and compressibility as follows:

$$Q_{in} = D\omega_p - K_{ilp}(p_1 - p_2) + K_{elp}(p_2 - p_{cdr}) + \frac{V_1}{\beta_e}\dot{p_1} \qquad (3.1)$$

$$Q_{out} = D\omega_p - K_{ilp}(p_1 - p_2) - K_{elp}(p_1 - p_{cdr}) - \frac{V_2}{\beta_e}\dot{p}_2 \tag{3.2}$$

where D : Displacement of pump, m^3/rad

p_1, p_2 : Outlet and inlet pressure of pump, Pa

p_{cdr} : Case Drain Pressure, Pa

ω_p : Rotational speed of pump, rad/s

K_{ilp} : Internal leakage coefficient of pump, $m^3/s/Pa$

K_{elp} : External leakage coefficient of pump, $m^3/s/Pa$

V_1, V_2 : Volume of fluid at pump inlet and outlet port, m^3

β_e : Effective bulk modulus of fluid, Pa

Q_{in} : Inlet flow of pump, m^3/s

Q_{out} : Outlet flow from pump, m^3/s

Due to dead volumes V_1 and V_2 in the pump is very small, the effect of oil compressibility inside the pump is ignored. Therefore, Eq. (3.1) and (3.2) can be considered as:

$$Q_{in} = D\omega_p - K_{ilp}(p_1 - p_2) + K_{elp}(p_2 - p_{cdr}) \tag{3.3}$$

$$Q_{out} = D\omega_p - K_{ilp}(p_1 - p_2) - K_{elp}(p_1 - p_{cdr}) \tag{3.4}$$

In four-quadrant operation which means the pump is operated whether in pump mode or motor mode, Eq. (3.3) and (3.4) are satisfied while the equations are

written in terms of the port pressures and the sign of the coefficients will automatically be corrected, regardless of the operation mode [30].

Internal leakage coefficient of the pump, K_{ilp}, stands for explaining the leakage between two ports of the pump, high pressure (outlet) port and low pressure (inlet) port. Leak flow occurs across the gears from high pressure to low pressure, as a result of pressure difference between two ports of the pump. Other reason is the fluid that trapped between gears' teeth directed backward while the pump gears are rotating.

External leakage coefficient of pump, $K_{elp,}$ is used to define the flow to case drain due to leakage between radial gap between gear tooth and case wall, transverse surface gap between gear flat face and case wall.

MATLAB Simulink® environment is used to develop a simulation model of the overall system according to the formulation given in Eq. (3.3) and Eq. (3.4). Simulink® sub-system for the pump is shown in Figure 24. Angular velocity of the pump whose unit is radian per second [rad/s] is input of the sub-system and flow rates to and from the hydraulic cylinder and the pump external leakage are outputs of the pump sub-system. Flow rates are given in unit of cubic meter per second [m^3/s]. The units are also demonstrated under or top of the connection lines at the figure.

To determine the internal and the external leakage coefficients, some tests are performed and compared with the values given in the manufacturer's data sheets. They are also reviewed in the lights of open loop test results due to improper results between the real system response and the modeled system response. A look-up table whose inputs are pressure difference of inlet and outlet ports of the pump and angular velocity of the pump is formed for internal leakage coefficient as seen in Figure 25. The leakage coefficients are in unit of m^3/s/Pa and compatible with pressure unit of the three pressure ports of inlet, outlet and the case drain.

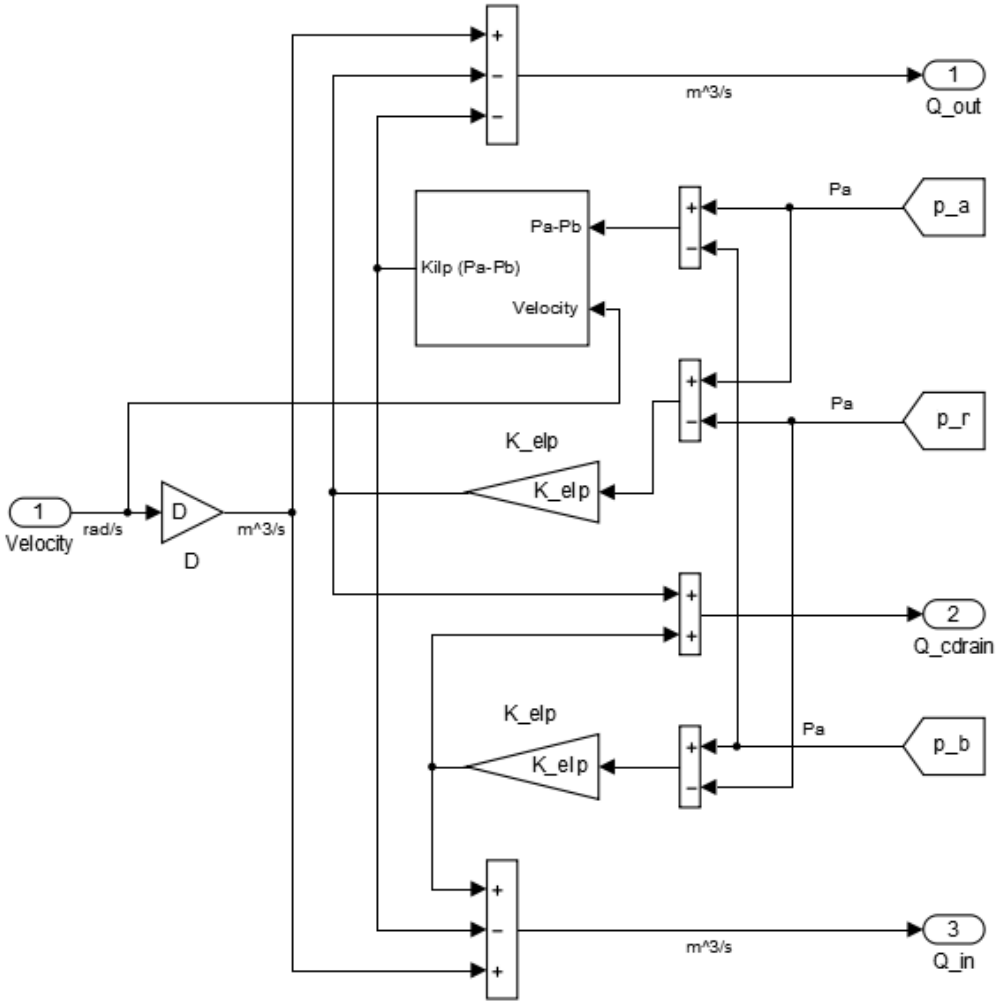

Figure 24: Simulink® Model of the Pump

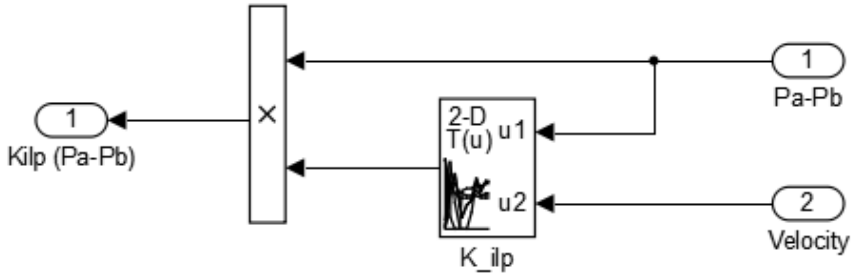

Figure 25: Simulink® Sub-Model of Internal Leakage of the Pump

3.3.2 Hydraulic Cylinder Equations

Hydraulic linear actuator for the EHA system is chosen as symmetrical and double acting cylinder to have same dynamic performance while moving in both directions and make the system less complex. However, it reasons unnecessary space for side of the piston that the load is not attached. According to chosen configuration of the hydraulic cylinder, it is modeled by making following assumptions.

Leakage between two chambers in the hydraulic cylinder is accepted as laminar and the leakage flow is defined as a function of pressure differential of two chambers. Furthermore, the leakage occurred in the cylinder can be lumped with pump leakage flow due to the pump has higher leakage flow than the cylinder and it can be assumed that their pressure differential is equal. While the leakage flow term is kept in the flow equation as follows, it is not included in the modeled system and considered in pump internal leakage flow.

$$Q_a = A\dot{x} + \frac{A(x_0 + x)}{\beta_e}\dot{p_a} + K_{ilc}(p_a - p_b) \tag{3.5}$$

$$Q_b = A\dot{x} - \frac{A(x_0 - x)}{\beta_e}\dot{p_b} - K_{ilc}(p_a - p_b) \tag{3.6}$$

$$A(p_a - p_b) = M\ddot{x} + K_{vp}\dot{x} + F_{bk} + F_{ex} \tag{3.7}$$

where A : Active area of hydraulic cylinder, m^2

p_a : Pressure in actuator chambers A, Pa

p_b : Pressure in actuator chambers B, Pa

K_{ilc} : Internal leakage coefficient of cylinder, $m^3/s/Pa$

β_e : Bulk modulus of hydraulic fluid, *Pa*

x : Position of the actuator, *m*

x_0 : Initial position of the actuator, *m*

M : Total mass of piston and load, *kg*

K_{vp} : Viscous friction coefficient of actuator, $m^3/s/Pa$

F_{bk} : Breakaway (static) friction force of the actuator, *N*

F_{ex} : External load, *N*

Q_a : Flow to/from the chambers A, m^3/s

Q_b : Flow to/from the chambers B, m^3/s

Because of symmetric design of the hydraulic actuator, cylinder chambers have the same effective area as Eq. (3.5) and (3.6). The volume that oil compressibility affects is defined as a function of piston displacement. When the EHA prototype evaluated alone, cylinder piston mass is assumed as the only mass that accelerated while piston moving. However, considering inertial load tests, mass loads of the inertia via transmission mechanism is added to the overall mass.

Friction between the piston seal and cylinder wall is accepted as viscous and modeled as proportional with piston velocity. Moreover, static friction is assumed in the hydraulic cylinder which is given as breakaway friction that the force required to start the cylinder motion. Both of these friction values are found by experiments.

In Figure 26, the Simulink® model of the hydraulic cylinder is demonstrated. Inputs of the model are inlet and outlet flow rates of hydraulic cylinder pressure chambers. Outputs of the model are pressure values of two pressure chambers of the hydraulic cylinder and the load force generated by pressure difference between

these pressure chambers. Inlet and outlet flow rates are in unit of [m^3/s], pressure of chamber A & B, p_a & p_b, are in unit of Pascal [Pa] and the load force generated is in unit of Newton [N].

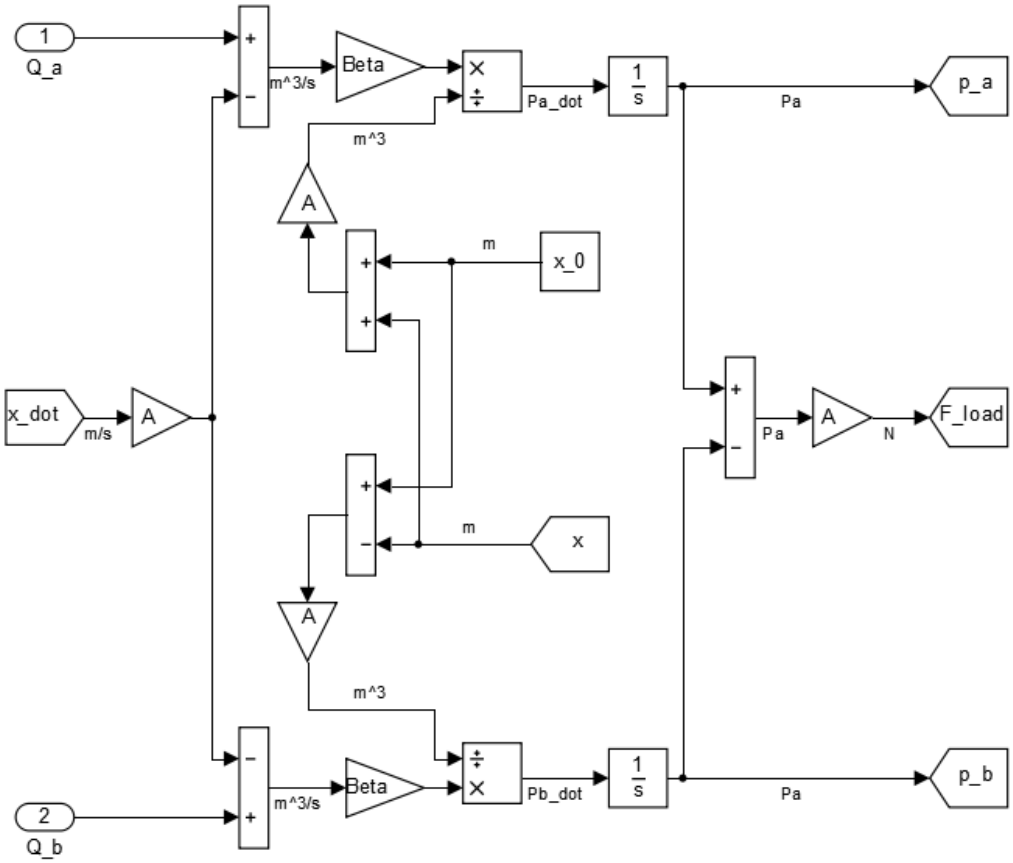

Figure 26: Simulink® Model of the Hydraulic Cylinder

The initial volumes of the pressure chambers and variation of volumes by the cylinder movement are modeled as a function of initial cylinder position and its change by time. Owing to this, compressibility in the pressure chambers is calculated by varying cylinder volumes. The hydraulic cylinder position and its speeds are given in terms of meter [m] and meter per second [m/s] respectively.

The load on the hydraulic cylinder is modeled in the same sub-model and is shown in Figure 27. Force summation on the cylinder which is load force generated by pump, external force and friction force of the cylinder is converted to acceleration, speed and position by order of the simulation flow. Besides, cylinder motion range is limited with a basic saturation block.

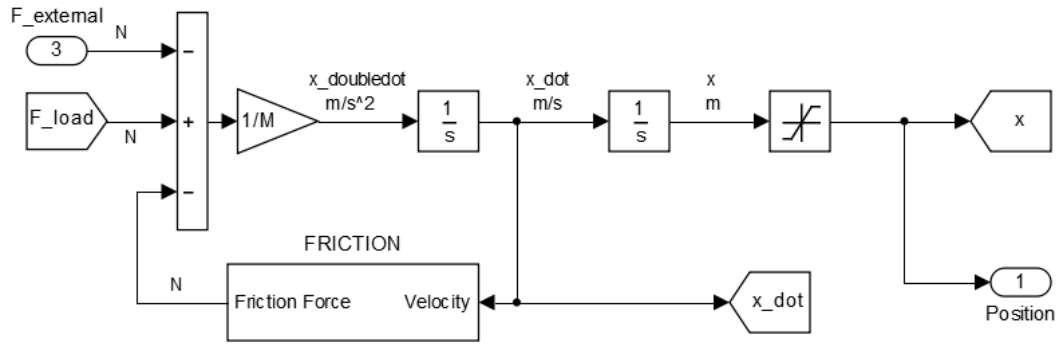

Figure 27: Simulink® Model of Loads Acting on the Hydraulic Cylinder

As given in the mathematical model, only two types of the friction is modeled which are viscous friction and static friction of the cylinder. Viscous friction is assumed as a function of the actuator velocity and static friction is assumed as constant force that the actuator experience during its motion. The cylinder friction model is illustrated at Figure 28.

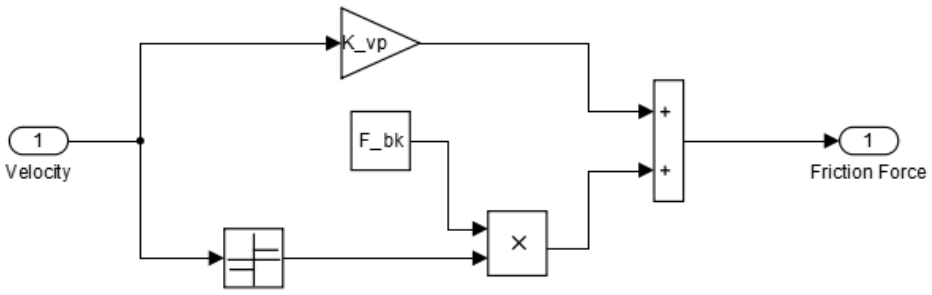

Figure 28: Simulink® Model of the Hydraulic Cylinder Friction

3.3.3 Accumulator & Inner Hydraulic Circuit Flow Equations

There are different types of accumulators according to their energy storage characteristics, spring loaded, weight loaded and gas charged. In the EHA prototype, a gas charged bladder type accumulator is utilized.

In Eq. (3.8), the accumulator pressure formula is shown for isothermal expansion or compression of gas. However, the accumulator dynamics is assumed insignificant and not included in the system mathematical model. It is modeled as a constant pressure source in the inner hydraulic circuit. It is because of the fact that the capacitance of the accumulator is relatively high in comparison with the hydraulic cylinder. Their volumes are 568 ml (1 Pint in Imperial Unit) and 24 ml, respectively.

$$p_{ac} = \frac{p_{ac0} V_{g0}^{k}}{(V_{g0} - \int Q_{ac} dt)^{k}} \tag{3.8}$$

where p_{ac} : Current pressure of the accumulator, *Pa*

p_{ac0} : Initial pressure of the accumulator, *Pa*

V_{g0} : Initial volume of gas, m^3

k : Polytropic exponent of gas (1-1.4)

Q_{ac} : Flow to/from the accumulator, m^3/s

In Figure 29, the inner hydraulic circuit is demonstrated. According to the accumulator's role in the system, if the pressure difference between accumulator and the main hydraulic circuit lines is bigger than cracking pressure of the check valve, accumulator gives fluid to the line connecting to inlet or outlet of the pump or receives fluid from the pump case drain.

The inner hydraulic circuit flows are made conditional as shown in Eq. (3.9), (3.10) and (3.11) below:

$$\begin{aligned} &p_{ac} - p_a > p_{cv}\,, && Q_{ac1} = K_{cv}(p_{ac} - p_a) \\ &p_{ac} - p_a < p_{cv}\,, && Q_{ac1} = 0 \end{aligned} \tag{3.9}$$

$$\begin{aligned} &p_{ac} - p_b > p_{cv}\,, && Q_{ac2} = K_{cv}(p_{ac} - p_b) \\ &p_{ac} - p_b < p_{cv}\,, && Q_{ac2} = 0 \end{aligned} \tag{3.10}$$

$$\begin{aligned} &p_{cdr} - p_a > p_{cv}\,, && Q_{ac} = Q_{cd} \\ &p_{cdr} - p_a < p_{cv}\,, && Q_{ac} = 0 \end{aligned} \tag{3.11}$$

where p_{cv} : Check valve cracking pressure, *Pa*

k_{cv} : Flow resistance in check valve, $m^3/s/Pa$

Q_{ac1} : Flow from accumulator to chamber A, m^3/s

Q_{ac2} : Flow from accumulator to chamber B, m^3/s

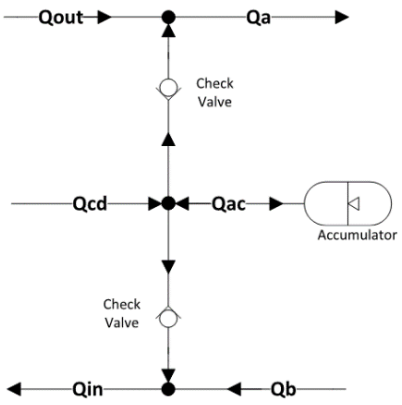

Figure 29: Inner Hydraulic Circuit Flow Schematic

In the inner hydraulic circuit, check valves are modeled as Figure 30. Their resistance to flow is assumed as a linear function of the pressure difference at upstream and downstream of the valves.

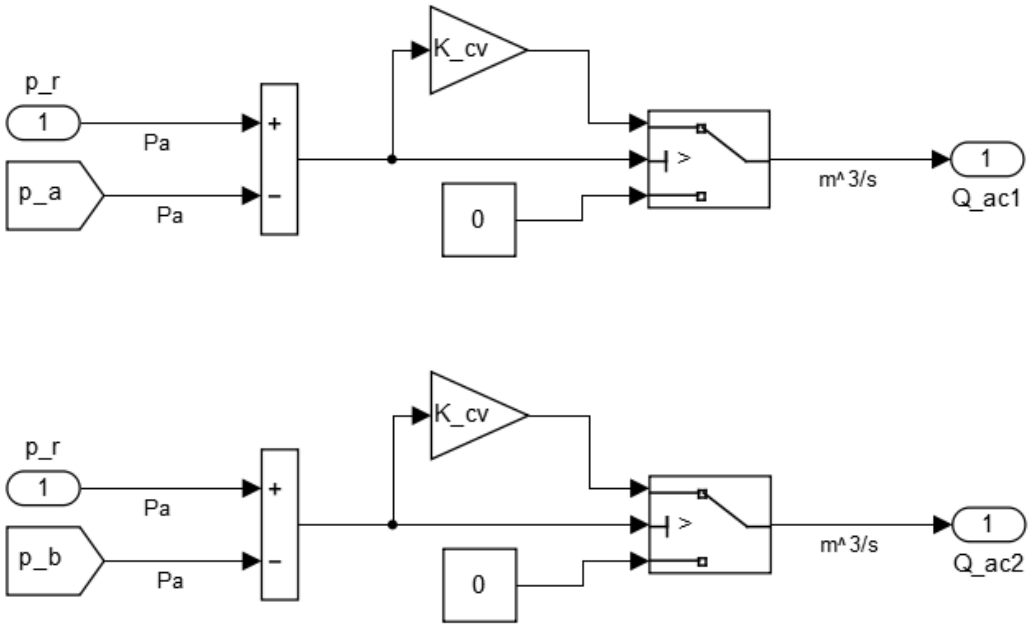

Figure 30: Simulink® Model of the Check Valve

3.3.4 Main System Flow Equations

Casing and connection elements are assumed as rigid; so, any structural compliance or volume change does not taken into account.

In the actuator, there are no hydraulic piping or long distance flow channels between components, it can be assumed that pressure losses occurred in the flow between pump to hydraulic cylinder is zero. Therefore, pressure at ports of the pump and pressure of the chambers that connected to each other are accepted to be equal.

System pressures p_1 and p_2 cannot be lower than pressure at the accumulator line. If it happens inner hydraulic circuit is activated and accumulator provides flow to low pressure line. According to the inner hydraulic circuit is active or inactive, system has two modes of operation. When the inner hydraulic circuit is inactive, it is normal mode of operation and pressure difference of the pump is p_1-p_2. If the inner hydraulic circuit is active, pressure difference of the pump is p_1-p_{cdr}.

The flow enters and exits the actuator is equal to the flow enters and exits the pump, the main flow can be defined as in Eq. (3.12).

$$Q = \frac{Q_a + Q_b}{2} = \frac{Q_{in} + Q_{out}}{2} = D\omega_p \tag{3.12}$$

3.3.5 Servomotor Equations

Servomotor performance has a big impact on the overall system dynamic performance. When servomotor and pump selection is done, some performance characteristics of the designed actuator have been decided. Also, the optimum performance is searched with design parameters that are shared with the pump and the servomotor such as rotational speed and nominal torque.

The hydraulic system obviously has lower dynamic response with respect to the servomotor. Moreover, servomotor has to at least ten times faster dynamics in order to be insignificant dynamically. Regarding to these kind rules of thumbs, servomotors are assumed as ideal angular velocity source or modeled as first and second order transfer functions in the literature [30, 31]. In this thesis work, it is modeled as an electric motor with embedded speed controller. It is because of the fact that during performance test with inertial and external loads, the second order transfer function is not sufficient to reflect real dynamics of the servomotor.

Electrical and mechanical equations representing the dynamic behavior of an electric motor are as follows:

$$V_m = K_w\omega + L\frac{di}{dt} + Ri \tag{3.13}$$

$$T_m = K_t i \tag{3.14}$$

$$T_m = J_{mp}\dot{\omega} + K_{vm}\omega + T_l \tag{3.15}$$

where V_m : Input voltage of the motor, *V*

K_w : Speed constant of the motor, *V/rad/s*

ω : Rotational speed of the motor, *rad/s*

L : Inductance of the motor, *H*

i : Current, *A*

R : Resistance of the motor, *Ohm*

T_m : The motor torque, *Nm*

K_t : Torque constant of the motor, *Nm/A*

J_{mp} : Inertia of the motor-pump couple, kgm^2

K_{vm} : Viscous friction of the motor, *Nm/rad/s*

T_l : Load torque on the motor, *Nm*

Simulink® model of the electric motor is built as shown in Figure 31. It defines relation between the motor input voltage in unit of [V] and the motor rotation speed in unit of [rad/s].

After the electric motor model is constructed, current and voltage controller are added to the model and final control variable, speed, is become to be manipulated. The electrical and mechanical delays in the servo system are added to the model. Afterwards, the servo system model is finalized for rotational speed control as illustrated in Figure 32 which is named as servomotor.

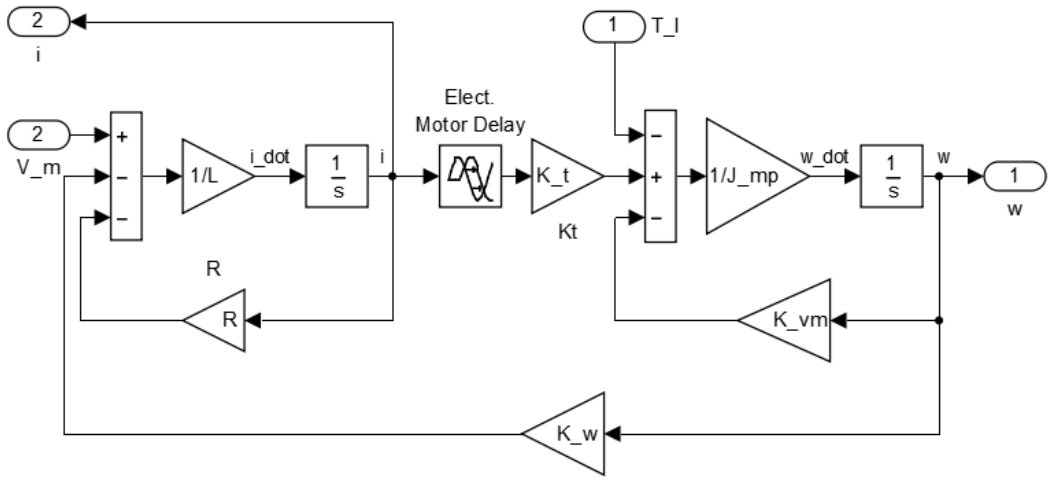

Figure 31: Simulink® Model of the Electric Motor

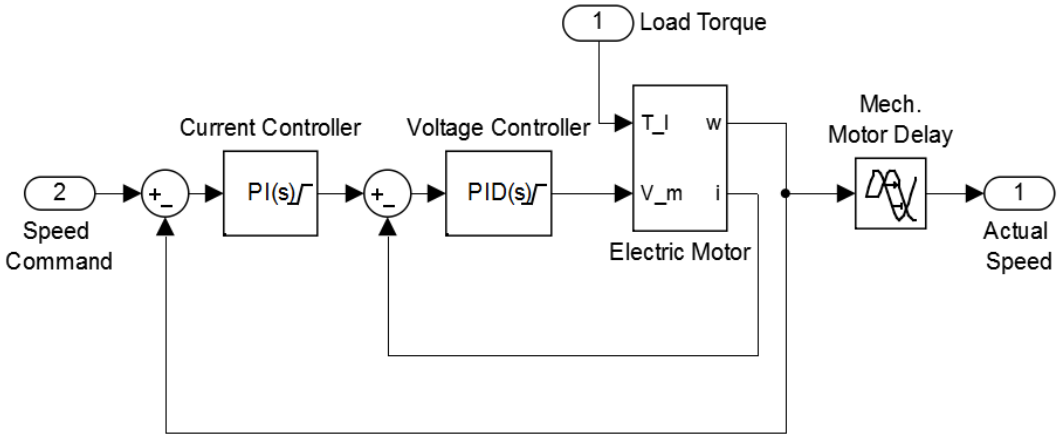

Figure 32: Simulink® Model of the Servo System

3.3.6 System Equations

Servomotor rotor and pump shaft is connected directly with conical seat and a keyway. They are assumed as backlash-free and rigid connection at torsional loading since they are not long slender shafts. There is not any twist angle between servomotor rotor and pump shaft. Therefore, their rotation speeds are equal to each other and their total inertia is lumped as J_{mp} which is defined in modeling of the electric motor. The viscous friction that occurs in electric motor and the pump is defined overall as K_{vm}. T_l is the load torque which represents the torque occurred at motor-pump shaft due to supplying pressurized flow by the pump.

The motor torque output defined in Eq. (3.15) is rearranged to express torque balance between the motor-pump regarding to the assumptions as follows:

$$T_m = J_{mp}\dot{\omega}_p + K_{vm}\omega_p + \frac{D(p_1 - p_2)}{\eta_{mech}} \tag{3.16}$$

In Figure 33, gains K_v, K_s and K_p represent the gains of current loop, speed loop of the motor driver and position loop of the EHA, respectively.

3.4 Mechanical and Hydraulic Design of EHA

According to the system architecture defined in 3.2, mechanical parts design process and component selection is described in this section.

Hydraulic system design process typically starts with determining nominal operating pressure of the system and selecting an actuator size. After determining nominal operating pressure, other components can be chosen with respect to pressure rating. To begin with, the actuator is considered. A symmetrical hydraulic cylinder is used in the available servo valve controlled actuation system.

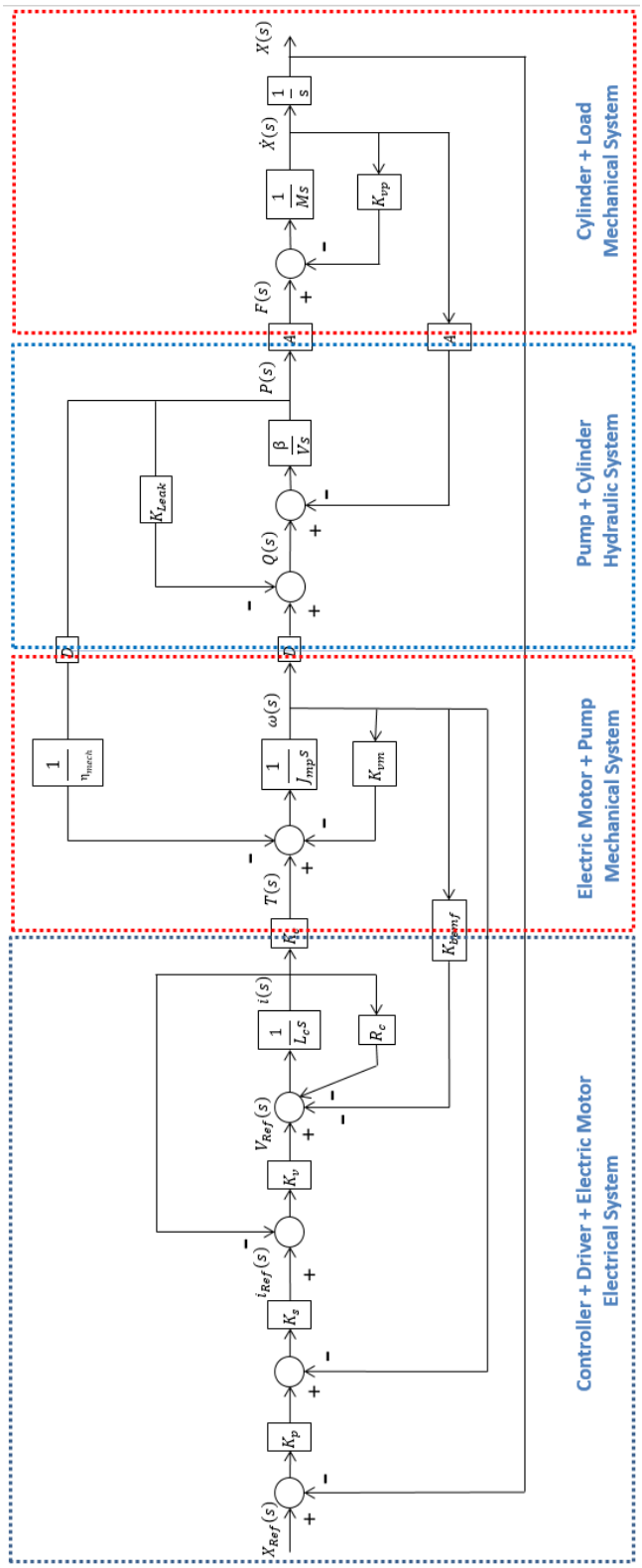

Figure 33: The Block Diagram of Position Closed Loop EHA

The same hydraulic cylinder is used for EHA to make the comparison between the valve controlled system and EHA. Also, it makes easier to evaluate while having same parameters such as cylinder areas, mass and stroke etc. and keeps the same connection interfaces with the actuation mechanism.

By having the symmetric cylinder, effective piston areas of the cylinder (A_{ef}) at two sides of the cylinder are equal. If maximum force output is considered, operating pressure of the system (153 bar) is calculated. The system nominal operating pressure as 160 bar seems to be enough. However, while external gear pumps are very capable to work efficiently under high pressure ratings, the pump and the other hydraulic components are selected at above this pressure rating, at 207 bar. In Eq. (3.17), necessary system pressure to satisfy the given maximum force output specification is calculated and in Eq. (3.18), the maximum force output (F_{mx}) for chosen system pressure is calculated.

$$p = \frac{F_{mx}}{A_{ef}} = \frac{9500\ N}{620\ mm^2} * \frac{10\ mm^2 * bar}{N} = 153\ bar \tag{3.17}$$

$$F_{mx} = A_{ef} * p = 620\ mm^2 * 210\ bar * \frac{10^{-1}\ N}{mm^2 * bar} = 13020\ N \tag{3.18}$$

Due to possible increased force output in the cylinder piston, the rod diameter is evaluated again for highest force value. Material of the cylinder piston is structural alloy steel of 45CrNiMoVa according to the Chinese GB/T3077-1999 standard and its material properties are given in Table 4. This material has high yield and ultimate tensile strength and corrosion resistant.

Safety factor is calculated for new maximum loading condition and one given in the specifications. Previous safety factor was 21 and for new maximum loading it is found as 15.7 in Eq. (3.19) where S_y is the yield strength of the material, A is the

cross sectional area of the rod. The safety factor is still high enough for reliable operation.

$$n_{safe} = \frac{S_y * A}{F_{mx}} = \frac{1330\ MPa * \pi * (7\ mm)^2}{13020\ N} \approx 15.7 \qquad (3.19)$$

Table 4: 45CrNiMoVa Alloy Steel Mechanical Properties [14]

Yield Strength	1330 MPa
Ultimate Tensile Strength	1470 MPa
Elongation	7 %
Reduction of Area	35 %
Max. Brinell Hardness	269

In Figure 34, technical drawing of the hydraulic cylinder piston is demonstrated and the major parameters are as follows:

- Rod diameter : 14 mm
- Cylinder diameter : 32.4 mm
- Effective piston area : 620 mm^2
- Stroke : ± 20 mm

The pump size, in other words, its displacement is chosen according to satisfy no-load velocity criterion in the specifications. Also, it affects resolution and

bandwidth of the system. The flow rate to satisfy the maximum cylinder speed under no load condition (Q_{mx}) is calculated in Eq. (3.20). Regular rotation speed values for external gear pump are investigated and for a common driving speed of 3000 rpm, displacement of the pump (D) is found in Eq. (3.21).

$$Q_{mx} = 297\frac{mm}{s} * A_{ef} * \frac{6 * 10^{-5}\, l * s}{mm^3 * min} = 11\ l/min \tag{3.20}$$

$$D = \frac{Q_{mx}}{3000rpm} * \frac{10^3 cc}{l} = 3.7\ cc/rev \tag{3.21}$$

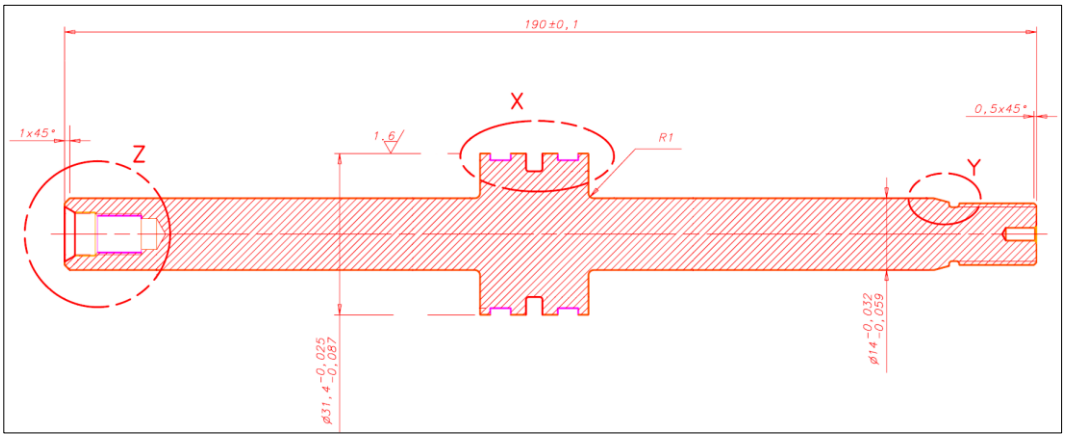

Figure 34: Technical Drawing of the Hydraulic Cylinder Piston

Pump mechanical and volumetric efficiency, working pressure, volumetric displacement, nominal speed are main factors that affect the pump overall performance. However, efficiency values at different working conditions are not tabulated at part catalogs and data sheets in general. According to the remaining factors such as volumetric displacement and working pressure and speed, a fixed displacement pump of the Parker Hannifin Corporation is chosen as illustrated at Figure 35. It is a 4.3 cc/rev external gear pump whose part number is 3309219025. It can operate up to 250 bar pressure and it is advised to rotate the

pump between 500 and 3500 rpm in the catalog and there is not a performance test result for rotation speed below than 500 rpm. Nevertheless, for closed loop position control of a hydraulic cylinder in which the hydraulic cylinder makes small displacements, flow rates from close zero to maximum pump speeds must be supplied by data sheets. In closed loop control, the pump may rotate at very low speed and produce small amount of flow when the hydraulic cylinder position change about a set point. Therefore, range of speed and pressure at which pump has zero displacement due to leakages is supposed to be known. In the chapter ahead, a characterization test to detect the region called “dead band” in the literature is mentioned in detail.

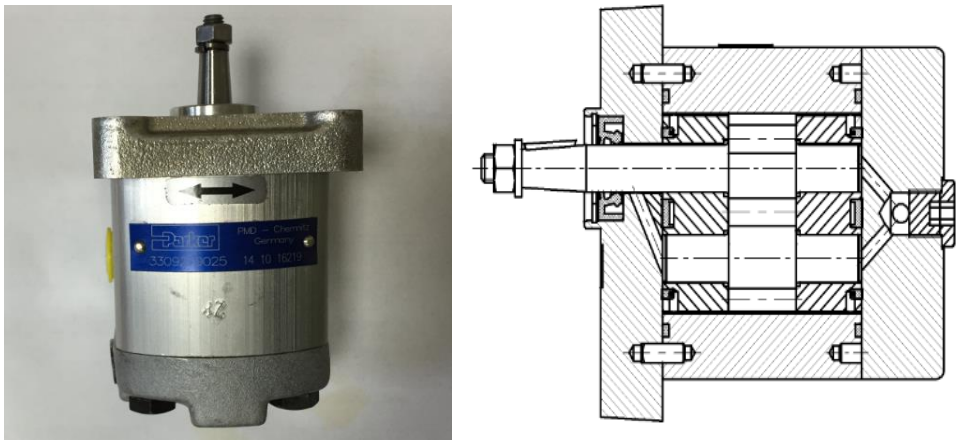

Figure 35: Parker External Gear Pump [15]

It should be considered that positioning accuracy of the hydraulic cylinder is affected by the pump displacement. Because the smaller displacement pumps, the lower amount fluid provided to the cylinder chambers and it causes finer motion; so, resolution of the motion gets superior with respect to bigger displacement pumps. Also, as mentioned before cylinder speed is proportional to the pump displacement. Therefore, a trade-off should be done between positioning accuracy

of the hydraulic cylinder and its speed. In this thesis work, to satisfy cylinder speed is one of the goals; so a bigger size pump selection is reasonable.

Electric motor is highly important element in the EHA system to have a great dynamic performance. When a selection is made, electrical and mechanical time constants, maximum speed, nominal torque should be considered primarily. Time constants are related with electrical and mechanical inner design of the motor. Catalog values of nominal speed and nominal torque is used for searching servomotors in the market. Necessary nominal speed is thought to be equal the pump rotation speed so it is chosen as 3000 rpm. The maximum hydraulic power of the pump is calculated in Eq. (3.22) and the necessary electric motor power for the worst efficiency is found in Eq. (3.23). For an intermittent duty cycle, the maximum torque requirement is derived in Eq. (3.24) and it means that the maximum output force at the maximum speed can be applied in intermittent region of the electric motor which can drop life of the electric motor if the duration of use exceeds pre-defined intermittent period of time.

$$\begin{aligned} P_h &= p_p * Q_{mx} \\ &= 160\ bar * 4.3\ \frac{cc}{rev} * 3000\ rpm \\ &* \frac{Pa * m^3 * min}{600\ bar * cc * s} = 3440\ W \end{aligned} \tag{3.22}$$

$$P_{em} = \frac{P_h}{\eta_e} = \frac{3.44}{0.8} = 4300\ W \tag{3.23}$$

$$T_{em} = \frac{P_{em}}{\omega_{em}} = \frac{4300\ W}{314.2\ rad/s} = 13.7\ Nm \tag{3.24}$$

Another constraint for servomotor is to work with 56 VDC which is the voltage can be supplied according to electrical architecture of the system. In the market, it is difficult to find a DC servomotor which has the related speed and torque specifications. Therefore, a custom design servomotor is asked for production which satisfies criteria and constraints in the domestic market. Performance parameters of the custom made servomotor are tabulated as follows:

Table 5: Servomotor Parameters

Nominal Voltage	56 V
No load Speed	3766 rpm
Nominal Speed	3000 rpm
Nominal Torque	7 Nm
Stall Torque	18 Nm
Nominal Current	40 A
Max. Efficiency	92 %
Terminal Resistance Ph. To Ph.	$35*10^{-3}$ Ohm
Terminal Inductance Ph. To Ph.	$34.8*10^{-6}$ H
Torque Constant	0.174 Nm/A

Speed Constant	$14.9*10^{-3}$ V/rpm
Mech. Time Constant	$0.62*10^{-3}$ s
Rotor Inertia	0.00042 kgm^2

After key components of the system is determined, the valve parts and other components of the inner hydraulic circuit are selected which are the pressure relief valves, the check valves and the accumulator.

To begin with, the pressure relief valves are used in the system for the safety issues such as overloading, instant pressure peaks and a possible stuck that may occur in the hydraulic cylinder. The valve chosen is a Parker Hannifin RAH081 Relief Valve, which is an adjustable pressure setting type and unidirectional; so, two of valves are utilized to connect high pressure line to low pressure line in both directions of the hydraulic circuit. By turning the knob in Figure 36, pressure setting for relief function can be adjusted and it is set to 210 bar for the EHA system.

The check valves are chosen with respect to low cracking pressure and small resistance as possible when the flow occurs. The reason is that the check valves' duty is to direct the flow without high pressure drop while the inner hydraulic circuit pressure is already low and to open at low pressure difference especially between the case drain of the pump and the accumulator. Parker Hannifin CVP081P Check Valve is selected with 0.3 bar cracking pressure and 2.6 bar pressure drop for maximum rated flow of 38 liters per minute (Figure 37).

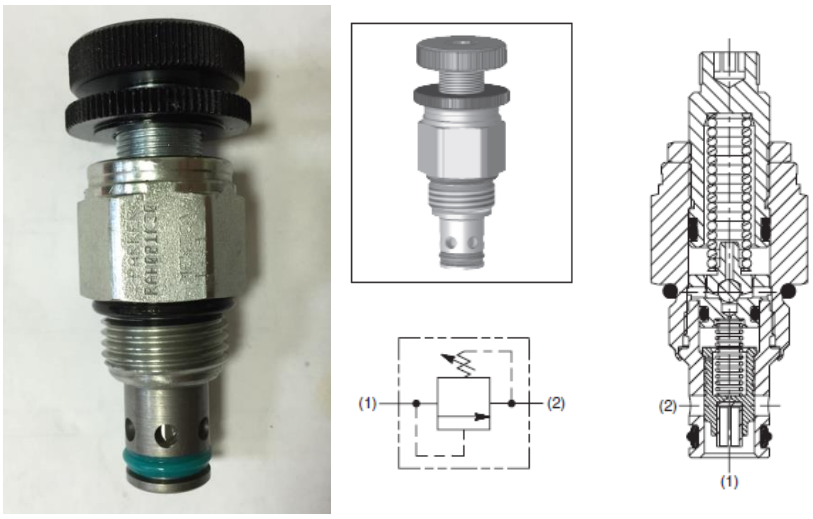

Figure 36: The Pressure Relief Valve [16]

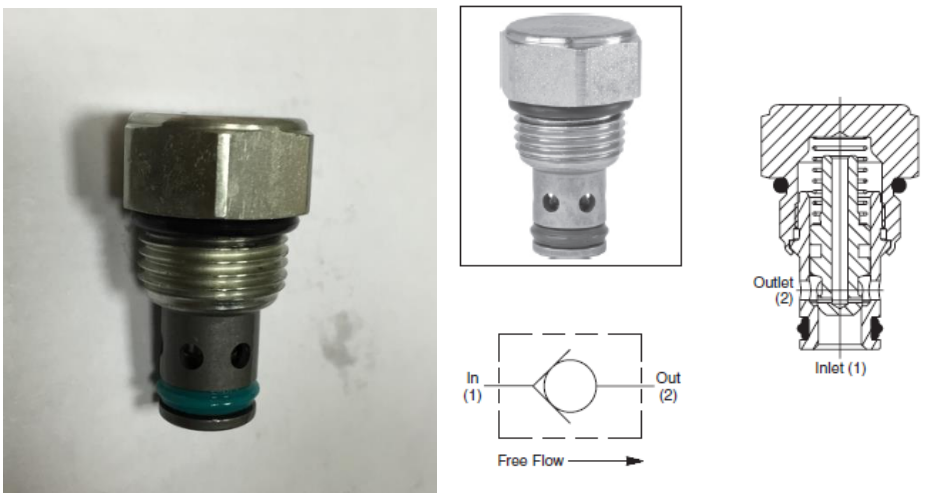

Figure 37: The Check Valve [17]

As explained in Section 3.2 the EHA has composed of high pressure main circuit and the inner hydraulic circuit with low accumulator pressure. The accumulator is responsible to re-feed the main hydraulic circuit for external leakages and prevent the pump cavitation and be a reservoir for the pump case drain. The selected accumulator is Parker Hannifin BA001B3 bladder type whose overall volume is

0.57 liter. The accumulator shown in Figure 38 is initially filled with 0.35 liter of hydraulic fluid and 3.5 bar of compressed gas. The maximum pressure of the pump case drain is 5 bar as indicated in the catalog in order not to damage the pump seals. Thus, 3.5 bar plus 0.3 bar the check valve cracking pressure is thought to be low enough to direct internal leakage of the pump to the inner hydraulic circuit and also, 3.5 bar of the inner hydraulic circuit pressure minus 0.3 bar of the check valve cracking pressure is thought to be high enough to eliminate the pump cavitation.

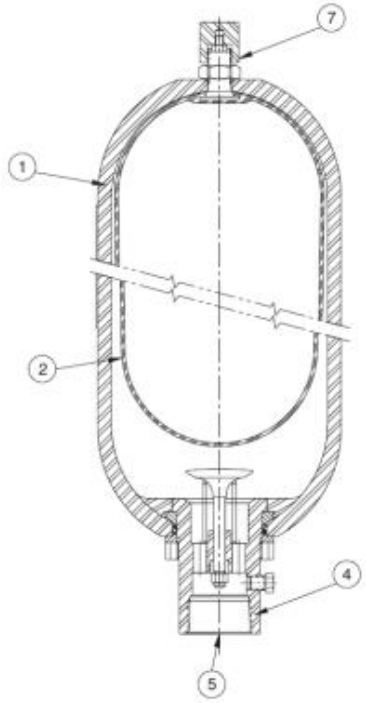

Figure 38: A Bladder Type Accumulator [18]

For proper application and long operation life two filters are employed in each direction of the circuit. The filter chosen is Parker Hannifin FL101 with permissible particle size of 30 microns as illustrated in Figure 39. It is thought to be enough particle size if it is compared with the 10 micron-particle size filter in the available servo valve controlled actuator while there is no component such as

narrow orifices, nozzles that is highly sensitive to the hydraulic fluid contamination in the hydraulic circuit.

After all necessary components are chosen and major design parameters are determined, in Figure 40, a valve manifold is designed to hold all elements of the valves, the cylinder, the pump, and sensors as a lumped unit and have a compact overall actuator design.

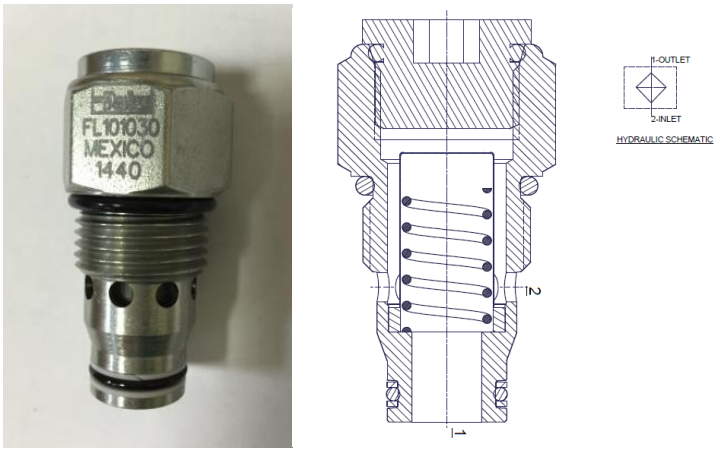

Figure 39: The Filter [19]

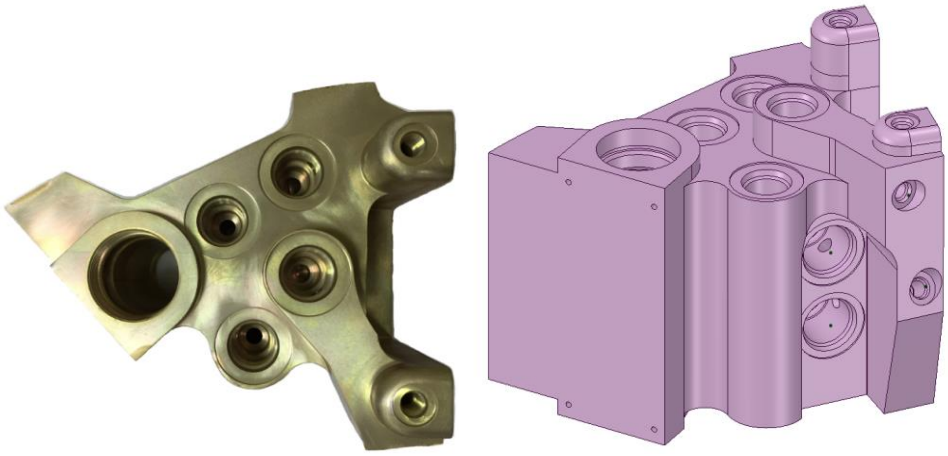

Figure 40: The EHA Valve Manifold

The determined conduit diameters of 8 mm inside the valve manifold is calculated to have a laminar flow regime at full flow of the pump as in Eq. (3.25) where "ν" is the kinetic viscosity (mm^2/s), "V" is the fluid velocity and "d" is the pipe diameter. However, instead of calculating the fluid velocity, the Reynolds Number can be calculated directly from the flow rate. The result shows that the flow stands in laminar flow regime at the maximum flow rate but, it is very close to transient regime ($2300 < Re < 4000$) which is in-between laminar and turbulent.

$$Re = \frac{Vd}{\nu} \text{ and } Q_{mx} = A * V$$

$$Re = \frac{dQ_{mx}}{A\nu} = \frac{4Q_{mx}}{\pi d\nu}$$

$$Re = \frac{4 * \frac{4.3cc}{rev} * 3000rpm}{\pi * 0.008\,m * 18\,mm^2/s} = 1901 < 2300 \qquad (3.25)$$

As the hydraulic fluid, MIL-PRF-5606H is selected. It is a mineral based aviation series hydraulic oil which has high viscosity index to be capable to operate wide range of temperatures, excellent low temperature properties, good chemical and oxidation stability to resists the formation of varnishes and deposits and super clean to ensure the reliable performance of pumps, servo valves and other hydraulic components. [20] The oil supplied is from Belgin Oil Hidrotex whose density is 868.8 kg/m^3 and bulk modulus is 1087 MPa at 15°C.

MIL-PRF-5606H compatible O-ring materials are investigated to support high and low temperature operating conditions. Acrylonitrile-Butadiene Nitrile, also known as NBR, which highly used in the industry, is determined to use in performance tests held in the laboratory. Its specifications are 70 Shore and it is suitable to be used between -34° to 121°C.

Filling operation of the closed hydraulic circuit of EHA is achieved by quick couplings which are embedded to system to connect the pressure sensors. As seen in Figure 41, filling valves are connected to the hydraulic circuit and at first, vacuum pressure of 0.3 bar is applied to discharge air inside the system and then, the hydraulic oil is filled with pressure of 3.5 bar. Next, the filling valves are disassembled from the system to attach pressure sensors.

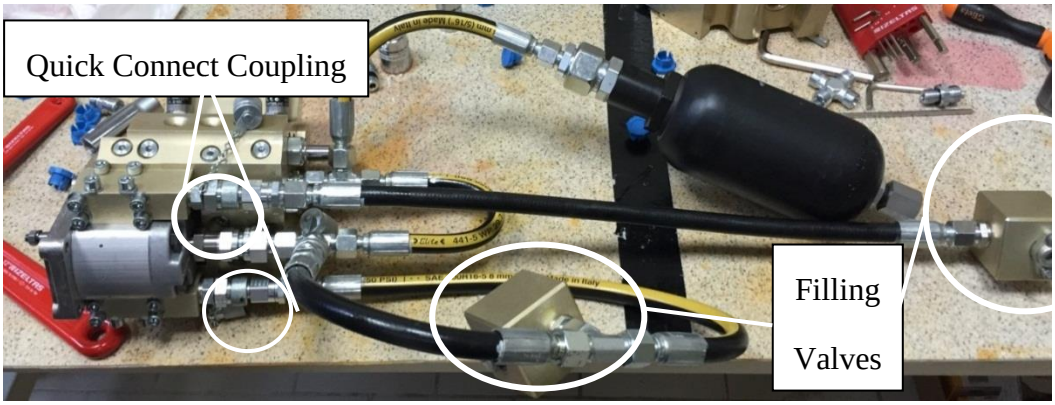

Figure 41: The EHA with Filling Valves

After the filling operation is completed, the pressure sensors with quick coupling interfaces are connected to the system. At the end, the servomotor is attached to the system and assembly operation of the prototype is finalized. In Figure 42, the solid model of the actuator is shown.

The prototype mechanical system parameters are given in Table 6.

Table 6: The EHA Mechanical System Parameters

Nominal Pressure	160 bar
Nominal Force Output	9500 N

Effective Cylinder Area	620 mm^2
Max. Flow Rate	12.9 l/min
Max. Cylinder Velocity	347 mm/s
Pump Displacement	4.3 cc/rev
Pump/Electric Motor Max. Rotation Speed	3000 rpm
Nominal Electric Motor Torque	7 Nm

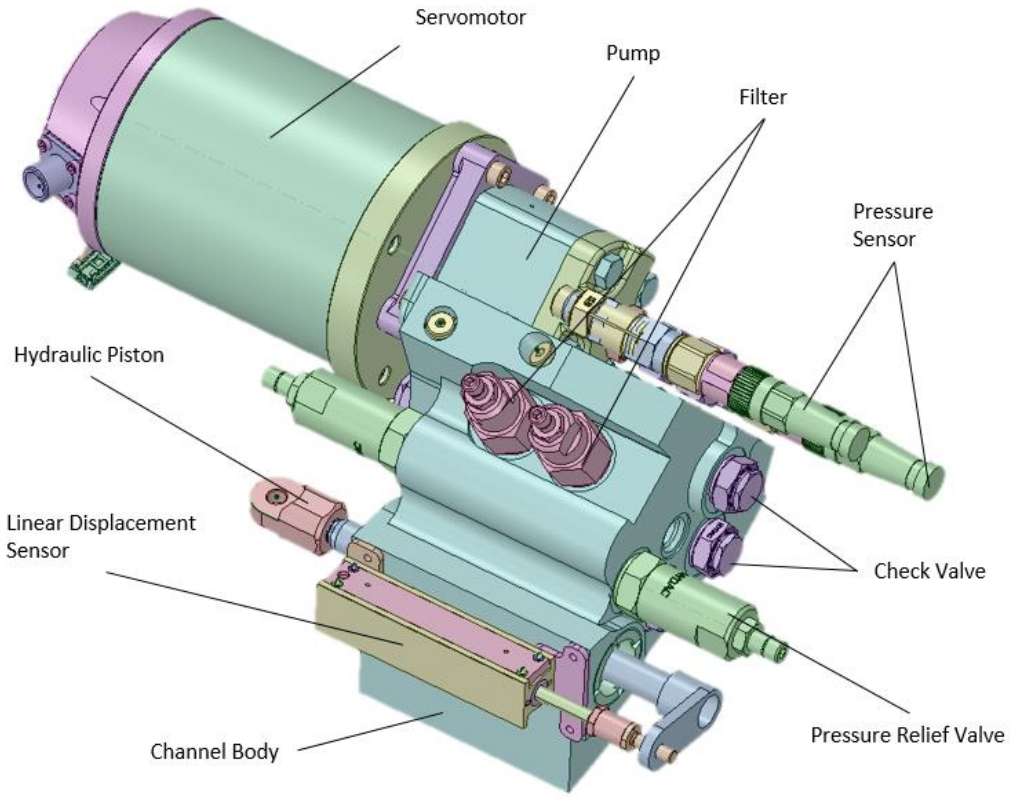

Figure 42: Solid Model of the EHA

3.5 Electrical Design of EHA

In electrical design section, components of the electrical system such as the motor drive, sensors, real time controller and data acquisition system are given in detail.

The electric motor is supplied from a domestic electric motor producer and the drive amplifier is taken from Unitek GmbH in Figure 43. The driver named Bamobil-D3 receives 56 VDC with nominal 40 Amperes and converts it into Pulse-Width Modulated (PWM) signal to drive the electric motor. Speed or torque control of the electric motor can be selected and ±10 V analog signal is utilized for control input signal. It is capable to work on four quadrants which mean that it can be used to drive or brake in both directions and made energy recuperation to the power supply. The set values of the servo drive's performance parameters; control mode, input and output type can be reached and adjusted by connection interface of RS232 and CAN bus via software on the computer [21].

There are five pressure sensors in the EHA system to monitor the system status, and emergency stop of the test software, to be used in identification process of unknown system parameters. The pressure sensor chosen is Trafag AG NAT 8252 and it has a Wheatstone bridge of thin film strain gauges on a stainless diagram for pressure sensing. As the diagram displaced, it causes voltage change in electrical circuit of in the sensor. The difference is outputted as current which proportional to the pressure [22].

As seen from Figure 44, two of the pressure sensors are located in each pressure chamber of the hydraulic cylinder; two of them are connected to inlet and outlet of the pump. The last one is at connection of low pressure inner hydraulic circuit, at the outlet of the accumulator. There are two types of pressure sensor used in the EHA with respect to the measurement ranges. One of them is for measuring low pressure and the other one is for high pressures. Pressure sensors with red

highlight indicate 0-250 bar high pressure range sensors in the figure. The blue highlighted pressure sensor is for sensing the 0-10 bar low pressure range.

Figure 43 : The Servo Drive Amplifier [21]

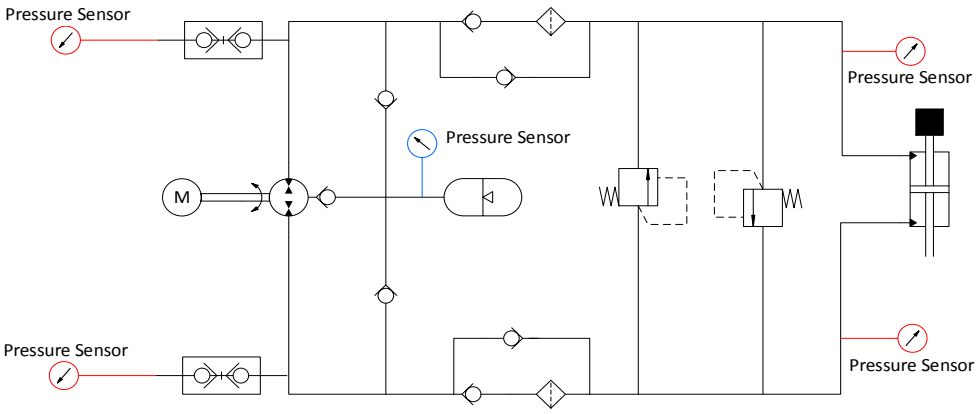

Figure 44: The Locations of the Pressure Sensors

The pressure sensors seen in Figure 45 have following specifications:

- Measuring Range: 0-10 bar and 0-250 bar
- Over Pressure: 48 bar (for 0-10 bar) and 750 bar (for 0-250 bar)

- Accuracy: 0.5 % FS
- Output Signal: 4-20 mA
- Supply Voltage: 24 (9-32) VDC
- Rise Time: 1 ms (5 %-90 %)

Figure 45: The Pressure Sensor [22]

For position measurement of the hydraulic cylinder, a Linear Variable Displacement Transducer (LVDT) is used. It is basically composed of core and coil assembly. When the core is displaced axially within the coil, it produces a voltage change in output which is directly proportional to displacement. The LVDT chosen is TransTek Incorporated 0244-0000Q that is shown in Figure 46 [36].

Figure 46: The Linear Variable Displacement Transducer [36]

The LVDT specifications are as follows [36]:

- Working Range: 25.4 mm
- Max. Usable Range: 38.1 mm
- Non-Linearity: 0.5 % FS
- % Ripple, RMS (nominal): 0.8
- Supply Voltage: 24 (6-30) VDC
- Bandwidth: 100 Hz
- Resolution: Infinite

For data acquisition and real time control, National Instruments real-time controller Compact RIO 9066 Chassis and signal input & output modules are used which are shown in Figure 47. The controller computer specifications are as such [23]:

- 667 MHz dual-core ARM Cortex-A9 processor
- 512 MB of nonvolatile memory for data logging
- 256 MB of DDR3 memory for embedded operations
- NI Linux Real-Time Operating System
- Artix-7 Field Programmable Gate Array (FPGA) for embedded control and monitoring applications

Figure 47: National Instruments Compact RIO 9066 Chassis [23]

The I/O modules that are used in measurements are listed as below:

- NI 9239 (±10 V, Simultaneous Analog Input, 50kS/s, 4 Channel Module)
- NI 9264 (±10 V, Analog Output, 25kS/s per channel, 16 Channel Module)
- NI 9485 (24 V, Sourcing Digital Output, 8 Channel Module)
- NI 9218 (Dynamic Universal Simultaneous Analog Input, 51.2kS/s, 24-bit, 2 Channel Module)
- NI 9411 (±5 to 24 V, Differential Digital Input, 6 Channel Module)

NI 9239 module is employed to get ±10 V analog signal of LVDT sensor for position measurement of the hydraulic cylinder. It is a channel to channel isolated module which leads elimination of measurement errors caused by ground loops. Also, it protects the measurement from harmful voltage spikes according to the isolation rating [23].

NI 9264 module is used to send ±10 V analog output to the servomotor driver. According to position error of the hydraulic cylinder, the position controller creates a speed command to the servomotor driver via NI 9264 with ±10 V analog output regarding to ±3000 rpm servomotor speed range.

NI 9485 module is preferred to be used as a switching element to change status of the servomotor between enable and disable. The aim to utilize such a switch in the test setup is to activate the servomotor under control of the test software. It provides that status of the servomotor which can be observed instantaneously and emergency stop conditions are checked to disable the servomotor simultaneously.

NI 9218 is multipurpose measurement module which supports quarter-bridge, half-bridge, 60 V, and ±20 mA current measurements. In the test setup, pressure measurements are obtained by this module.

NI 9411 is used to measure angular velocity of the servomotor. The module reads digital output of the encoder.

The electrical connections between control computer, modules, sensors and power suppliers are given in detail in Appendix A.

3.6 Controller Design of EHA

In this section, to control the position of the hydraulic cylinder, implementation of a basic proportional closed loop controller to the EHA prototype is given.

Control strategy of the EHA prototype is shown in Figure 48. As seen from the figure, a reference position signal is given to the position controller and according to difference between the reference and the measured positions of the hydraulic cylinder; a reference speed command is generated. Next, the reference servomotor speed is generated for the servomotor driver which is named as "Speed Controller" of the DC motor in the figure.

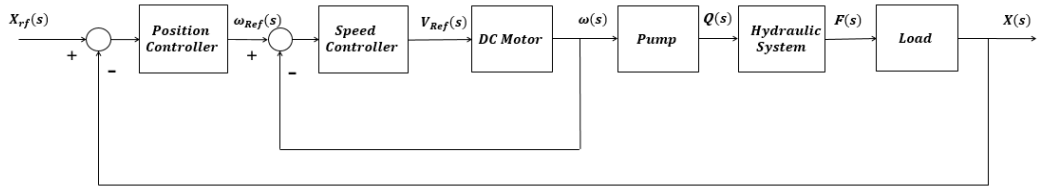

Figure 48: The Control Block Diagram of the System

As mentioned before, position of the cylinder is measured with a LVDT and the measurement is read via isolated channel voltage input module that minimizes the measurement noise. Therefore, the signal received is clean and no filter is needed. Furthermore, this measurement signal is used directly for comparison with the reference signal to generate the error input signal to the position controller.

In Figure 49, sample position measurement without any position reference input is shown. The noise amplitude in the measurement is about in a range of 3 microns which is acceptable when the full scale hydraulic cylinder motion of 40 mm is considered. In addition, the noise harmonics of position signal are investigated and power spectral density of the signal is obtained. It is seen from Figure 49 that the noise density reaches a peak at frequency about 73 Hz. It can be induced due to the servomotor in the system or other high frequency electronic components in the surroundings.

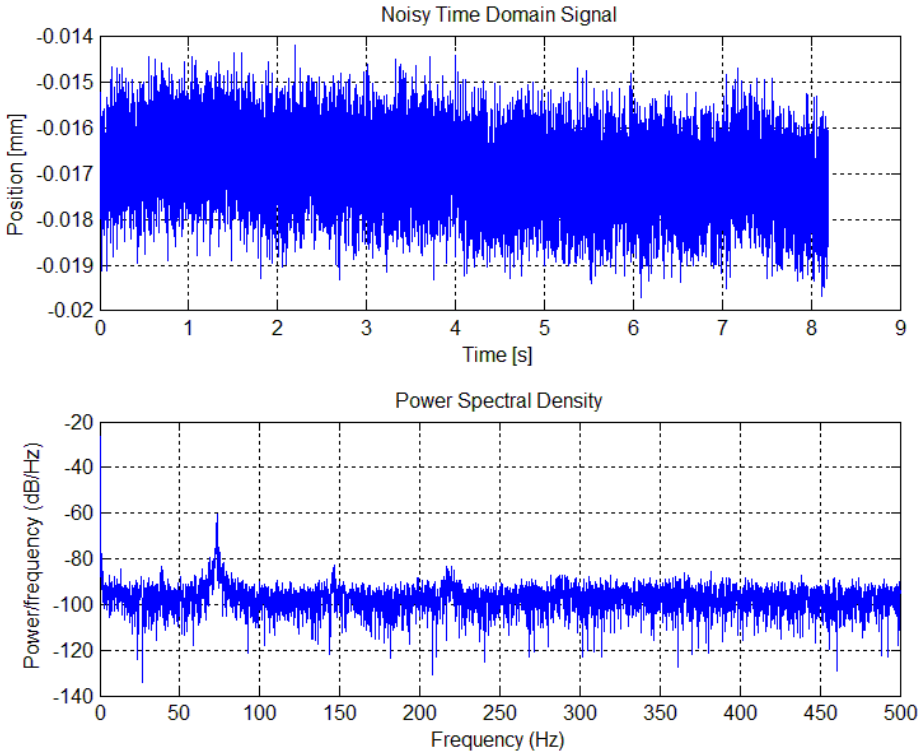

Figure 49: Position Signal in Time Domain and Power Spectral Density

To design the controller, MATLAB Simulink® Design Optimization Toolbox is utilized. The closed loop Simulink® model of the EHA is shown in Figure 50. Proportional gain of the position controller in the model is optimized by using

sub-toolbox of Simulink® Design Optimization which is called Response Optimization. The design requirements in time and frequency domains are input to the software and by considering response constrains, it solves an optimization problem.

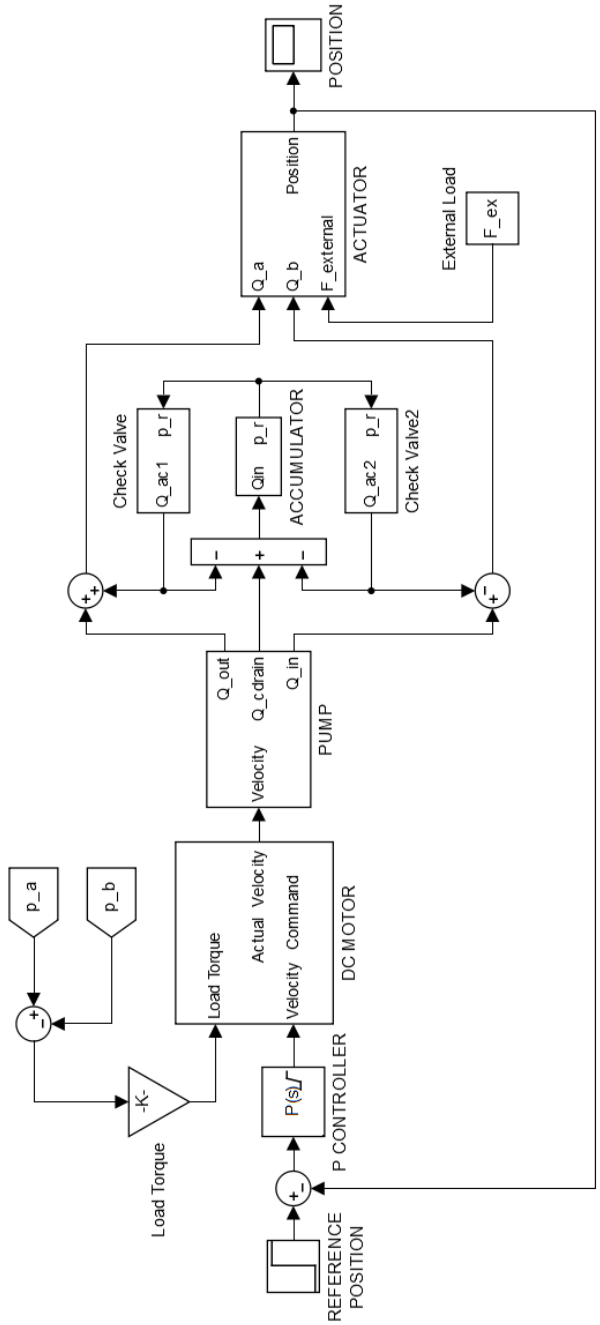

Figure 50: Simulink® Model of the Closed Loop Overall System

In Section 3.1, desired step response and frequency response characteristics are defined in Table 3. These desired characteristics are inputs to the software to specify the acceptance region of responses that are shown for time response in Figure 51 and for frequency response in Figure 52.

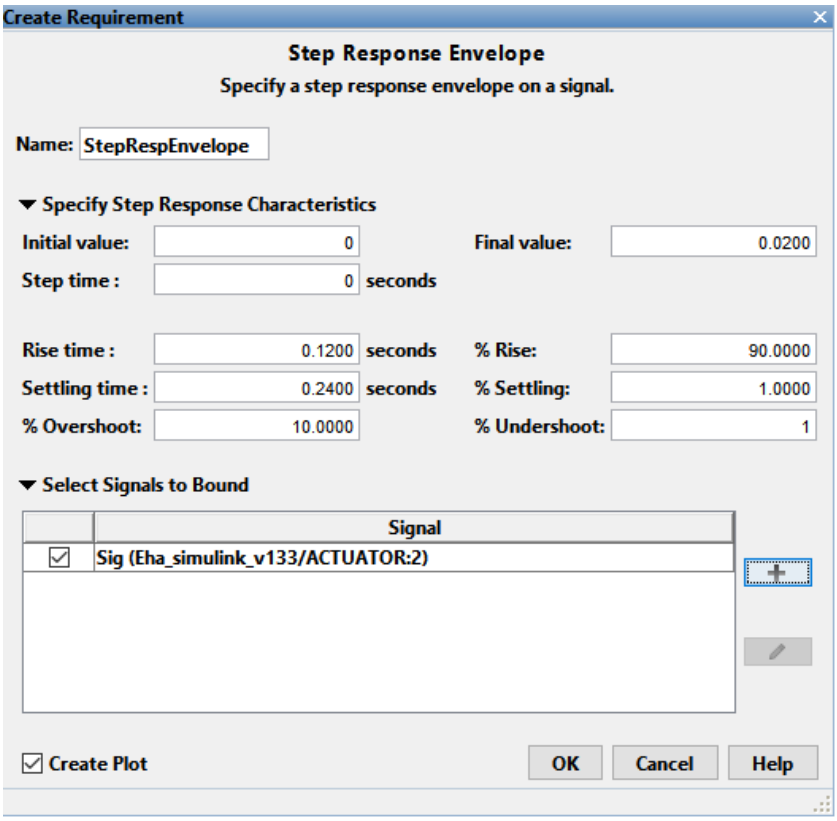

Figure 51: The Desired Time Response Characteristics

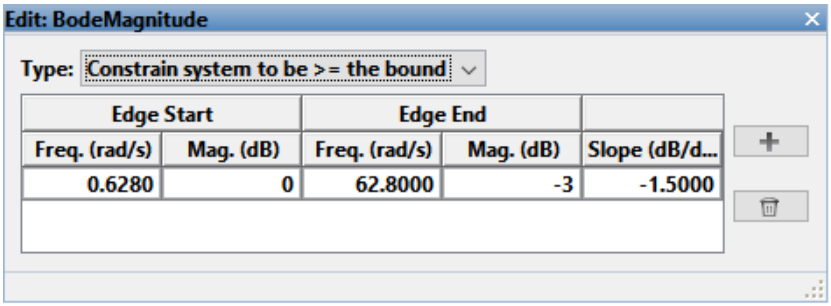

Figure 52: The Desired Frequency Response Characteristics

To shorten the optimization process, lower bound of the proportional gain is defined as 10000 rad/s/m and any upper bound is not defined. At the end of optimization, the proportional controller gain is found as 18705 rad/s/m and 45312 rad/s/m to satisfy the desired time and desired frequency responses which are shown in Figure 53 and Figure 54, respectively.

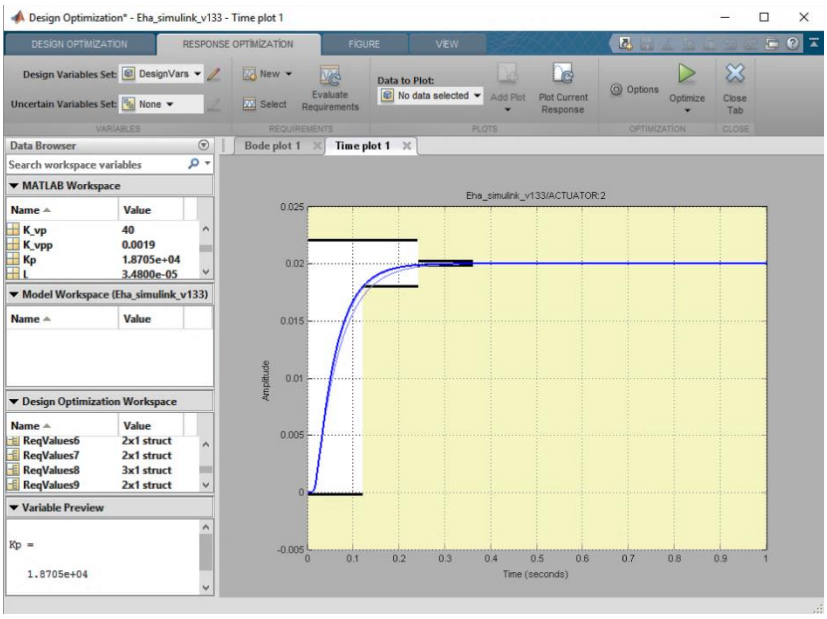

Figure 53: Response Optimization Results in Time Domain

Due to fact that the gain found in time response optimization is not sufficient to fulfill the frequency domain requirements, gain of the proportional controller is chosen as 45312 rad/s/m. After that, it is checked whether the time response characteristics are satisfied with this gain or not. As shown in Figure 55, the response makes an overshoot of amplitude 0.005 mm approximately. However, it is in the region enclosed with constrains defined by the time response characteristics. Thus, it is reasonable to select the proportional gain of the position controller as,

$$K_p = 45312 \frac{rad/s}{m}$$

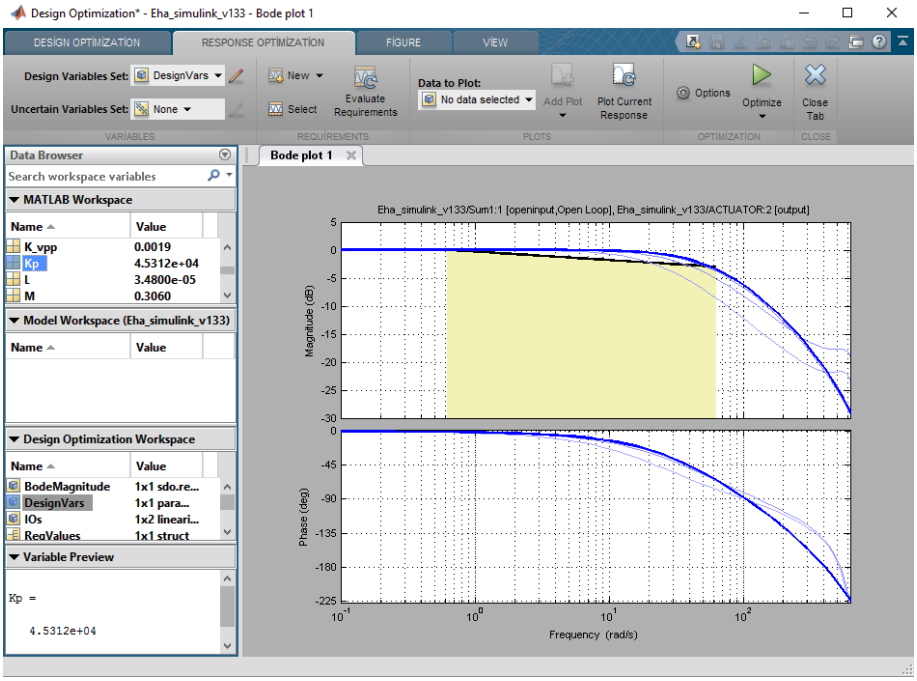

Figure 54: Response Optimization Result in Frequency Domain

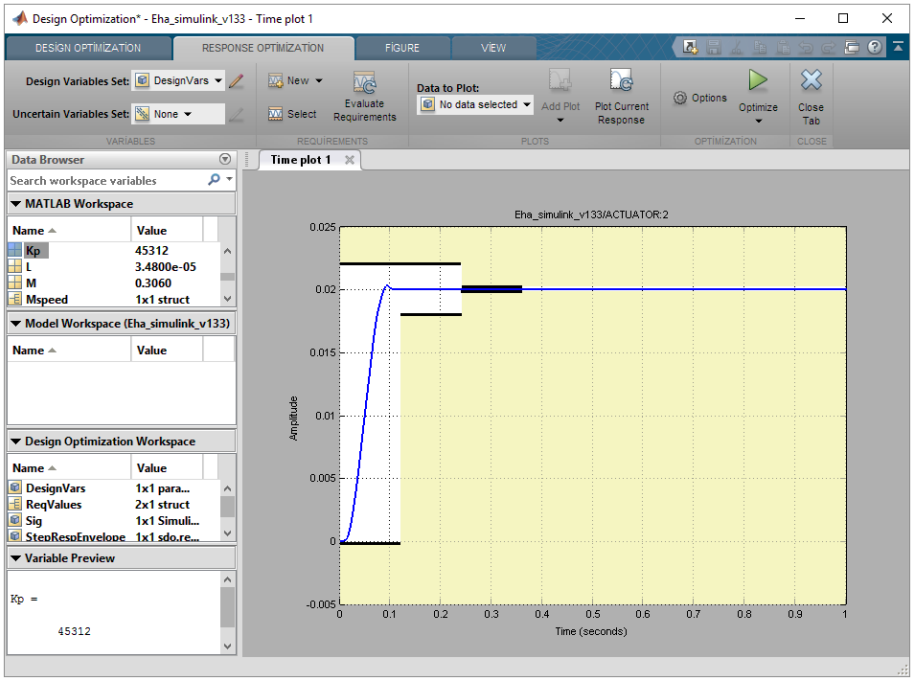

Figure 55: Time Response Result with the Chosen Proportional Controller

To observe the performance of the controller against a disturbance, a disturbing force is applied to the actuator in the model and the corresponding hydraulic cylinder position with respect to time is shown in Figure 56. The disturbance is applied as a ±200 N amplitude chirp signal that changes from 0.1 Hz to 30 Hz within 60 seconds. Under effect of this disturbance, the position error is still within the limits defined previously.

In Figure 57, the frequency response for disturbance rejection of the actuator in position control is shown. It can be concluded that since the overall gear ratio is very high, the controller can reject to disturbance loads successfully.

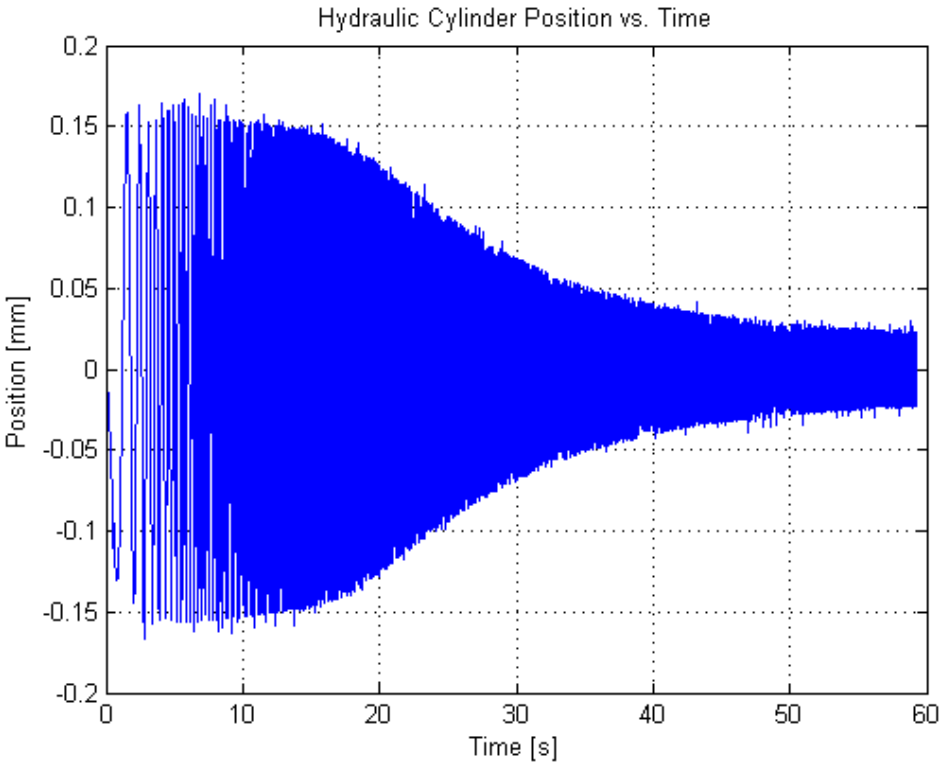

Figure 56: Hydraulic Cylinder Position vs. Time

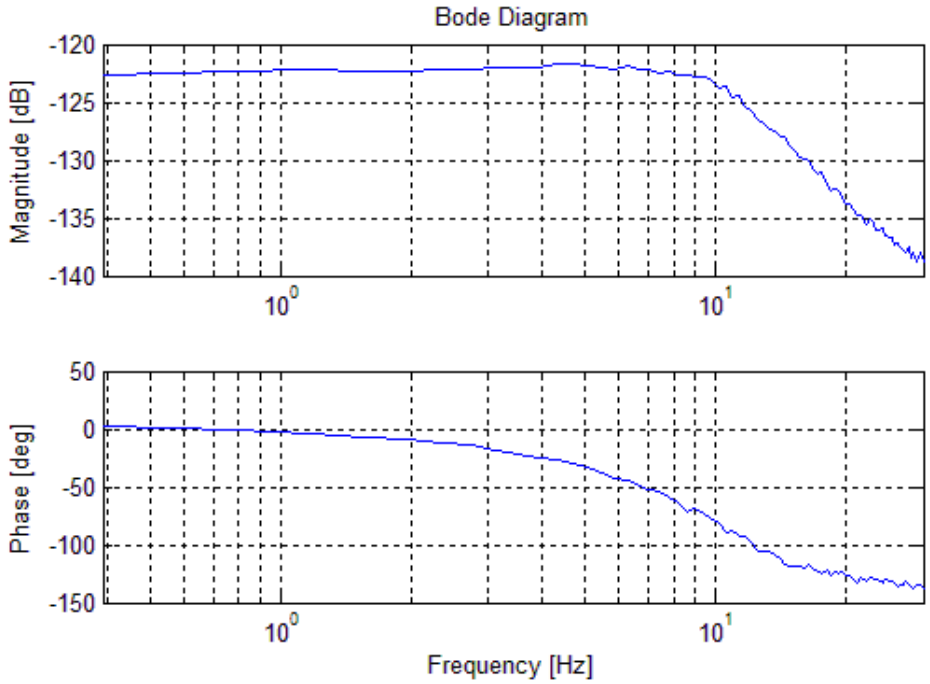

Figure 57: Frequency Response for Disturbance Rejection

CHAPTER 4

PERFORMANCE TESTS OF EHA SYSTEM

4.1 System Identification Tests

In this part of the study, tests conducted to identify the unknown system parameters used in mathematical model are explained. Hydraulic cylinder friction force, pump leakage coefficients and servomotor characteristics are the parameters investigated in this study.

4.1.1 Hydraulic Cylinder Friction

In this sub-section, the friction force in the hydraulic cylinder is measured. As mentioned in Section 3.3.2, two types of friction force are assumed for the hydraulic cylinder. These are static friction and viscous friction.

As the friction force is naturally very non-linear, it changes with altering physical conditions of the surroundings. The microstructural contacts between the cylinder bore and the piston seals lead different elastic deformations at each motion. Also, while the piston travels with different speeds, the lubricating film thickness may vary which leads different friction forces at different cylinder velocities. Moreover, even location of the piston in the cylinder can cause unalike friction behavior, because of machining tolerances of the cylinder bore and the piston.

Owing to being random process, the friction force is investigated with different processes in which they are dominant and significant. To derive static friction

force, step voltage inputs at different amplitudes are applied to the servomotor. In other words, step speed commands with different amplitudes are given to the servomotor. The maximum peak pressure of the measurement at which the hydraulic cylinder has zero velocity is taken and assumed as the static friction. The input signal amplitudes are between 1-10 V which covers all of amplitude range and corresponds to the actuator velocity between 0.034 m/s – 0.346 m/s. Furthermore, the tests are performed for both directions of the hydraulic cylinder motion.

The results of tests are illustrated at Figure 58 and Figure 59 with respect to the direction of the cylinder motion. It can be realized that the static friction does not increase with increasing velocity magnitude as expected. The average friction value for forward direction of the hydraulic cylinder motion is 14.9 N with a standard deviation of 4.8 N. The average friction value for the reverse direction of the hydraulic cylinder motion is 39.6 N with a standard deviation of 10.6 N. For this research, the static friction force (F_{bk}) in Eq. (3.7) is assumed regarding the mean value of the measurements as,

$$F_{bk} = 39.6\ N$$

To derive the viscous friction coefficient of the hydraulic cylinder, a low frequency chirp signal for closed loop position control system is applied and friction force is calculated according to Eq. (4.1). During the test, pressures of the cylinder chambers are measured and low frequency is chosen to reduce inertial effects of the cylinder in the pressure values. The accelerations of the cylinder piston are obtained from the MATLAB Simulink® model of the system.

$$F_{friction} = (p_a - p_b)A - m\ddot{x} \tag{4.1}$$

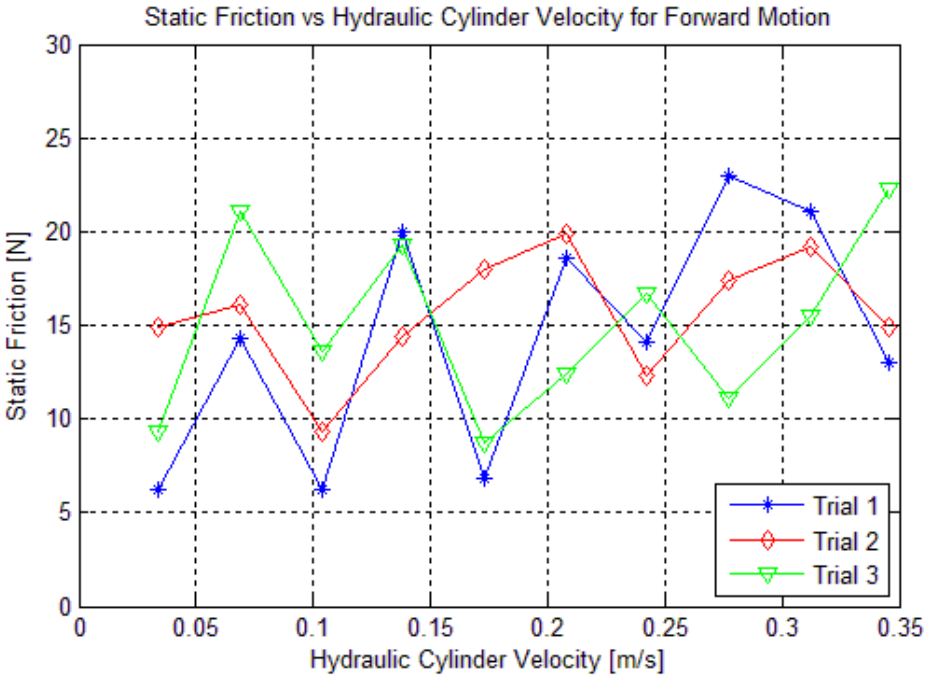

Figure 58 : Static Friction vs. Cylinder Velocity for Forward Motion

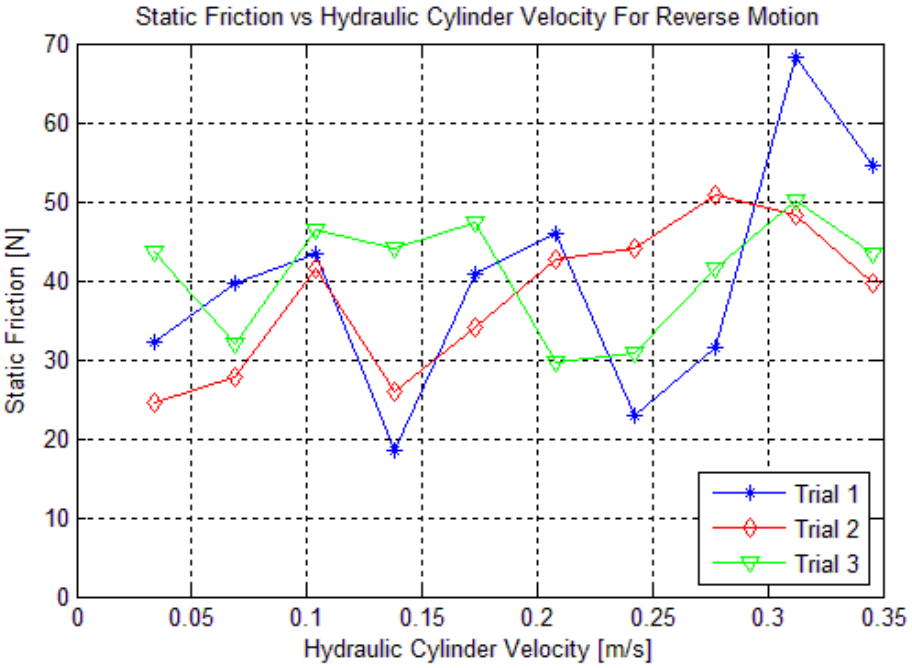

Figure 59 : Static Friction vs. Cylinder Velocity for Reverse Motion

A chirp signal which is an increasing frequency sinusoidal signal is used with magnitude of ±5 mm between 0.1 Hz and 10 Hz for the test. The frequency of the signal increases by the test duration that is 40 seconds. The variation of cylinder piston position with respect to time during the test is shown in Figure 60.

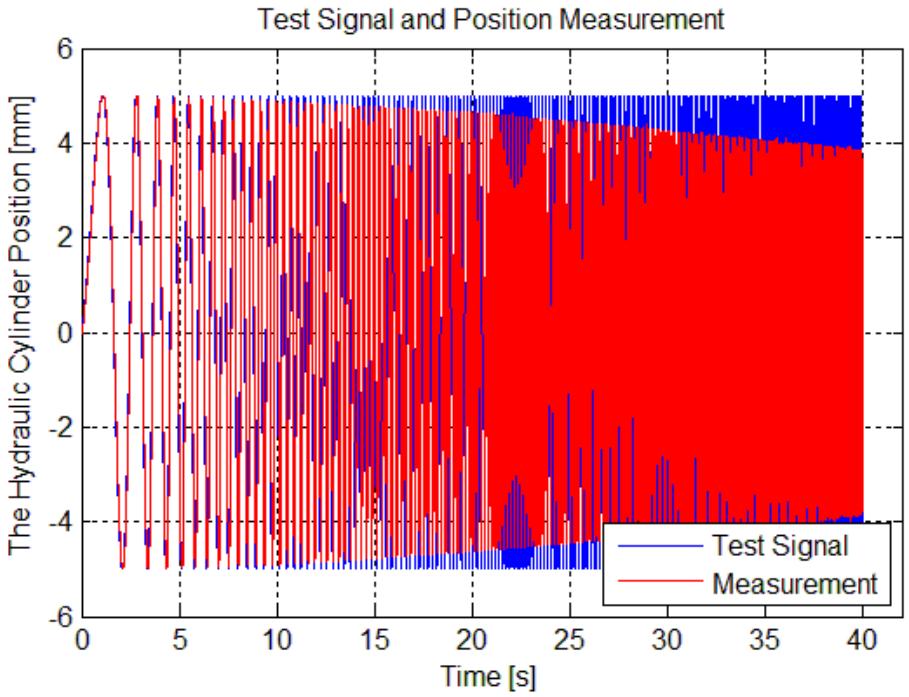

Figure 60: Friction Test Signal & Measurement

To determine effects of the inertial forces, the mathematical model is used. From simulated test conditions, acceleration data of the cylinder is obtained and plotted as shown in Figure 61. If amplitude of the inertial forces is compared with the friction forces, it can be concluded that inertial forces are not significant.

Friction force is calculated according to Eq. (4.1) versus the cylinder velocity is shown in Figure 62. While different cylinder velocities lead different friction forces, the overall result gives such a data distribution. The velocities close to zero are assumed to be static friction and ignored in evaluation. Also, in the static

friction test, it was realized that friction force is different regarding direction of the cylinder motion. The same trend can be realized from the figure.

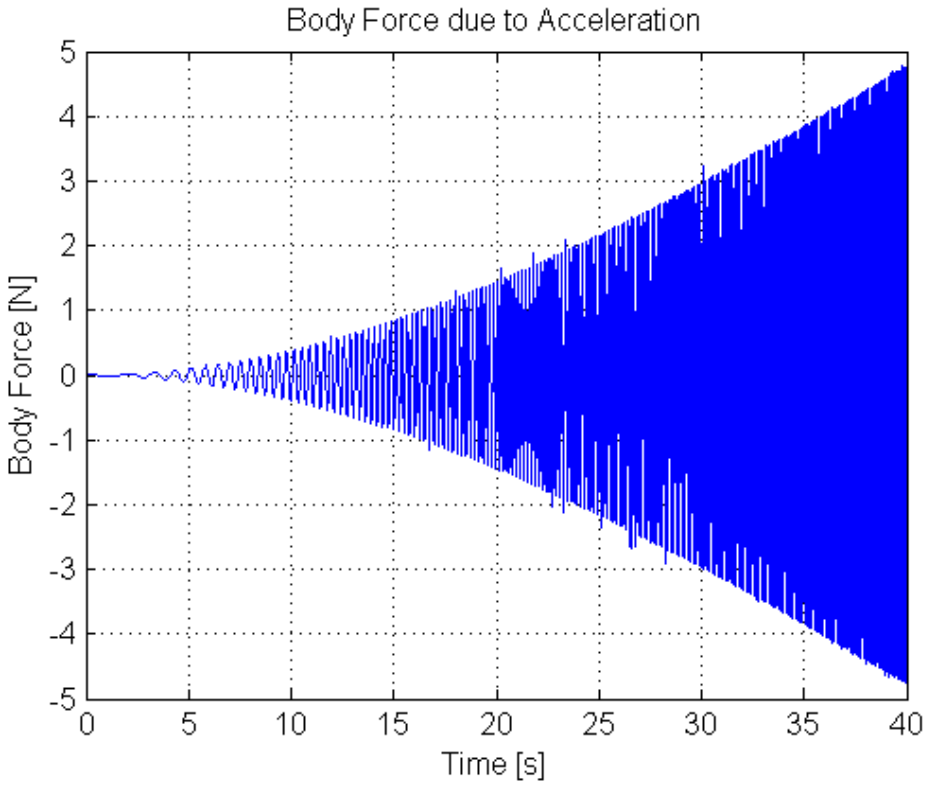

Figure 61: Inertial Force Due To the Acceleration

While it is hard to estimate the values of the viscous friction coefficient from Figure 62, the data is separated to 18 sub-groups of velocities. The average values of these sub-groups are calculated as shown in Figure 63. Afterwards, red curves are drawn from the average values of sub-groups as shown in Figure 62.

If the slopes between two consecutive points in Figure 63 are considered, the viscous friction coefficient of the hydraulic cylinder for forward and reverse motion can be determined as,

$$K_{vp} = 40\ N.s/m$$

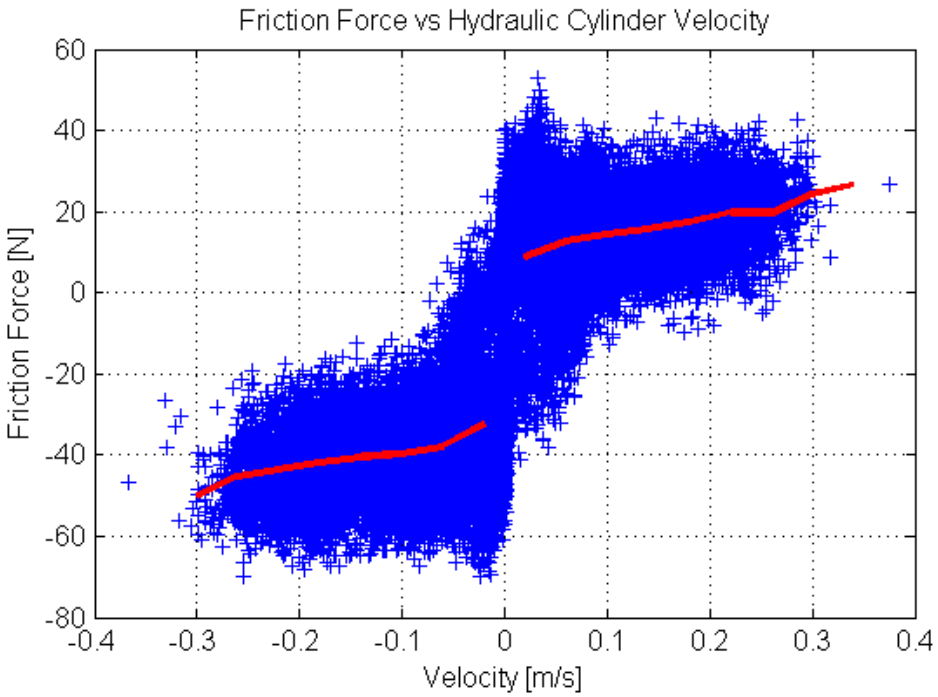

Figure 62 : Friction Force vs. Cylinder Velocity

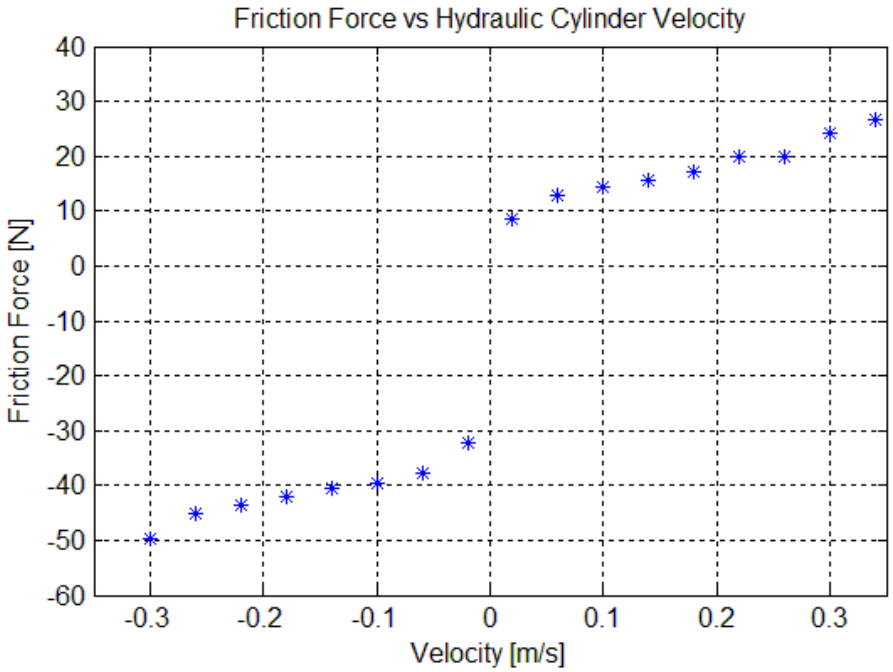

Figure 63 : Average Friction Force vs. Cylinder Velocity

According to the static friction values found at the beginning of this section; as the cylinder starts motion, the friction force decreases which is described as Coulomb friction in the literature and then increases with increasing velocity. The results of the system friction characteristics are consistent with complex friction models described in the literature with static, Coulomb and viscous friction.

4.1.2 Pump Performance Characterization Tests

As introduced in Section 3.3, the pump used in the prototype is an external gear pump from Parker Hannifin Corporation. Its performance data is given in Appendix B. From the data given, it can be seen that for rotation speeds slower than 500 rpm, there is no information for flow rates of the pump for varying pressure difference between pump inlet and outlet ports. The aim of this section is to find internal and external leakage coefficients of the pump with respect to altering conditions of pressure difference across the pump and rotation speed.

Another interest to characterize the pump performance is that, there is a range of speed under a specific load pressure called as “dead band” in the literature at which pump has zero displacement due to leakages occurring in the pump. The no-flow region is detected in order to estimate the lowest necessary electric motor speed gain in order to pass this region in small duration of time for closed loop control of the system.

The pump is tested alone with a test setup whose details are given in the following section. Afterwards, the tests performed below are explained:

- Constant pressure - variable pump speed test
- Variable pressure - constant pump speed test

4.1.2.1 Test Setup of the Pump

The test setup for pump tests is shown in Figure 64.

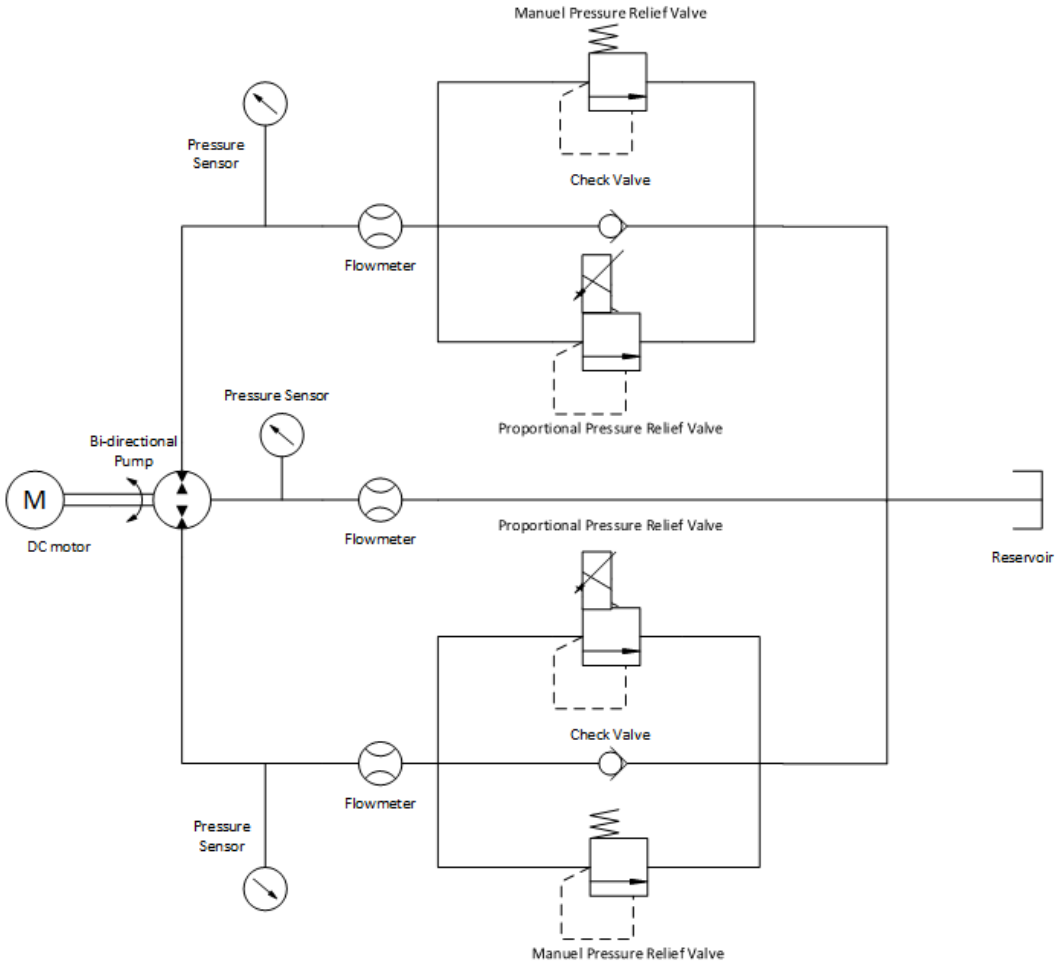

Figure 64: Hydraulic Circuit of the Pump Test Setup

The pump is actuated with a speed controlled electric motor. Speed feedback corresponding to the pump rotation is obtained from an encoder embedded in the electric motor. Because of the pump is bi-directional, characterization tests are performed in both directions. Also, the hydraulic circuit is designed in symmetric manner to have the same test conditions in each direction. A proportional pressure relief valve is utilized in order to change pressure at the outlet of the pump and a manual relief valve is used for safety reasons such as unexpected sticking in valves, sudden pressure increase and failure of proportional pressure relief valve. A check valve is used between the reservoir and the pump suction port for proper

suction of the pump. To circulate the fluid and eliminate pump cavitation, a pressurized reservoir is integrated to the system. The pump case drain line is also connected to the reservoir to return external leakage occurred in the pump to the system.

Two pressure sensors are attached at inlet and outlet of the pump to measure pressure difference across the pump and a pressure sensor is used for case drain line to measure pressure at the drain line. Three flow meters are used in the test setup, one at inlet, one at outlet of the pump and the remaining one for measuring the case drain flow.

A photograph of the pump characterization test setup constructed is shown in Figure 65. A valve block is manufactured for mounting of valves and pressure sensors used in the test. Detailed information of the pump test setup is given in Appendix B.

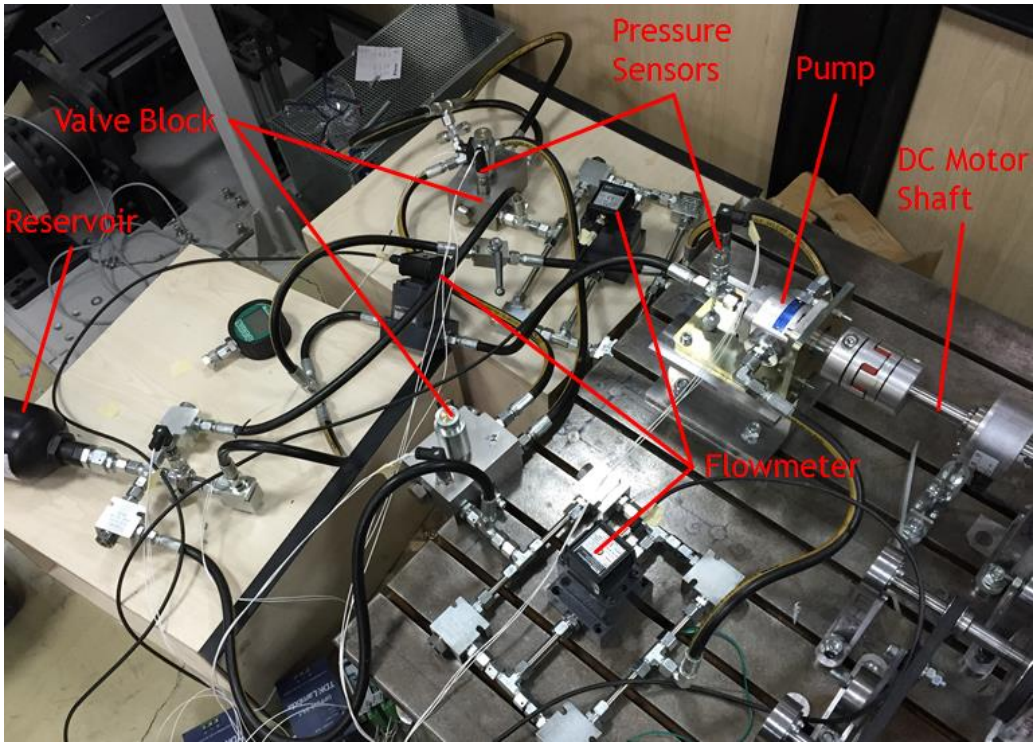

Figure 65: Pump Characterization Test Setup

4.1.2.2 Constant Pressure - Variable Pump Speed Test

Pump inlet and outlet flow rates are defined in Section 3.3.1 with Eq. (3.3) and (3.4), respectively. According to these equations, output flow of the pump is basically theoretical flow of the pump minus external and internal leakage flows. Therefore, if the pump rotation speed, pressure differences between pump ports and flow rates at output and drainage are measured, there are only unknown parameters of the internal leakage and external leakage coefficients.

In this test, the pump is kept under a specific pressure difference between its ports and its performance is evaluated with changing rotation speed. The test results which are conducted at different pressures are given in Appendix B.

To apply such a test scenario, the proportional pressure relief valve at the outlet of the pump is energized and set to a pressure relief value. Afterwards, the electric motor speed is increased with time as a ramp signal which saturates at 3000 rpm. In Figure 66, speed of the electric motor is shown for test duration of 95 seconds. The test data acquisition is performed with 1000 Hz sampling rate and averaged at every 100 data interval.

The pressure difference is set to 115 bar between the pump inlet and outlet ports and with given speed signal, the flow rate is measured as shown in Figure 67. Since there are two flow rate values for one speed value, average value of these two flow rates is calculated. The red line shows theoretical flow rate defined as multiplication of the pump displacement and its speed. In addition, the blue line represents measured flow rate regarding to the pump speed range. The deviation of measured flow rate from theoretical flow rate gives internal and external leakages occurred. The external leakage is measured directly and shown in Figure 68.

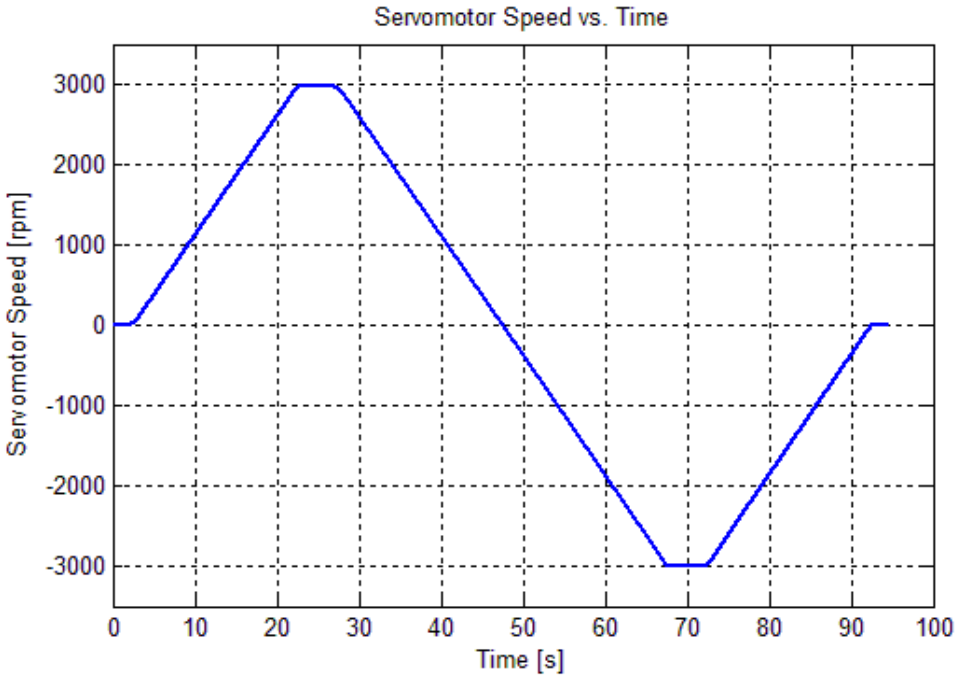

Figure 66 : The Electric Motor Speed Profile at the Test

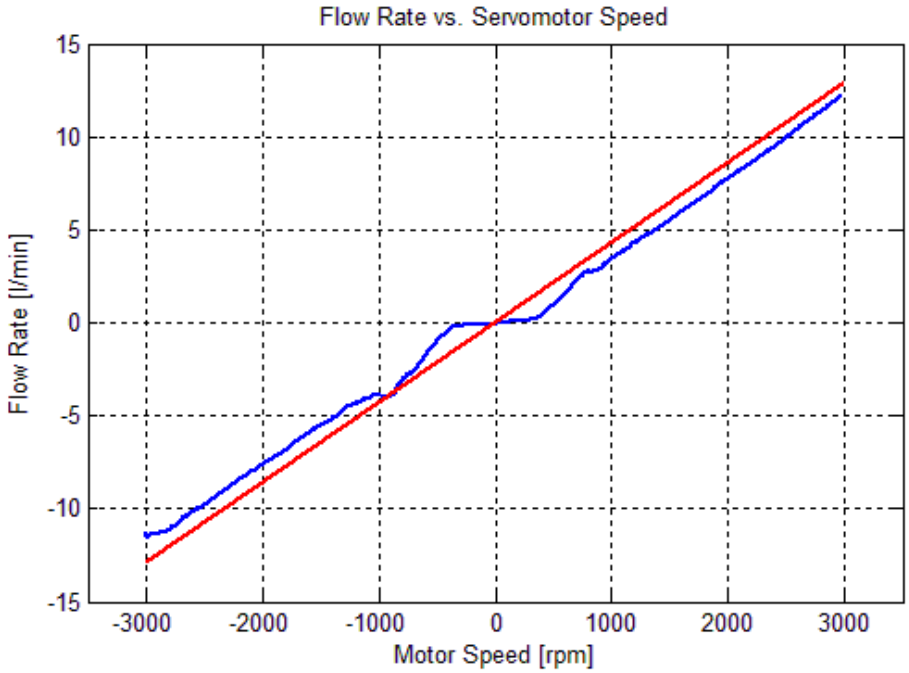

Figure 67: Flow Rate vs. Motor Speed

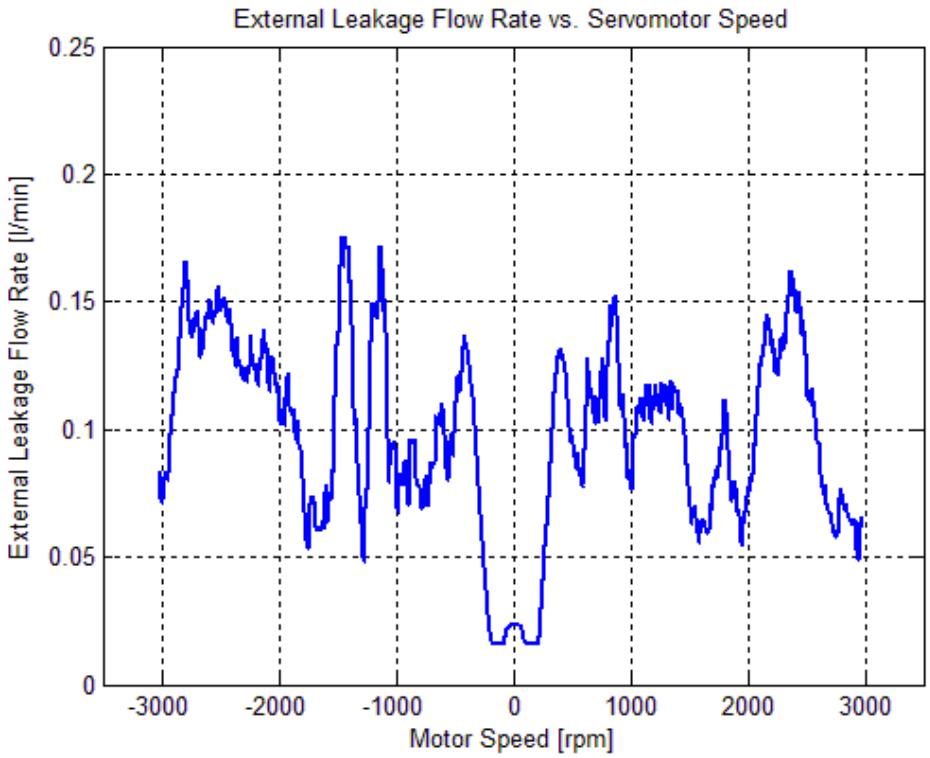

Figure 68: External Leak Flow Rate vs. Motor Speed

The internal leakage coefficient of the pump is calculated by using Eq. (4.2). However, for low velocities since the flow is not reached steady state, the pressure difference between the pump ports is very small and the internal leakage coefficient converges to a value that no flow is supplied by pump analytically.

$$K_{ilp} = \frac{D\omega_p - Q_{out} - Q_{external\_leakage}}{(p_1 - p_2)} \tag{4.2}$$

In Figure 69, variation of the internal leakage coefficient of the pump with respect to electric motor speed is shown. Between 0-500 rpm the internal leakage coefficient increases drastically while it gets closer to the region called “dead

band". It can be observed from Figure 67 that, the no flow region which is about ±250 rpm speed range.

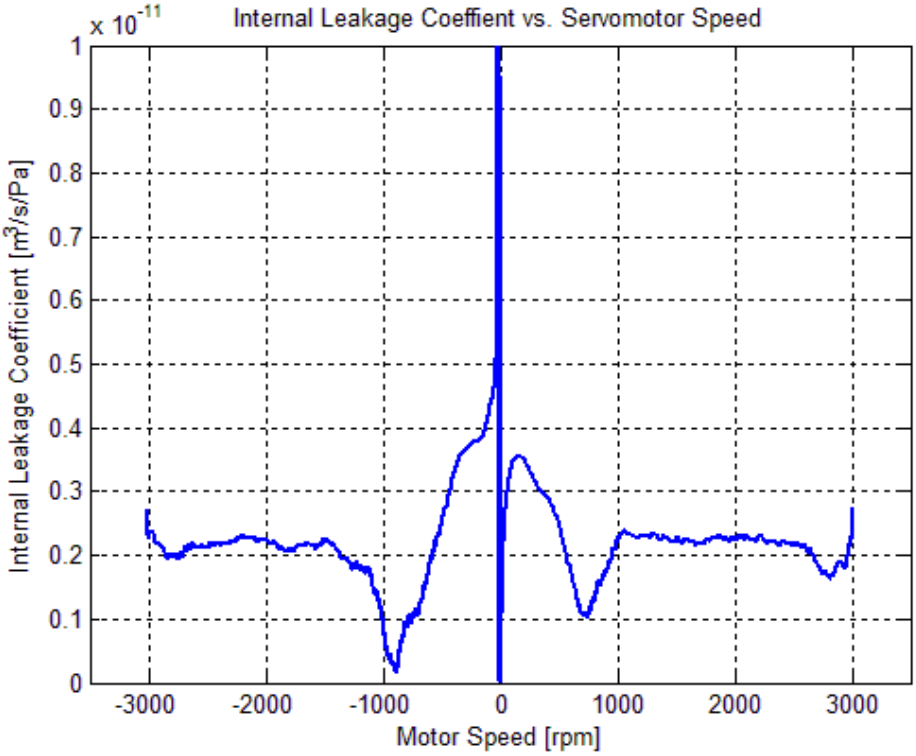

Figure 69: Internal Leakage Coefficient vs. Motor Speed

The external leakage coefficient of the pump is derived as given in Eq. (4.3). The external flow rate, pressure difference between pump ports and drain line are measured directly and the external leakage coefficient variation with respect to the motor speed is shown in Figure 70. Comparing with the internal leakage, the external leakage coefficient is much smaller. Moreover, it can be said that, external leakage is less sensitive to rotation speed of the pump.

$$K_{elp} = \frac{Q_{external\_leakage}}{(p_1 - p_{cdr}) + (p_2 - p_{cdr})} \tag{4.3}$$

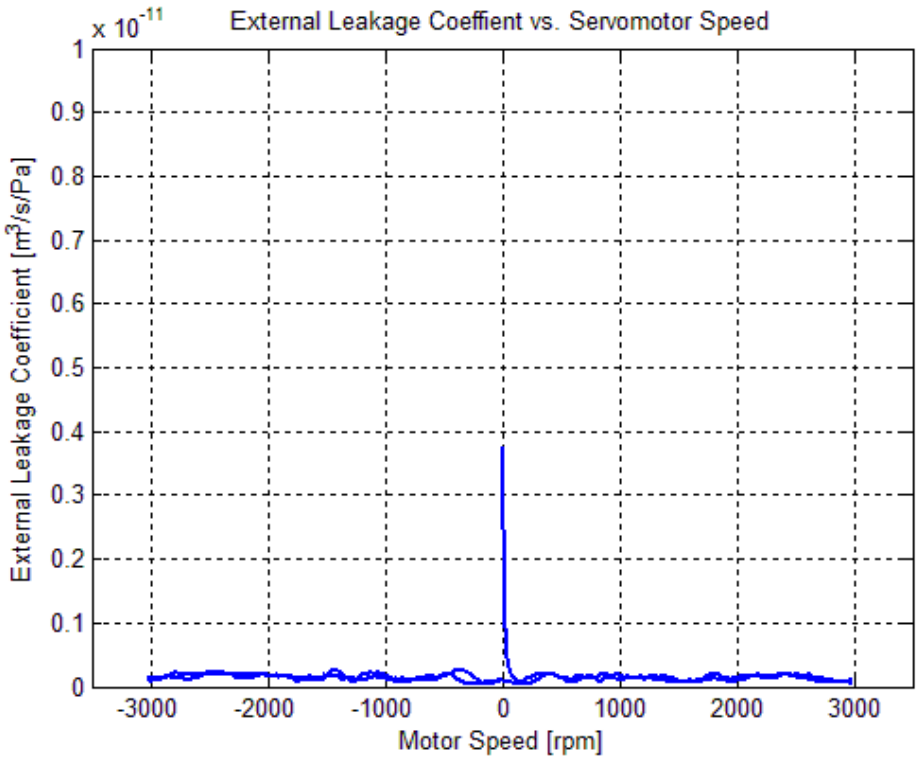

Figure 70 : External Leakage Coefficient vs. Motor Speed

As seen in Figure 71, the proportional pressure relief valves do not successfully keep the test pressure at the desired level while the flow rate increases. Also, there is difference between pressure levels of the set load pressure of the pump. Two identical proportional pressure relief valves are used for each direction of the pump rotation. However, they do not reach at the same load pressure level as shown in Figure 71 . It can be explained by manufacturing tolerances in the proportional relief valve. The same input signal leads different pressure set point which may be null shift or inadequate calibration of the valve driver cards.

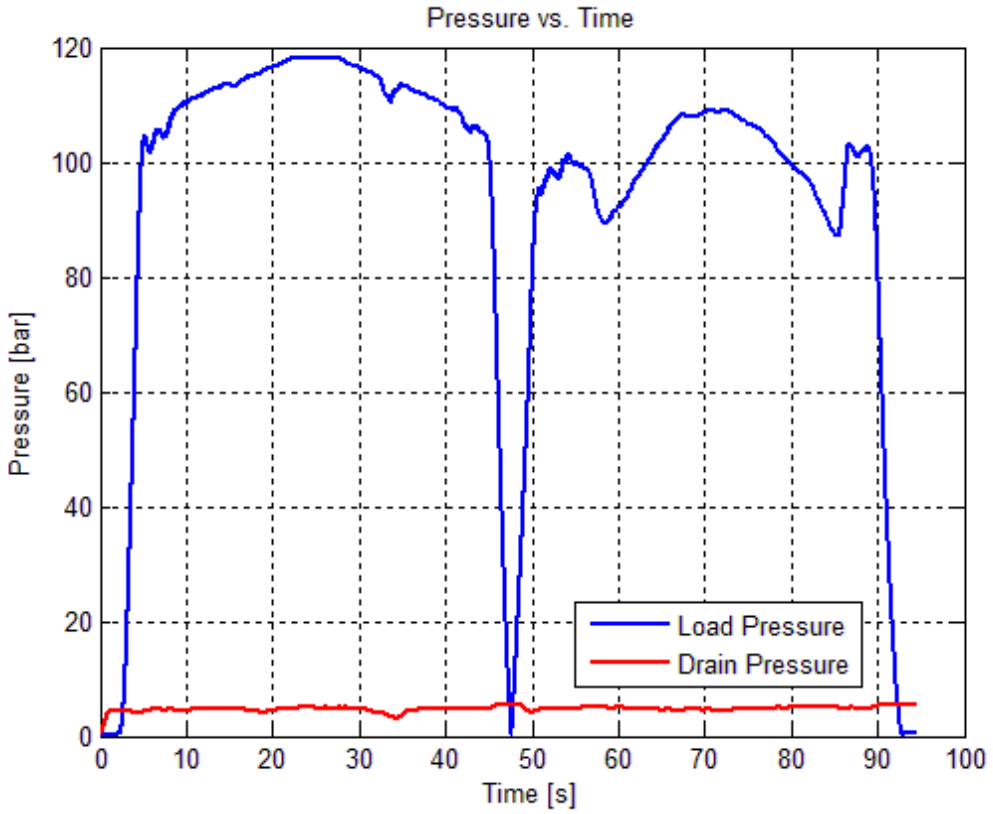

Figure 71 : Pressure Difference at the Pump Ports vs. Time

4.1.2.3 Variable Pressure - Constant Pump Speed Test

In this test, the pump is rotated at 3000 rpm which is the maximum constant speed of the EHA system and the proportional pressure relief valve is energized with a ramp signal up to a peak pressure of 200 bar. Therefore, the extreme performance points which can be experienced in the EHA duty cycle is tested by the pump itself.

To apply this test scenario, the electric motor is kept at a constant speed; meanwhile, a trapezoidal signal is applied to the proportional relief valve. The pump outlet is loaded in this manner. Pressures at the pump inlet, outlet and case drain are shown at Figure 72.

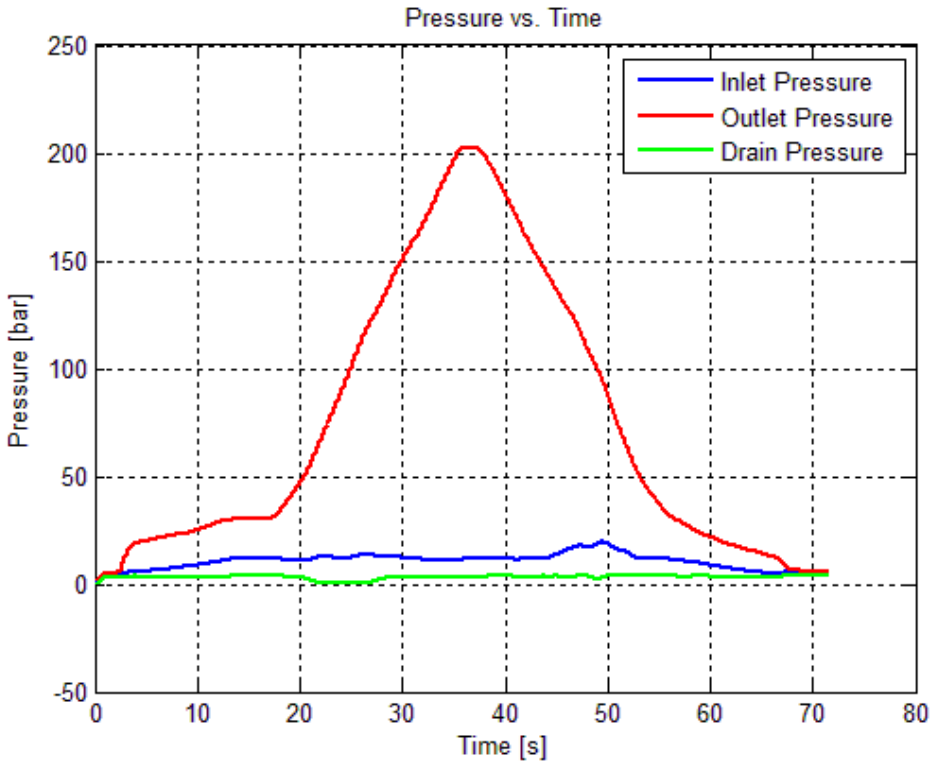

Figure 72 : Pressure at Pump Ports vs. Time

In Figure 73, the flow rate change with varying outlet pressure is shown. The flow rates which are illustrated with blue and green colors are named according to direction of rotation, clockwise (CW) or counter-clockwise (CCW). In the manufacturer's catalog, it is given that this test is performed with 4000 rpm and 1500 rpm. The flow rate result for 3000 rpm is scaled from these catalog test results. Furthermore, since the pump is bi-directional, flow rates with different load pressures are very close to each other. Also, it is realized that the catalog results are very close to the results of the tests carried out. There is about 1.4% deviation between the catalog and the test results.

In Figure 74, the external leakage coefficient with changing load pressure is shown. The coefficients are calculated by Eq. (4.3). It can be realized that the

results do not change with varying load pressure. Moreover, the constant pressure – variable speed test results in Section 4.1.2.2 has similar amplitude of external leakage coefficient as seen in Figure 70. Therefore, change in rotation speed and load pressure does not change the coefficient significantly. Thus, it can be assumed as a constant. The mean value of the external leakage coefficient is assumed as,

$$K_{elp} = 2.5\ x\ 10^{-13}\ m^3/s/Pa$$

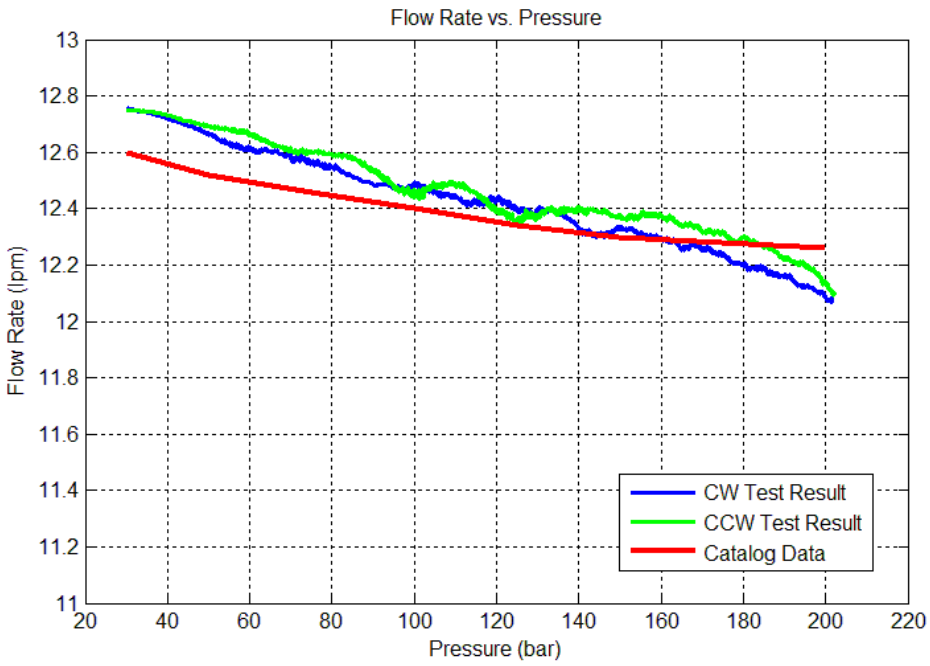

Figure 73 : Flow Rate vs. Pressure

The internal leakage coefficient is calculated by using Eq. (4.2). In Figure 75, the internal leakage coefficient results are illustrated with respect to pressure change at the pump outlet. It can be observed from the figure that the internal leakage coefficient is not affected from pressure change considerably as occurred in pump rotation speed change as shown in Figure 69. However, there is a constant rise in

the internal leakage coefficient up to 80 bar and it is comparatively small in the low pressure region.

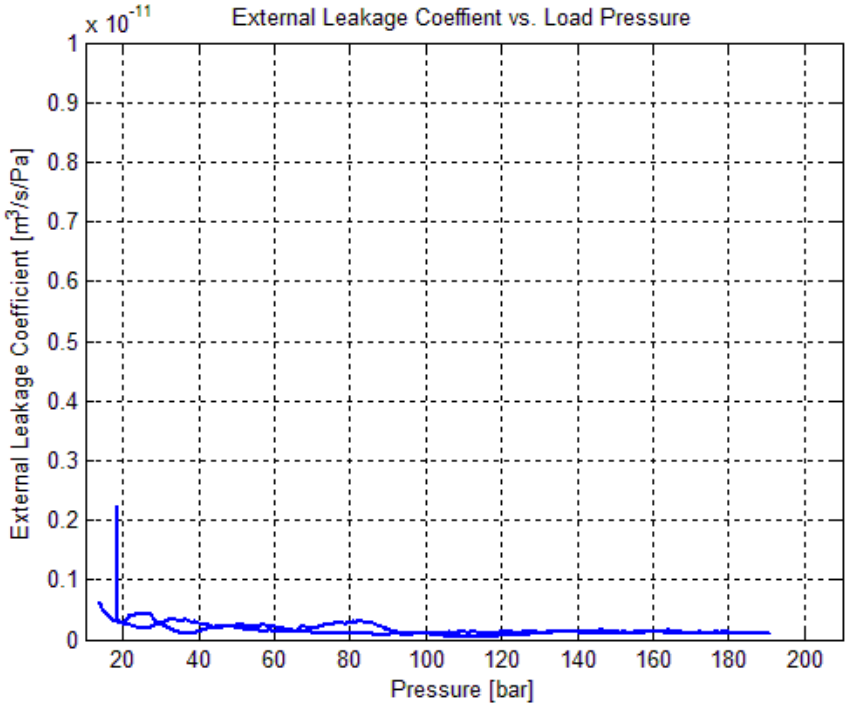

Figure 74: External Leakage Coefficient vs. Load Pressure

It is observed that pump rotation speed with load pressure change affects the internal leakage directly. A look-up table is created whose inputs are pump rotation speed and pressure difference between pump output and input ports. It is embedded in the MATLAB Simulink® Model of the EHA as Look-Up (2-D) Table Block. The block keeps two dimensional information of speed and load pressure at specific values called as breakpoints. Besides, it maps the internal leakage coefficients as output values between the breakpoints with a method of interpolation. The internal leakage coefficient results found in the tests are given in Table 7. In the table, the rotation speed breakpoints are illustrated in the rows with the unit of rad/s and the load pressure breakpoints are shown in columns with the unit of Pa.

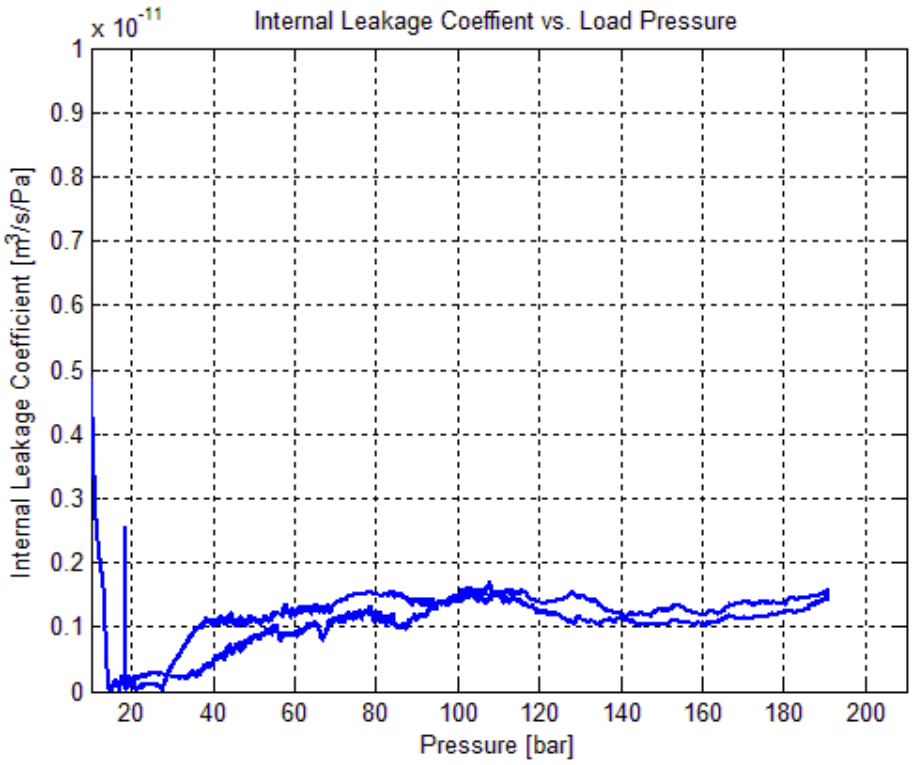

Figure 75: Internal Leakage Coefficient vs. Load Pressure

Table 7: Look-Up Table of Internal Leakage Coefficient

Breakpoints	Column	(1)	(2)	(3)	(4)	(5)	(6)
Row		*0*	*1500000*	*7000000*	*11500000*	*16000000*	*18000000*
(1)	*0*	2.6e-12	2.6e-12	5.1e-13	3.2e-13	2.2e-13	2.24e-13
(2)	*5.236*	2.6e-12	2.6e-12	5.1e-13	3.2e-13	2.2e-13	2.24e-13
(3)	*15.708*	2.07e-12	2.07e-12	1.54e-12	9.4e-13	6.7e-13	6.72e-13
(4)	*20.944*	1.9e-12	1.9e-12	2.05e-12	1.25e-12	8.96e-13	8.96e-13
(5)	*33.511*	1.75e-12	1.75e-12	1.54e-12	2e-12	1.4e-12	1.43e-12
(6)	*41.889*	1.57e-12	1.57e-12	6.3e-13	2.49e-12	1.79e-12	1.79e-12
(7)	*67.02600...*	2.09e-12	2.09e-12	1.4e-13	1.09e-12	1.75e-12	1.4e-12
(8)	*100.5410...*	1e-12	1e-12	1.4e-13	2.6e-13	1.46e-12	1.3e-12
(9)	*134.056*	5.5e-13	5.5e-13	1.4e-13	1.5e-12	1.4e-12	1.27e-12
(10)	*167.5710...*	9.8e-13	9.8e-13	1.4e-13	1.6e-12	1.39e-12	1.28e-12
(11)	*201.086*	1.18e-12	1.18e-12	7.4e-13	1.6e-12	1.38e-12	1.24e-12
(12)	*234.601*	1.94e-12	1.94e-12	1.85e-12	1.74e-12	1.55e-12	1.32e-12
(13)	*268.116*	1.55e-12	1.55e-12	1.33e-12	1.72e-12	1.36e-12	1.29e-12
(14)	*301.631*	1.85e-12	1.85e-12	1.35e-12	1.79e-12	1.44e-12	1.26e-12
(15)	*335.1459...*	1.85e-12	1.85e-12	1.35e-12	1.79e-12	1.44e-12	1.26e-12

4.1.3 Servomotor Characterization Tests

During initial performance tests, it is realized that modeling the servomotor with a first order or second order transfer function is not sufficient to represent actual speed response characteristics since load torque deeply affects speed output at peak load values. Also, dynamics of the servomotor driver has an influence on response of the servomotor. Therefore, an overall model of the servomotor driver and the electric motor is developed.

In Section 3.3.5, a Simulink® Model for the servomotor is given. Some of necessary parameters are taken from the supplier. However, proportional, integral and derivative gains in current and voltage control loops of the servomotor driver and time delays in the servomotor are not known.

As discussed in Section 3.3.5, two delays are utilized in the servomotor model. One of these is modeled at current output of the motor which is named as electrical delay and the other one is at speed output of the motor named as mechanical delay. To find duration of the electrical delay, servomotor service mode is change from speed control to torque control in which the current controller in Figure 32 is eliminated and an analog input applied to the servomotor driver corresponds to torque output. In other words, the input signal controls current through the driver. To find delay duration, a step current is applied and the time lag between the step time and the response time of the current is accepted as electrical delay in the servomotor which is measured as 2 milliseconds. The similar procedure is applied to find out the mechanical delay. The servomotor is switched back to speed control mode and time lag between the input and response time is accepted as combined delay of electrical and mechanical which is measured about 6 milliseconds. Therefore, it is assumed that the mechanical delay is 4 milliseconds.

Voltage and current controller gains are investigated by using the Parameter Estimation Toolbox® of the MATLAB Simulink® Software. It is used to estimate

the Simulink® model parameters and calibrate the model parameters with respect to the test outputs. The software puts estimating parameters into an optimization problem and solves it to find the estimated parameter values [35].

Due to lack of necessary equipment to load the servomotor alone, the tests are performed without applying any loads. Step speed commands are given to the servomotor and speed measurements are obtained from the encoder. The investigated parameters are specified within a guess range as shown in Figure 76. Estimated parameters are investigated iteratively with a cost function, and after some iteration, the estimation process is ended. In Figure 77, a comparison between the experiment data and the servomotor model response with estimation of unknown parameters is shown. There is a difference in the damping characteristics between experiment and model responses. The reason can be the known parameters in the model do not represent the real values of the system parameters.

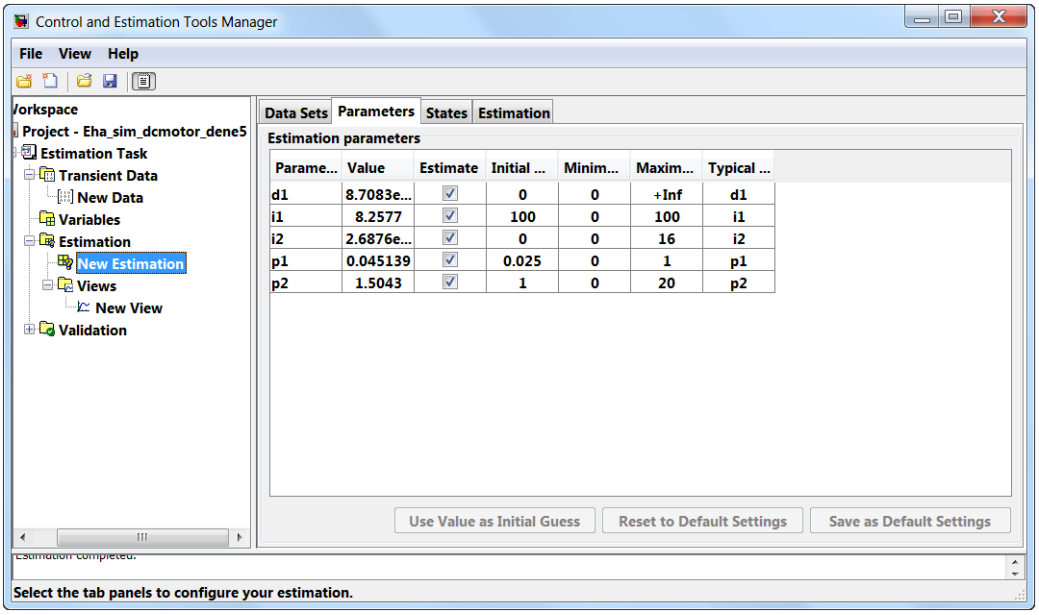

Figure 76: Parameter Estimation Toolbox® Interface

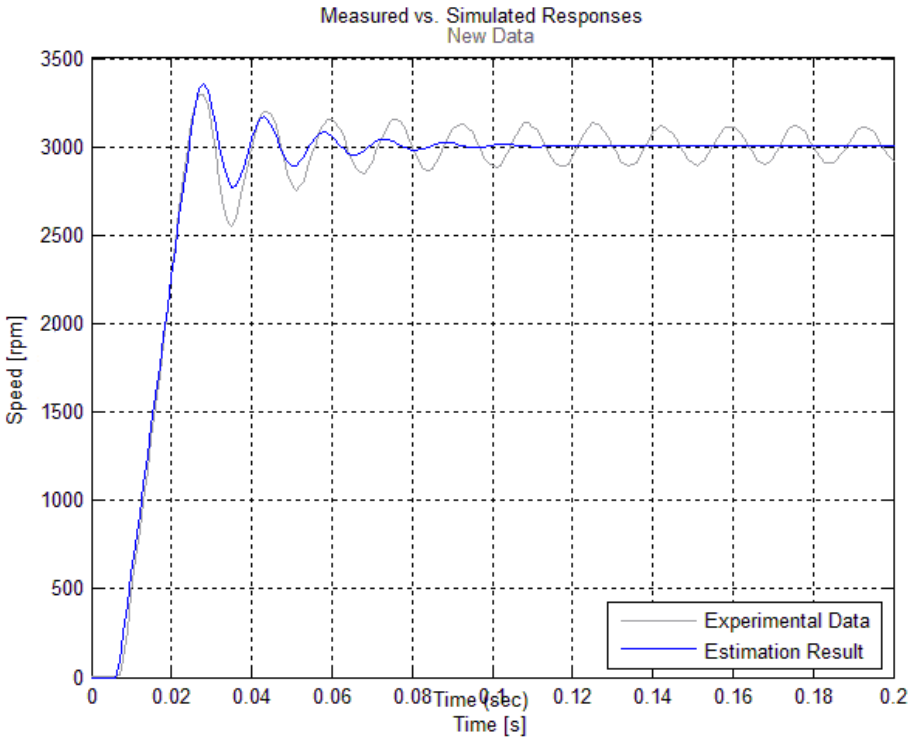

Figure 77: 3000 rpm Step Response of Estimation Result vs. Experiment Data

A bandwidth test is applied to the servomotor in order to validate the model in useful frequency range and observe its bandwidth. In the test, a chirp signal of magnitude ±600 rpm is chosen, in order to eliminate risk of exceeding voltage and the current limits. The signal is varied from 0.1 to 100 Hz within 50 seconds as a speed command. The frequency responses of the test and the model are shown in Figure 78. After 35 Hz, the test and the model responses are very different. It seems that the higher order terms which are not modeled become dominant in servomotor response.

The servomotor model results are very compatible with the measurement results up to 35 Hz. Since the frequency range of interest for the EHA prototype is 10 Hz, it can be concluded that the servomotor model can be used for the overall system simulation.

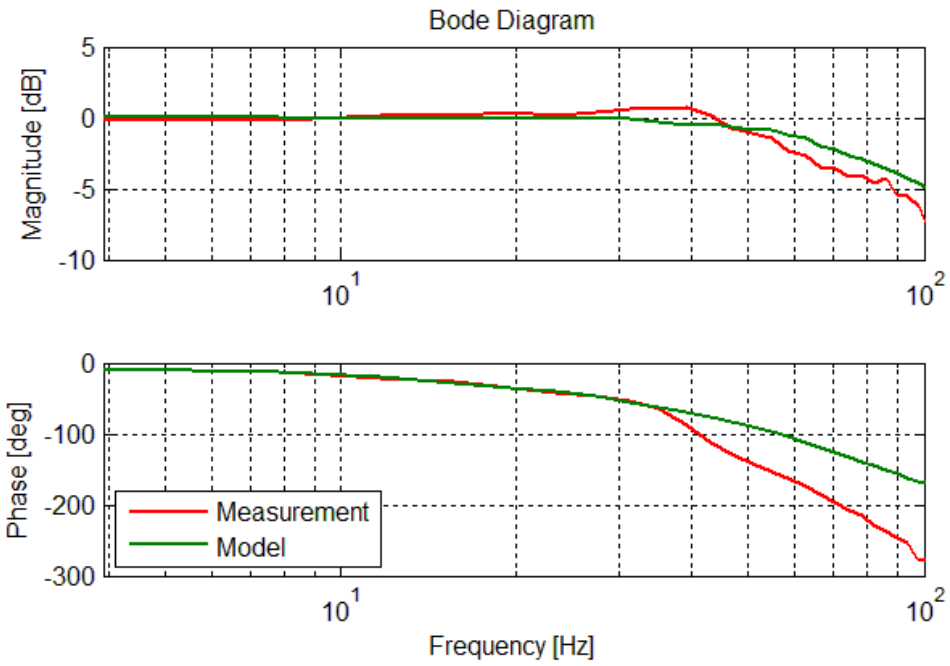

Figure 78: Frequency Response of Servomotor and the Servomotor Model

4.2 System Performance Test

In this sub-section, the tests applied to the EHA prototype are explained in detail. To begin with, open loop system tests for actuator itself and actuator with an inertial and an external load are performed. Then, according to the controller designed in Section 3.6, closed loop performance tests are carried out.

To conduct tests, perform data acquisition and real-time control applications, National Instruments LabVIEW® software is utilized. Basic test software and a user interface are built up for this purpose. The test scenarios are embedded in to this software. Detailed information of this software is given in Appendix C.

4.2.1 Open Loop Performance Tests

To observe consistency between the test and the simulation results and validate the mathematical model, open loop performance tests are performed.

In this test configuration, the input signal is actually speed command to the servomotor and the output signal is the hydraulic cylinder position.

As a test signal, a square wave voltage is applied to the servomotor driver. Two different magnitudes of square wave are applied with frequency of 4 Hz and 8 Hz according to amplitudes of the test signal by considering the hydraulic cylinder stroke does not exceed the maximum stroke. The test duration is chosen as 1 second to lower the external leakage and contribution of the inner hydraulic circuit.

At first, the EHA prototype is tested alone in open loop. Then, regarding to the actuator working condition, the inertia is attached the test system and same open loop test procedure is repeated again.

4.2.1.1 Open Loop Tests of the EHA Prototype

In open loop tests of the EHA prototype, input signals are applied with a square wave form, 1-10 V amplitude, 4-8 Hz.

Amplitude of 3 V input signal which corresponds to 900 rpm of command speed is applied and position measurement of the hydraulic cylinder and position response of the simulation model are compared as shown at Figure 79. It can be observed that the model response and the measurement results have very close slope in hydraulic cylinder position.

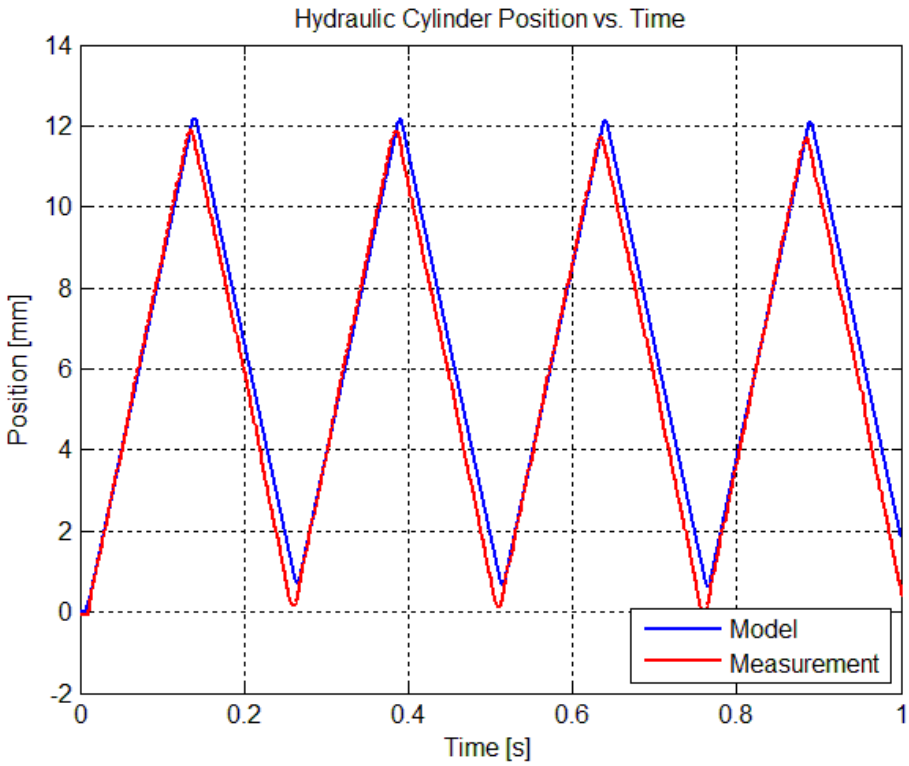

Figure 79: Cylinder Position vs. Time for 3 V Input Test Signal

In Figure 80, the pressure difference between pressure chambers of the hydraulic cylinder which is called as load pressure in sections ahead is shown for the model and the measurement results. As mentioned before, static friction characteristics are different in both directions of motion. The measurement results are in different magnitude with respect to direction of motion. According to the hydraulic cylinder friction model given in Section 3.3.2, direction of motion is not an input of the friction model. Therefore, static and viscous friction coefficients found in Section 4.1.1 represent the average friction force acting on the cylinder.

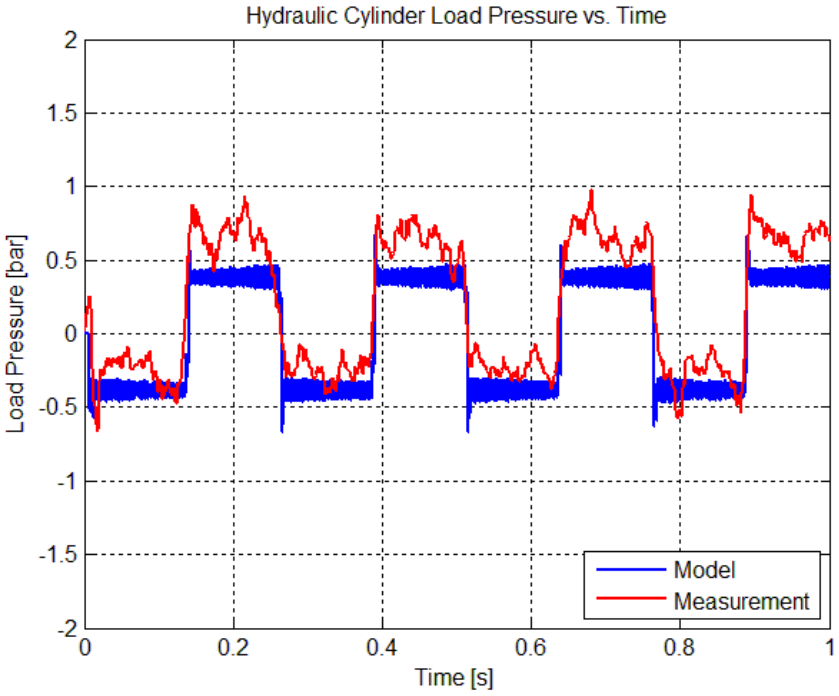

Figure 80: Load Pressure vs. Time for 3 Volt Input Test Signal

4.2.1.2 Open Loop Tests of the EHA Prototype with an Inertial Load

The open loop tests explained in the previous section is repeated in this sub-section with inertia of 0.32 kgm^2 attached to the EHA prototype.

To have a comparison with the previous results, amplitude of 3V input signal which corresponds to 900 rpm of command speed is applied again. Position measurement of the hydraulic cylinder and position response of the simulation model is shown in Figure 81. The load pressure at the hydraulic cylinder is shown at Figure 82. Due to contribution of inertial load to the system, loaded characteristics of the pump and the servomotor begin to affect the system response. There is a deviation between the measurement result and the model response when the load pressure on the hydraulic cylinder maximizes. Load pressure variations of the model and the measurement are similar in amplitude.

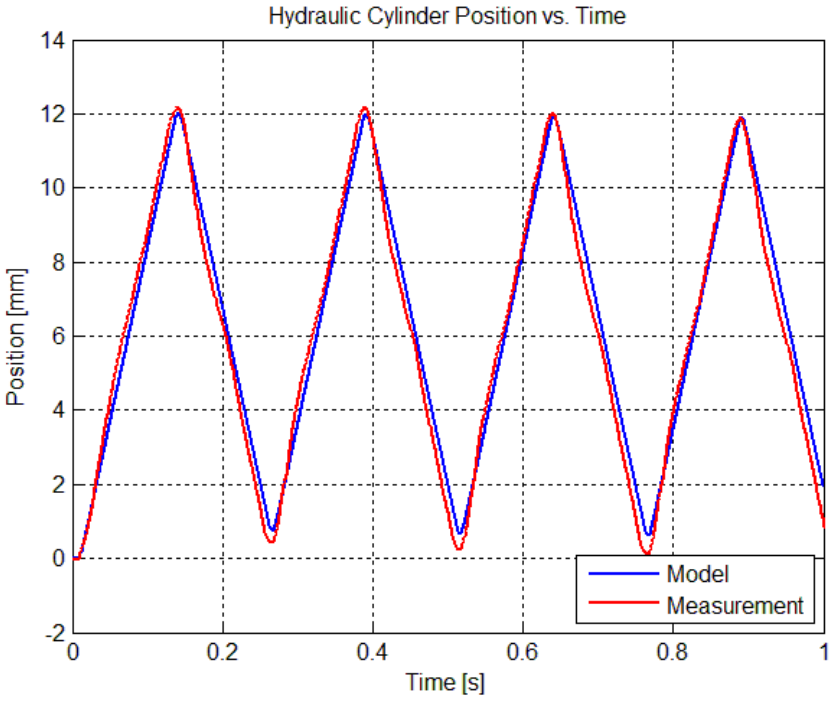

Figure 81: Cylinder Position vs. Time for 3 V Input Test Signal

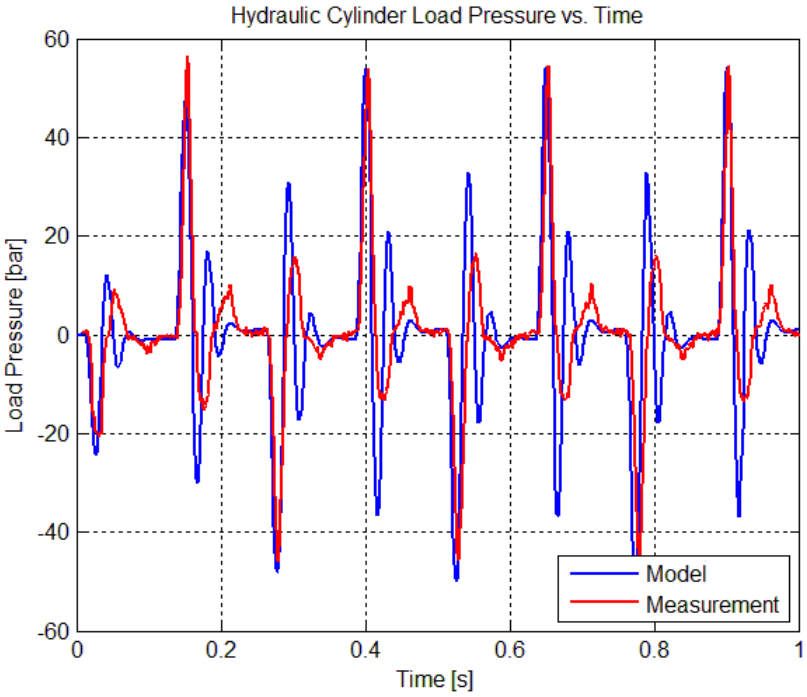

Figure 82: Load Pressure vs. Time for 3 Volt Input Test Signal

However, there is difference in settling times. The reason for that the bulk modulus and leakages in the hydraulic cylinder do not sufficiently represent the real system.

4.2.2 Closed Loop Performance Tests

In Section 3.6, a controller to satisfy the given design considerations and performance criteria in Section 3.1 is designed for position control of the hydraulic cylinder.

The input signal in the open loop system in the previous section is the speed command to the servomotor. In this section, it becomes a closed loop system with a position controller. Therefore, the input signal is the hydraulic cylinder position command.

The tests are performed with two different configurations. At first, the EHA prototype is tested for time response characteristics and then, frequency response characteristics of the system are checked. Secondly, while the actuator operates under inertial load in normal operational conditions, the tests are repeated with inertial load.

4.2.2.1 Closed Loop Tests of the EHA Prototype

In this sub-section, results of the step response of the EHA prototype are given. As discussed in Section 3.6, position control of the hydraulic cylinder is achieved with a basic proportional controller.

The proportional gain is set to a value of 45000 rad/s/m which is rounded value of the gain found in Section 3.6. A step signal with 20 mm amplitude is assumed to be the reference signal in the test. The step responses of the model and the EHA prototype are given in Figure 83.

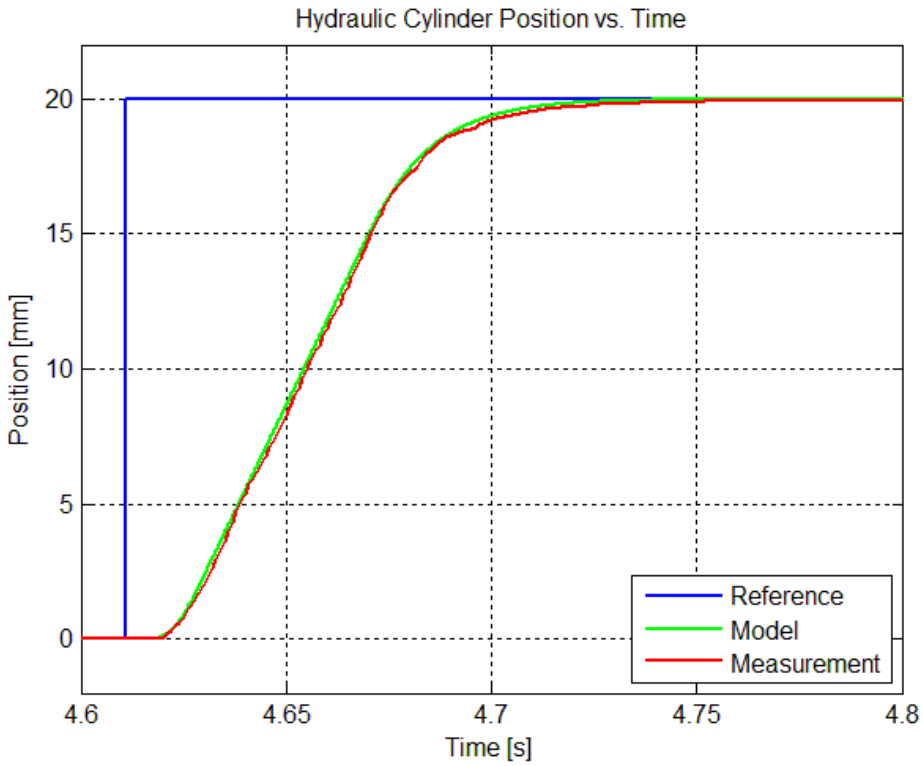

Figure 83: Step Response of the EHA Prototype with K_p=45000 rad/s/m

To observe the frequency response characteristics, ±3 mm chirp signal from 0.1 Hz to 10 Hz within 40 seconds is applied. To eliminate speed saturation and the servomotor current and voltage limitations, it is decided to be suitable. MATLAB System Identification Toolbox® is utilized to plot the test results in frequency domain and it is shared with the time domain data as shown in Figure 84. It can be seen from the Bode diagram at 10 Hz, the magnitude is still higher than -3 dB as expected. However, while the phase shift of the model and the measurement are matches superbly, there are difference in the model and the measurement amplitudes.

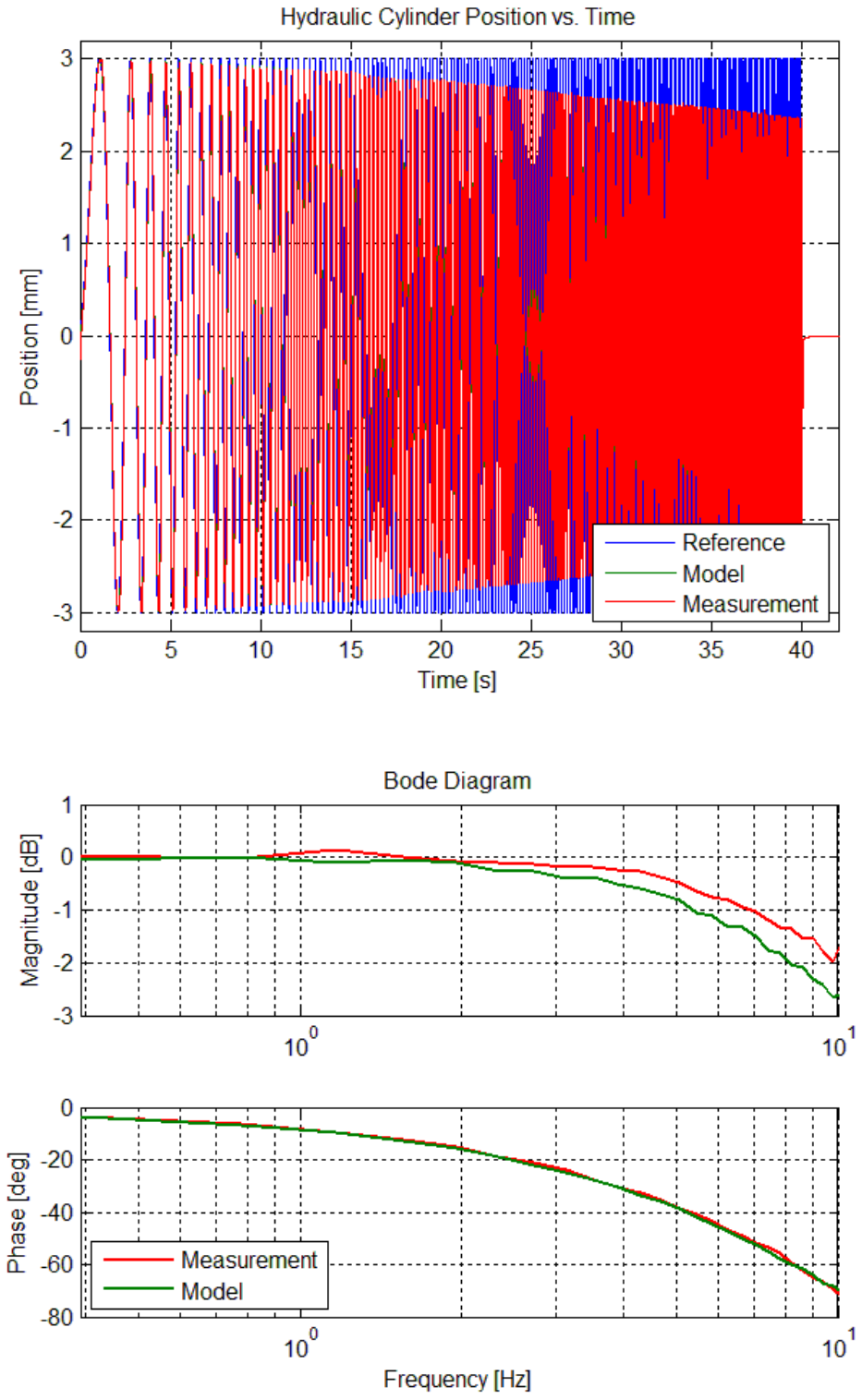

Figure 84: Frequency Response Test of the EHA Prototype with K_p=45000 rad/s/m

4.2.2.2 Closed Loop Tests of the EHA Prototype with an Inertial Load

The closed loop tests are repeated with the inertia attached EHA prototype. A step signal with 20 mm amplitude is applied as the reference signal in the test and proportional gain of the position controller is set to 45000 rad/s/m.

The step responses of the model and the EHA prototype are given in Figure 85. The figure shows that the model and the measurement data are close to each other. During settling period, the model data makes an overshoot; unlikely, the measurement data has an undershoot response and then it settles. Overshoot is due to the deviation occurred in the servomotor responses between the model and the test response.

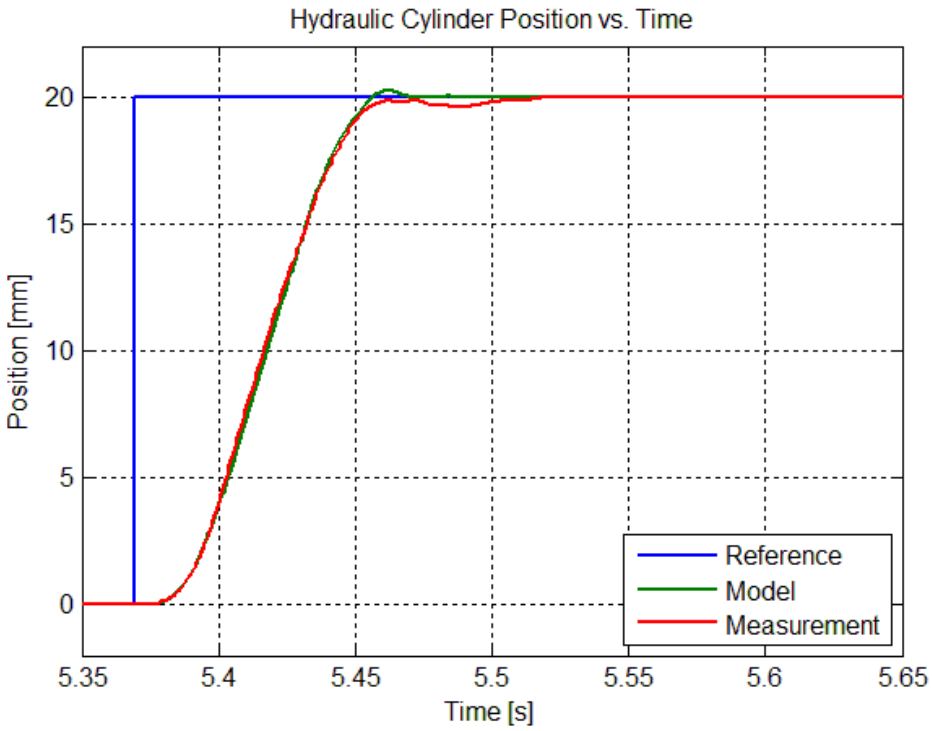

Figure 85: Step Response of the EHA Prototype under Inertial Load with K_p=45000 rad/s/m

The reference, model and measured servomotor speeds are illustrated at Figure 86. The model response has the same trends with measured speed; but it has higher values. Hence, it makes an overshoot in the model response.

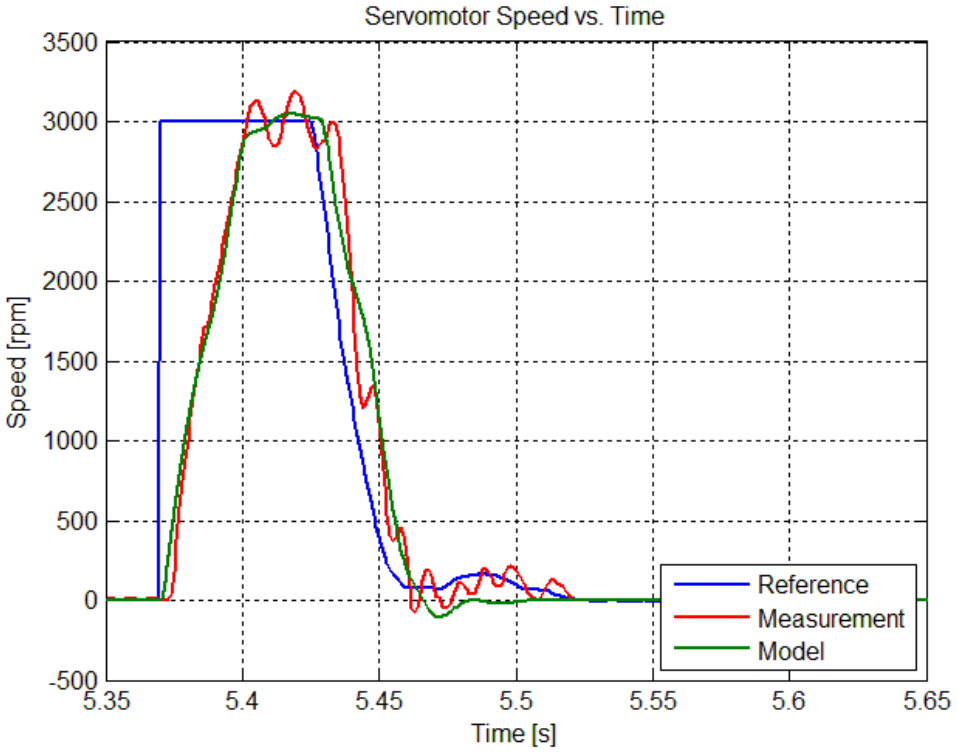

Figure 86: The Servomotor Speed at Closed Loop Test with K_p=45000 rad/s/m

The reference speed is basically created with multiplication of positional error and the proportional gain. If the position of the hydraulic cylinder passes the reference position while approaching the reference, the sign of the position error changes and an opposite reference speed is created. Therefore, to have negative servomotor speed as shown in Figure 86, the cylinder must have an overshoot. According to the measurement data in Figure 85, the cylinder moves in reverse direction, although the cylinder does not make overshoot. The main reasons are the oscillations in the servomotor speed and structural flexibility. The EHA prototype is connected via an auxiliary apparatus to the test bench and it is not

rigid enough to eliminate small displacements that LVDT experienced while acceleration or deceleration motion of the inertia. Moreover, if the inertia attached to the transmission mechanism is converted to an equivalent mass attached to the hydraulic cylinder, it corresponds to a mass of 145 kg. Thus, it can be expected to observe distortion in the LVDT data due to structural flexibilities at higher dynamic responses of the system.

The model and the prototype results are very close and they satisfy the time response characteristics of the controller defined in Section 3.1. It can be said that, rise time (between 5% and 95% of the input amplitude) is 60 milliseconds and settling time is 58 milliseconds from Figure 85. In addition, the steady state error is about 0.01 mm for which the maximum allowable value is 0.2 mm.

In order to minimize excitation of the structure and interference to the hydraulic cylinder position measurement, proportional gain of the position controller is set to a lower value. Therefore, deceleration and acceleration of the inertia are decreased. The proportional gain is set to a new value of 30000 rad/s/m and the step response test is repeated. Figure 87 demonstrates the test result of position response of the system. As seen from the figure, the response is slower and structural intervention to measurements is reduced at the cost of performance degradation.

In order to investigate the frequency response characteristics of the system and the simulation, a chirp signal is applied to the system. Test signal amplitude is selected as ±4 mm while the inertia is attached to the system, pressure difference across the pump increases and dead band of the pump expands and become significant, it is aimed to test the system outside this region as much as possible. Test signal is varied from 0.1 Hz to 15 Hz within 60 seconds and proportional gain of the position controller is set at 45000 rad/s/m. The test results are shown in Figure 88. As seen from the Bode diagram, change in magnitude of the model and the measurement is compatible. However, while inertial load increases with

increasing excitation frequency, there are small distortions at amplitude of the responses. However, phase shifts of the model and the measurement are a bit different. It may occur due to insufficient modeling of the servomotor. Its dynamics are dominant in the overall system and since the servomotor model is developed with unloaded test results, it is possible to observe deviations in loaded response characteristics of the servomotor.

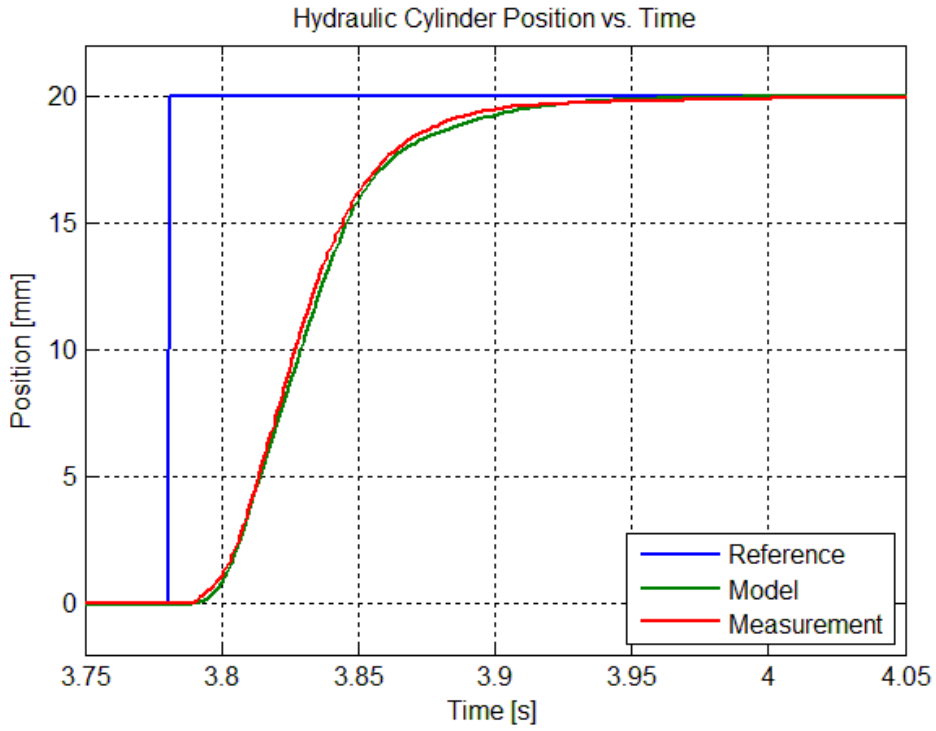

Figure 87: Step Response of the EHA Prototype under Inertial Load with K_p=30000 rad/s/m

In Section 3.1, no-load speed of the actuator is given as one of the performance criteria. To calculate the speed, the displacement of the cylinder in Figure 86 during peak speed region of the servomotor in Figure 85 is observed. The average cylinder speed at that region is calculated as 336 mm/s which is above the given criteria. If the frequency response characteristics are examined, -3 dB amplitude occurs at the 10.8 Hz and 90° phase shift takes place at 9.9 Hz.

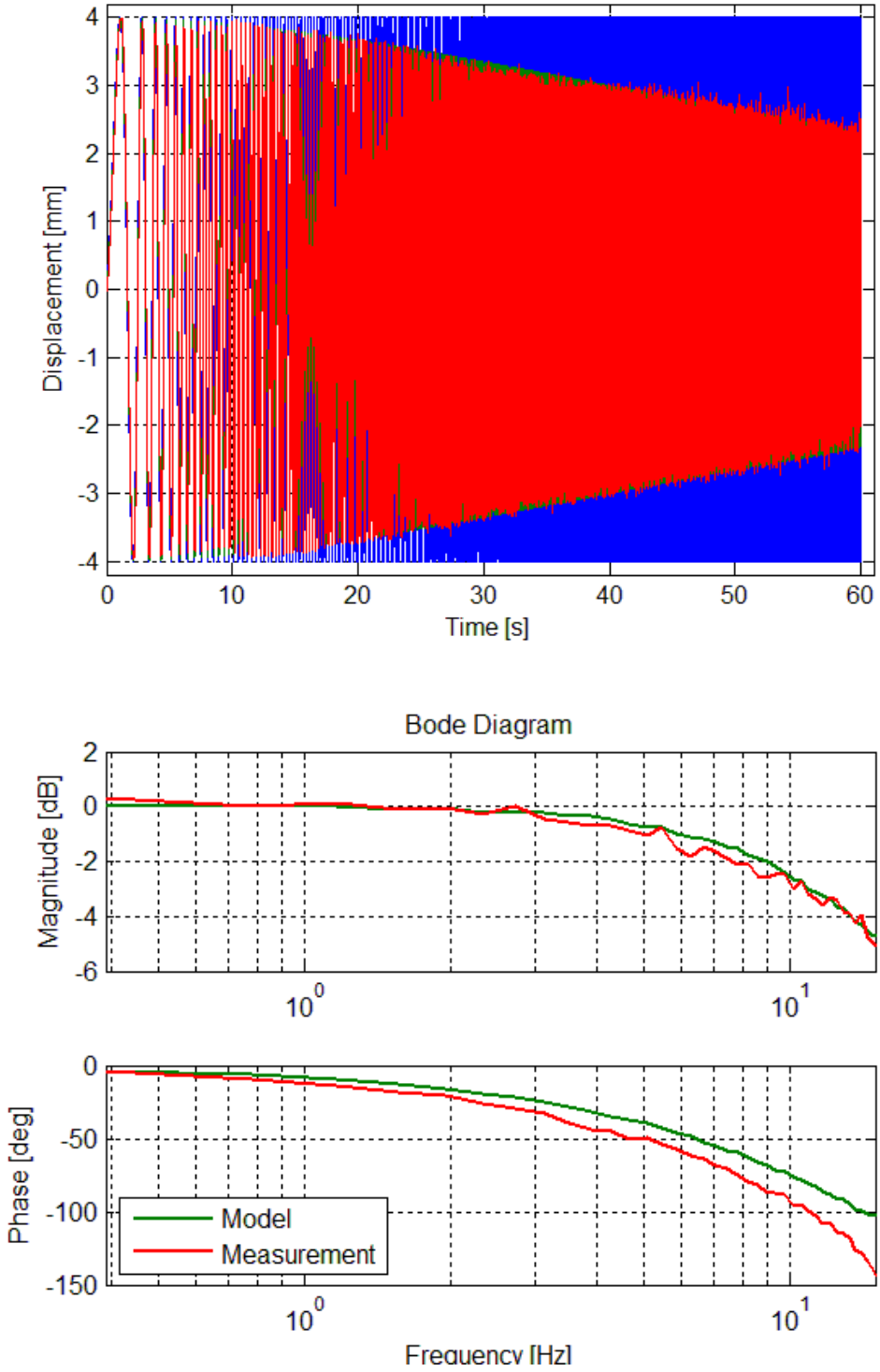

Figure 88: Frequency Response Test with EHA Prototype under Inertial Load with K_p=45000 rad/s/m

Since the data at high frequency is distorted by the reason of structural flexibility of the test assembly and results are very close to desired frequency, it is assumed that the criteria are satisfied.

4.3 System Performance Test with External Loading

In operational conditions, the EHA prototype controls position of the inertia and an external loading on the actuator is expected to occur. Therefore, the EHA prototype is tested under external loading conditions and checked whether if the given loaded performance criteria is satisfied.

A test setup which is illustrated in Figure 89 is constructed to apply necessary external load to the EHA prototype. A servomotor is utilized as a load generator and connected to a gear box to amplify generated torque by the load motor. Moreover, the inertia is attached between the transmission mechanism and the gear box. The load motor is used in torque mode and desired torque is applied to the EHA prototype. From analog output channel of the load motor driver, amplitude of the given torque data is collected. Detailed information of the external load test setup and additional results is given in Appendix D.

A step signal with 20 mm amplitude is applied as the reference signal in the test and proportional gain of the position controller is set 45000 rad/s/m as in the tests given in the previous section. 110 Nm load torque is selected to be applied to check the performance criteria given for loaded speed of the actuator. The load torque is applied before giving the step command of position and the EHA prototype tries to keep the hydraulic cylinder position at the zero. Next, the step command is applied to the system and step response characteristics of the model and the EHA prototype are observed.

Result of the test is shown in Figure 90. The experiment results and the model response are compatible while they share the same trend during the motion of the

hydraulic cylinder. Nevertheless, their steady state error amplitudes are different. In external loading test, the pump only pressurizes the fluid that works against to the external load. Therefore, the pump delivers only pressurizing amount of fluid and the remainder fluid become leakage. If mathematical equations of the pump are considered, during the dead band, while the pump keeps rotating, all of the theoretical flow supplied turns into internal and external leakage. The leakage coefficients of the pump are found by the tests explained in Section 4.1.2. However, in these tests, the pump rotation speed is changed as a ramp signal from 0 to 3000 rpm to scan whole possible speed range and the tests are repeated for some pressure levels. The intermediate values of leakage coefficients are interpolated in the pump model. Therefore, it seems that, the leakage coefficients do not sufficiently represent the real leakage characteristics at low rotation speeds and high load pressures of the pump.

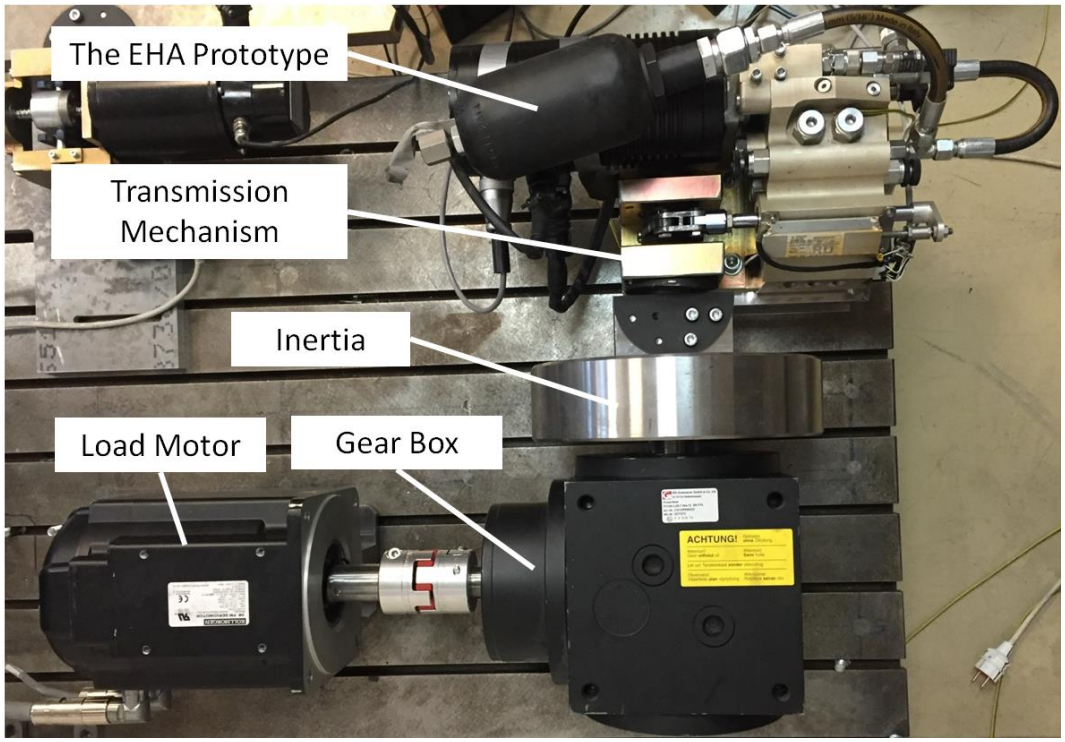

Figure 89: External Load Test Setup

In Figure 90, the steady state error for 110 Nm external loading test is measured as 0.2 mm which corresponds to 1 % of the 20 mm amplitude of step input.

In Section 3.1, loaded speed of the actuator is given as one of the performance criteria. To calculate the speed, the displacement of the cylinder in Figure 90 during peak speed region of the servomotor in Figure 91 is observed. The average cylinder speed at that region is calculated as 288 mm/s. The performance criterion is satisfied. However, the servomotor cannot reach the reference speed due to the external loading. Deviation of the servomotor rotational speed from the reference speed corresponds nearly 36 mm/s decrease of the cylinder speed. If the total decrease of 48 mm/s (with respect to no-loaded speed) is considered, it can be said that the servomotor speed response is more effective than pump leakages regarding the decrease in the hydraulic cylinder speed.

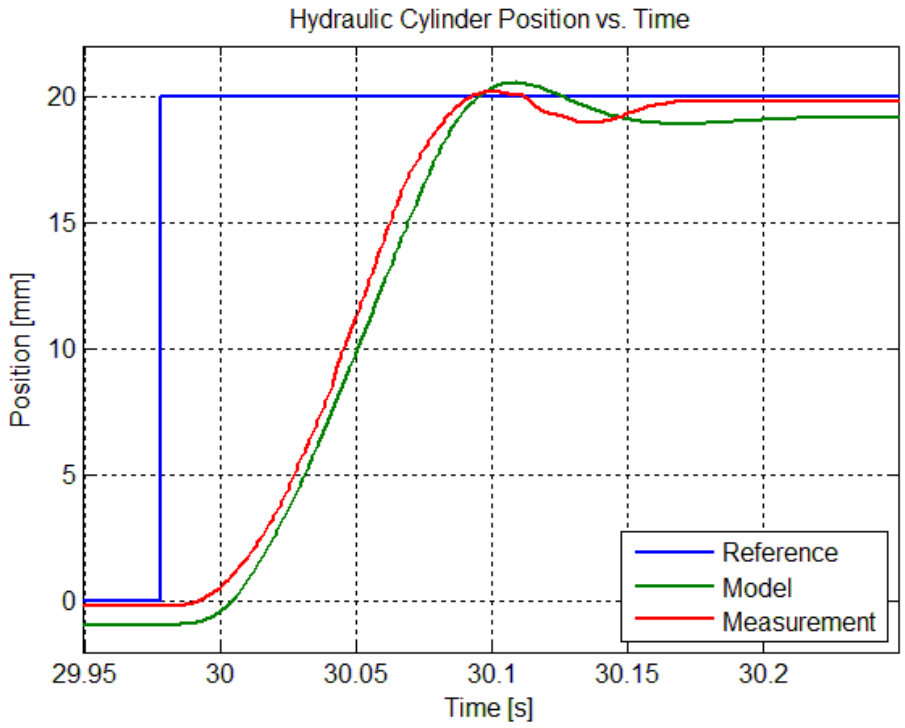

Figure 90: Step Response of the EHA Prototype under Inertial and 110 Nm External Load with K_p=45000 rad/s/m

In Figure 91, the servomotor speed during the external load test is shown. The servomotor is commanded to rotate about 88 rpm, and rotational speed of the servomotor model is higher while the position error of the model is higher than the measurement.

From the load motor analog output, the load torque is obtained. It is calculated as 110 Nm considering the gear box. Furthermore, using kinematics of the transmission mechanism, it can be converted to the load force acting on the EHA prototype. It is found as;

$$F = \frac{110\ Nm}{0.0486\ m} = 2263\ N$$

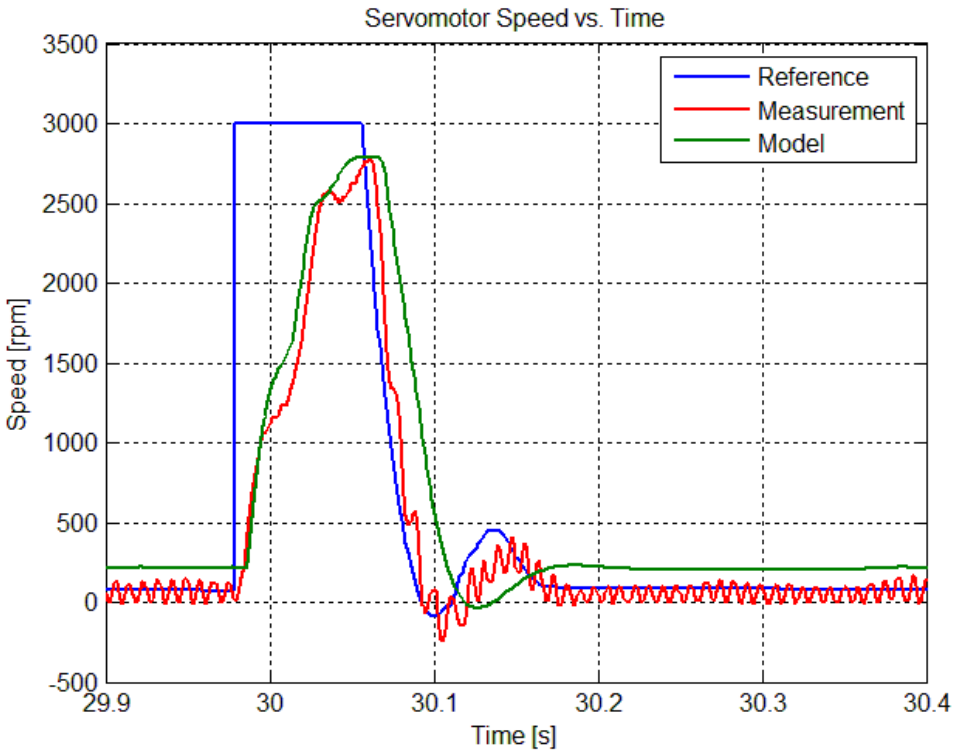

Figure 91: The Servomotor Speed at External Load Test with K_p=45000 rad/s/m

In Figure 92, variation of load pressure in the hydraulic cylinder with respect to time is shown. According to steady region of the load pressures, the force acting on the system can be found as,

$$F = 36bar * 620\ mm^2 \frac{0.1\ N}{bar * mm^2} = 2232\ N$$

The forces calculated are very close to each other; therefore, it can be said that small amount of supplied torque is lost along the torque transmission over components like coupling, gearbox and transmission mechanism.

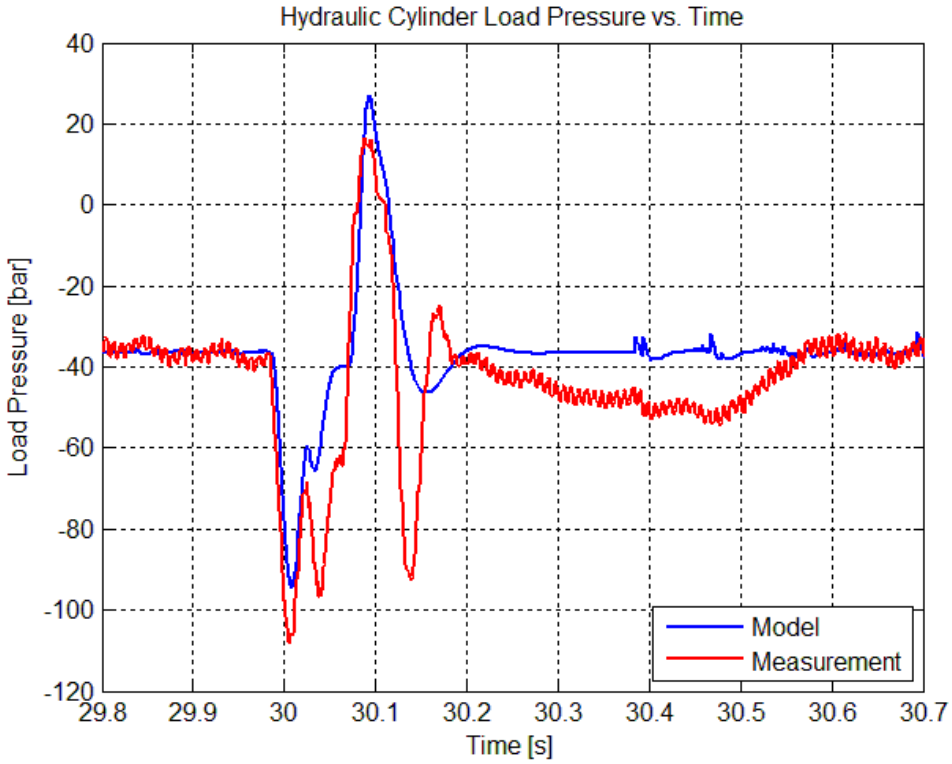

Figure 92: Load Pressure vs. Time for 110 Nm External Load Test

CHAPTER 5

DISCUSSIONS AND CONCLUSIONS

5.1 Summary and Discussions

This thesis addresses the design and manufacturing of an Electro-Hydrostatic Actuator (EHA). The design considerations and performance criteria are designated as performance specifications of an available servo valve controlled actuation system.

Theses, patents, and research papers available in literature are investigated in the preliminary design period as well as the architecture of hydraulic circuit to be used. Using this architecture, mechanical and hydraulic sub-systems are designed by considering the performance criteria. Sensor requirements, their placements, electrical circuit of control and data acquisition system, and electronic components are selected.

In order to simulate the behavior of the overall system, mathematical models of the EHA's sub-systems are derived. These sub-systems are basically servomotor, pump, inner hydraulic circuit, and actuator. The overall non-linear model is developed in MATLAB Simulink® Library for numerical analysis of the system.

Before the EHA is assembled, a series of component based tests are performed. In order to find leakage coefficients of the pump, a pump characterization test is conducted. The servomotor is tested for its step response and frequency response characteristics. After these tests, the EHA is assembled and system identification

tests are performed to estimate the unknown hydraulic cylinder friction. By executing open loop tests on the set-up, the system simulation results obtained by MATLAB Simulink® are validated.

In the controller design of the EHA, it is decided to use position control of the hydraulic cylinder with a proportional controller from the feedback supplied by a linear variable differential transducer (LVDT) connected to the cylinder rod.

Since a variety of operation conditions exist for an EHA, a set of performance tests are performed in different combinations. First, the EHA alone is tested for its time domain and frequency domain characteristics. Considering ordinary operation of the EHA in which it is expected to rotate a specific inertia, a cylindrical mass to simulate the inertia is connected to the actuator via a transmission mechanism. This mechanism transforms the translational cylinder motion of the actuator into a rotational motion. As another operational condition, external loading is applied by adding a load motor to the test assembly.

In all tests, magnitude and frequency of the test signals are selected such that the servomotor will not saturate and the hydraulic cylinder will not crash to its bounds. In tests, LabVIEW® software is utilized for data acquisition and control purposes. Therefore, test software is created to conduct all tests in the LabVIEW® environment. The real-time control of the EHA is performed in LabVIEW® supported National Instrument's Compact RIO platform.

To sum up, an EHA system which has a high force output (nominal 9.5 kN), a remarkably good bandwidth (10 Hz), and a fairly high positioning accuracy (0.02 mm) is presented by this thesis work.

5.2 Conclusions

The EHA, variable speed pump control technique, is a trend topic in hydraulic control systems and it is getting preferred in application areas to replace conventional valve controlled hydraulic systems.

The main reasons of hydrostatic actuators gaining popularity are energy concerns, improvements in electric motor technology, and changing approach in flight surface actuation systems. To begin with, in valve controlled systems throttling losses lead to only small portion of the hydraulic energy available and more than half of overall hydraulic energy is wasted. Due to the removal of control valves in pump controlled systems, these losses are eliminated; however, there are still some losses occurred in pump and servomotor. Secondly, improvements in electric motor technology and servomotors become accessible; it affects developments of the EHA's in positive manner. Before utilizing servomotors in pump controlled systems, a constant speed electric motors and variable displacement pumps were used to make a hydrostatic actuator. These pumps are complex and expensive components, and still control valves are used to control pump displacement such as swash plate angle. Servomotor with a constant displacement pump, which is relatively basic component, decreases the complexity of this technique. Lastly, in aviation, flight surface control systems generally have a centralized hydraulic power unit and from there the hydraulic power is distributed to control actuators which are controlled by control valves. This architecture is called as Fly-by-Wire. However, in the industry, there is a desire to replace it with Power-by-Wire architecture in which, all sub-units are packed as consist of a single power and actuation unit and only electric power is supplied to each of these sub-systems. This technique increases system reliability, energy efficiency, modularity and decreases system complexity and maintenance costs.

In this thesis study, it is shown that a flight control actuation system that satisfies necessary performance criteria can be design as an EHA and can be packed as a compact monoblock design. However, due to using standard industrial components the overall package volume is increased with respect to the hydraulic actuator.

5.3 Recommendations for Future Work

In this thesis work, the oil bulk modulus is assumed as from data sheet of the oil supplier. However, it is a one of the key parameters to find stiffness value of the hydraulic system. The hydraulic system's stiffness is affected by bulk modulus, volume of fluid and elasticity of the material that contains the hydraulic fluid. The entrained air in the oil affects bulk modules of the oil. Since the oil does not return back to a reservoir, the air entrained cannot diffuse from the system. Therefore, measuring bulk modulus of the oil in the filled system or knowing amount of entrained air is important.

In this thesis work, performance characterization tests are performed to figure out performance of the pump. These tests are done for specific pressure setting with continuously changing pump speed to observe change of the leakage coefficients under varying pump speed and pressure. Moreover, the model and test results are compatible for dynamic conditions of the hydraulic cylinder. However, for static conditions of the hydraulic cylinder which is observed during the external loading tests, modeled pump leakages does not represent the real case. Therefore, more comprehensive tests for low speed with high pressure may be done for better characterization of the pump.

During the performance tests, it is observed that for low frequency excitation of the EHA alone, the hydraulic part is dominant and servomotor can be assumed as an ideal speed source. At higher frequency of operation, the servomotor response is not fast enough and a phase shift and attenuation are observed in the test results.

Although the servomotor driver dynamics are not known and cannot be determined easily with parameter estimation, more detailed characterization of servomotor should be made. In this study, the servomotor driver is assumed as a black box. The gains of inner loops of it are not tuned, since they are not known. However, if they were known, they can be tuned for improved response of the system.

In this thesis work, the servomotor is used in speed mode; however, it can be used in the torque mode and speed loop of the servomotor can be closed in the real time control computer. Consequently, the torque commands can be given to the servomotor and comparison of two methods for the system response can be investigated for future work.

In this study, a basic proportional position controller is employed in the EHA. Since all of the performance criteria are satisfied, the more complex control algorithms are not tested. However, for further researches, different control strategies can be developed whose examples are found in the literature such as “Sliding Mode Control”, Adaptive Control” and “Fuzzy Logic Control”.

REFERENCES

[1] Bloomfield, Louis (2006). How Things Work: The Physics of Everyday Life (Third Edition), John Wiley & Sons. p. 153. ISBN 0-471-46886-X.

[2] Habibi, S., Goldenberg A., "Design of a New High-Performance Electrohydraulic Actuator", IEEE/ASME Transactions on Mechatronics, Vol. 5, Issue 2, pp. 158-164, 2000.

[3] Valdo, M., "Electro Hydrostatic Actuators – A New Approach In Motion Control" 2nd Workshop on Innovative Engineering for Fluid Power, Sep 2-3, 2014.

[4] Blackburn, J.F., Reethof, G., and Shearer, J.L., Fluid Power Control, 1st Ed., MIT Press and John Wiley & Sons Inc., New York & London, 1960.

[5] J. Watton, Fluid Power Systems. Englewood Cliffs, NJ, Prentice-Hall, 1989.

[6] Guan, C., Jiao, Z., He, S., "Theoretical Study of Flow Ripple for an Aviation Axial-Cylinder Pump with Damping Holes in the Valve Plate" Chinese Journal of Aeronautics, Volume 27, Issue 1, February 2014, Pages 169–181.

[7] Patil B.J., Sondur, V.B., "Investigation into the Causes of Pulsation of Flow of Hydraulic Pumps and Its Effects" International Journal of Innovative Research in Science, Engineering and Technology (An ISO 3297: 2007 Certified Organization), Vol. 4, Issue 1, January 2015.

[8] Helduser, S., "Electric–Hydrostatic Drive - An Innovative Energy-Saving Power And Motion Control System", Proceedings of the Institution of Mechanical Engineers, Vol. 213, pp. 427-437, 1999.

[9] Kamiaga, H., Tanaka, H., Yasuda, K., Nakamura, Y., “Screw Pump for Electro-Hydrostatic Actuator that Enhances Backdrivability”, 11th IEEE-RAS International Conference on Humanoid Robots Bled, Slovenia, October 26-28, 2011.

[10] Zhang, Y., Fu, Y., Zhou, W., “Optimal Control for EHA-VPVM System Based on Feedback Linearization Theory”, 11th Int. Conf. Control, Automation, Robotics and Vision Singapore, 7-10th December 2010.

[11] Backe, W., "Resent Research Projects in Hydraulics", Proceedings of the Second JHPS International Symposium on Ruid Power, September 1993.

[12] Rahmfeld, R., Ivantysynova, M., "Displacement Controlled Linear Actuator with Differential Cylinder - A Way to Save Primary Energy in Mobile Machines", 5th International Conference on Fluid Power Transmission and Control, Hangzhou, China, pp. 316-322, 2001.

[13] Takahashi, N., Kondo, T., Takada, M., Masutani, K., Okano, S., Tsujita, M., "Development of Prototype Electro-Hydrostatic Actuator for Landing Gear Extansion and Retraction System", 7th JFPS International Symposium on Fluid Power, Toyama, Japan, September 15-18, 2008.

[14] Henan Gang Iron and Steel Co. Chinese GB/T3077 Standard. http://gangsteel.net/uploads/soft/120405/GB3077.pdf, last visited on April 2016.

[15] Parker Hannifin Corporation, 2016, “Gear Pumps / Motors”. http://www.parker.com/literature/PMDE/Catalogs/Gear_Units/PGP_PGM/HY30-3300-UK.pdf, last visited on April 2016.

[16] Parker Hannifin Corporation, 2016, “Pressure Control Valve”. http://www.parker.com/literature/Literature%20Files/IHD/PCsection.pdf, last visited on April 2016.

[17] Parker Hannifin Corporation, 2016, “Check Valve”. http://www.parker.com/literature/Literature%20Files/IHD/CVsection.pdf, last visited on April 2016.

[18] Parker Hannifin Corporation, 2016, “Series BA Bladder Accumulators”. http://www.parker.com/literature/Global%20Accumulator%20Division/Catalogs%20&%20Bulletins/Maintenance%20-%20BA's.pdf, last visited on April 2016.

[19] Parker Hannifin Corporation, 2016, “Hydraulic Cartridge Systems”. http://www.parker.com/literature/Literature%20Files/IHD/HY15-3502-US.pdf, last visited on April 2016.

[20] Exxon Mobil. “Mobil Aero HF Series – Aviation Hydraulic Fluids” http://www.exxonmobil.com/USAEnglish/Aviation/PDS/GLXXENAVIEMMobil_Aero_HF.aspx, last visited on April 2016.

[21] Unitek Industrie Elektronik GmbH., “BAMOBIL-D3/D2 Servo Driver”. http://www.unitek-online.de/en/produkte/batterie/bamobil_d2_d3.html, last visited on April 2016.

[22] Trafag AG., “NAT8252 - Industrial Pressure Transmitter” http://www.trafag.com/fileadmin/ms3/Datenblatt_WS/01_Datenblaetter/H72303h_EN_8252_NAT_Industrial_Pressure_Transmitter.pdf, last visited on April 2016.

[23] National Instruments. The CompactRIO Platform http://www.ni.com/compactrio, last visited on April 2016.

[24] Davis, M. A., “High Performance Electromechanical Servoactuation Using Brushless DC Motors”, MOTOR-CON’84, Conf. Atlantic City, April 1984.

[25] Frischemeier, S., “Electrohydrostatic Actuators for Aircraft Primary Flight Control-Types, Modelling and Evaluation”, SICFP’97, Proceedings, 5th Scandinavian International Conference on Fluid Power, 1997, pp. 1–16.

[26] Modern Industrial Hydraulics., “Tag Archives: Unbalanced Vane Pumps”. www.modernhydraulics.net/tag/unbalanced-vane-pumps, last visited on April 2016.

[27] Manring, N., D., “Valve-Plate Design for an Axial Piston Pump Operating at Low Displacements”, J. Mech. Des 125(1), pp. 200-205, March 21, 2003.

[28] Massachusetts Maritime Academy, “TSPS Engineering Manual”, 1995. weh.maritime.edu/campus/tsps/manual/steering4.html, last visited on April 2016.

[29] Modern Industrial Hydraulics., “Tag Archives: External Gear Pump”. www.modernhydraulics.net/tag/external-gear-pump, last visited on April 2016.

[30] Çalışkan, H., “Modeling and Experimental Evaluation of Variable Speed Pump and Valve Controlled Hydraulic Servo Drives”, Ms. Thesis, pp. 78, Middle East Technical University, September, 2009.

[31] Pastrakuljic, V., “Design and Modeling of a New Electro Hydraulic Actuator”, Ms. Thesis, pp.3, University of Toronto, 1995.

[32] Habibi, S., Roach, J., Luecke, G., “Inner-Loop Control for Electromechanical (EMA) Flight Surface Actuation Systems”, Journal of Dynamic Systems, Measurement and Control 130, pp. 1-13, August 01, 2008.

[33] Hewett, A. J., 1994, “Hydraulic Circuit Flow Control”, U.S. Patent No. 5,329,767.

[34] Çalışkan, H., Balkan, T., Platin, B. E., “A Complete Analysis and a Novel Solution for Instability in Pump Controlled Asymmetric Actuators”, Journal of Dynamic Systems, Measurement and Control 137, September 01, 2015.

[35] MATLAB Simulink Design Optimization, Parameter Estimation Toolbox., www.mathworks.com/help/sldo/parameter-estimation.html, last visited on April 2016.

[36] TRANS-TEK, Inc., "Series 240", www.transtekinc.com/products/series-240, last visited on April 2016.

[37] Michel, S., Weber, J., "Energy-Efficient Electrohydraulic Compact Drives for Low Power Applications" in FPMC'12, The 24th Fluid Power and Motion Control Symposium, 2012, pp.93-110.

[38] LeTron, X., "A380 Flight Controls Overview", http://www.fzt.haw-hamburg.de/pers/Scholz/dglr/hh/text_2007_09_27_A380_Flight_Controls.pdf, last visited on April 2016.

APPENDIX A

ELECTRICAL CONNECTIONS OF THE PROTOTYPE AND CONTROL COMPUTER

Figure A. 1 demonstrates electrical diagram of the EHA and Control Computer.

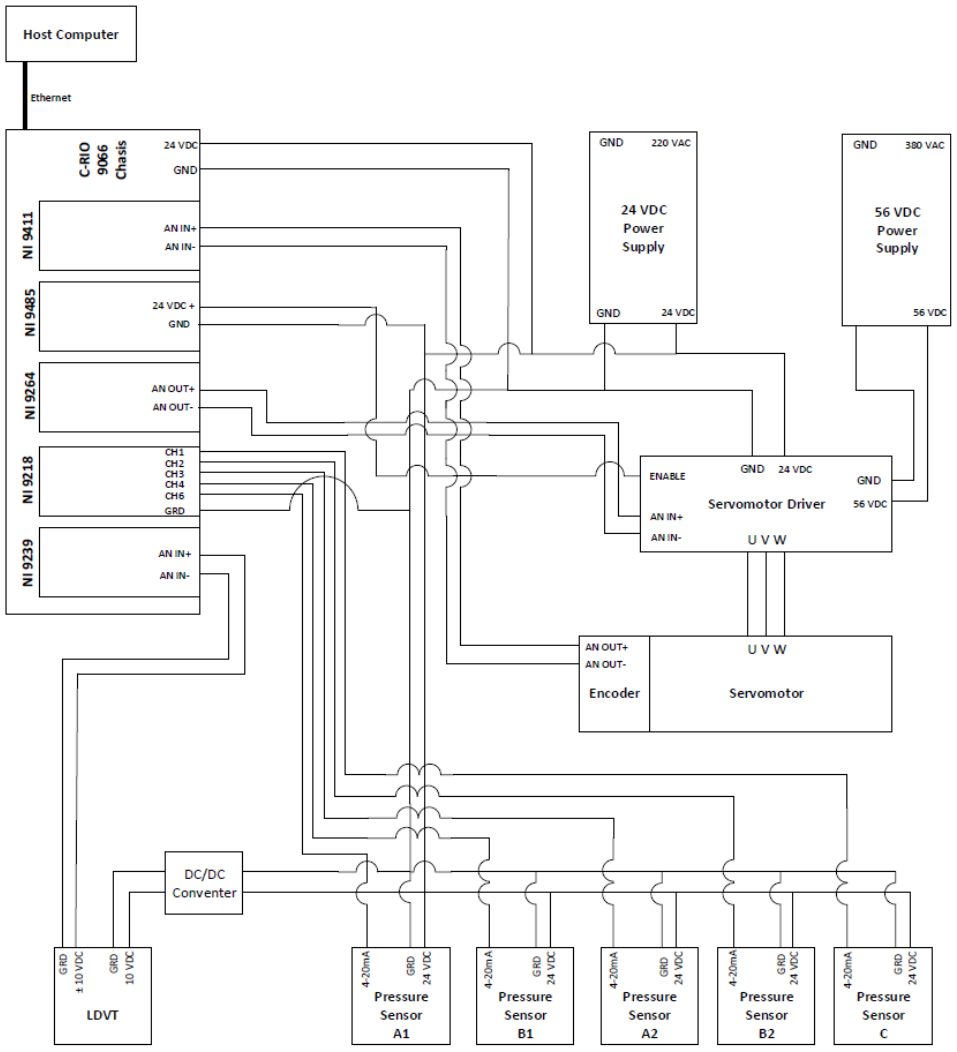

Figure A. 1: The Electrical Diagram of the EHA and Control Computer

APPENDIX B

PUMP CHARACTERIZATION TEST

B.1 Test Setup

The pump used in the EHA prototype is undertaken a pump characterization test and a test setup is proposed. The hydraulic circuit scheme of the test setup is shown in Figure 65. The products used are introduced in this section.

Kollmorgen AKM 73Q is utilized as a DC motor with servo drive AKD-X02407 that shown in Figure B. 1 and servomotor specifications are given below:

- Max. Rated DC Bus Voltage : 640 V
- Continuous Torque (Stall) : 41.5 Nm
- Continuous Current (Stall) : 24.5 A
- Max. Speed : 6000 rpm
- Peak Torque : 111 Nm
- Peak Current : 73.5 A

Figure B. 1: The Servomotor and Servo Drive

As proportional pressure relief valve, Walvoil MP10X spool type proportional pressure relief valve shown in Figure B. 2 is used. Its specifications are as follows:

- Max. Flow : 60 l/min
- Max. Pressure : 350 bar
- Nominal Voltage : 12-24 V
- Max. Control Current : 1.70 (12 V)-0.85(24 V) A
- Hysteresis : 5 %

As a manual pressure relief valve, Parker Hannifin RAH081 Relief Valve is utilized which is the same manual pressure relief valve whose specifications are given in Section 3.3. Furthermore, check valves that used are from Parker Hannifin CVP081P whose specifications are also given in Section 3.3.

Figure B. 2: Proportional Pressure Relief Valve

Two types of pressure sensors are utilized according to the measuring range, one of them is high pressure range 0-250 bar for inlet and outlet ports of the pump and the other is low pressure range 0-10 bar for drainage port of the pump. Trafag AG

NAT 8252 is chosen in the setup. The specifications of the sensor are given in Section 3.5.

The flow meters are product of the Parker Hannifin SCVF type volume flow sensors. Their measurement principle is to count the gearwheel volume by its rotation. Flow sensor with measurement range of 15 l/min for the inlet and outlet ports of the pump and flow sensor with measurement range of 4 l/min for the drainage port of the pump is selected.

Figure B. 3: The Flow Meter

B.2 Product Catalog

The pump data sheet is given Figure B. 4. As seen from figure, there are no information is given for rotation speed lower than 500 rpm.

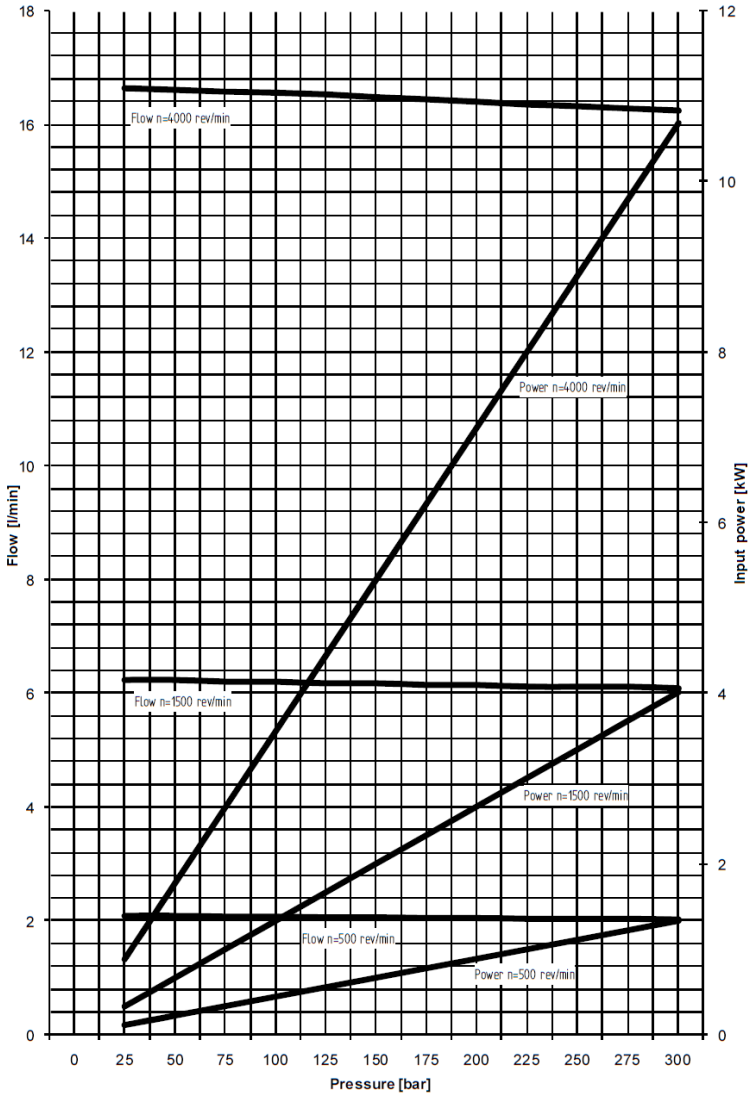

Figure B. 4 : The Pump Catalog Data

B.3 Additional Results of Pump Characterization Test

The results of the some of the test conducted in Section 4.1.2.2 which is constant pressure and variable speed test of the pump.

In Figure B. 5, flow rate measurement is shown for the test performed at 15 bar load pressure over the pump. Change in the internal leakage for the motor speed profile in Figure 66 is shown in Figure B. 6.

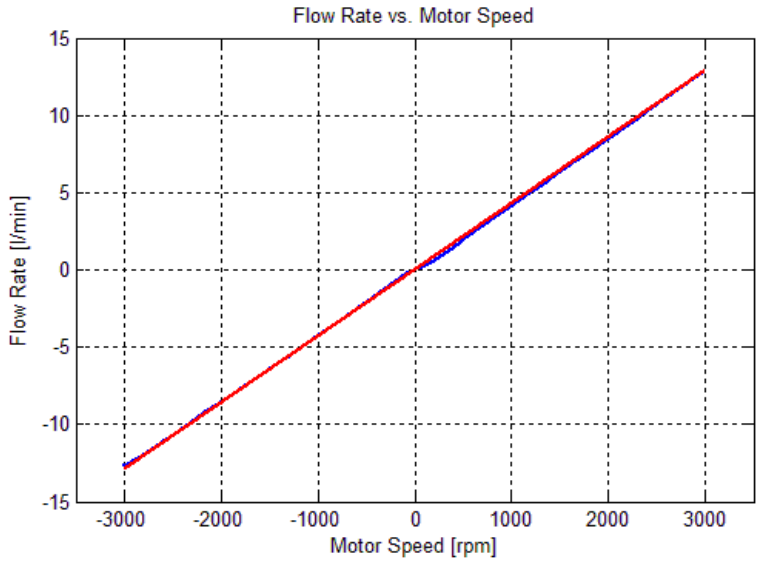

Figure B. 5: Flow Rate vs. Motor Speed at 15 bar Load Pressure

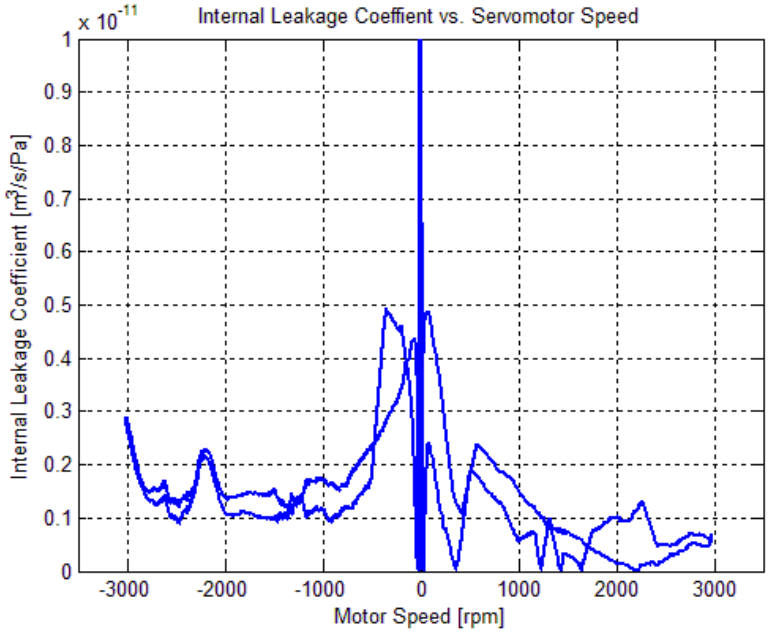

Figure B. 6: Internal Leakage Coefficient vs. Motor Speed for 15 bar Load Pressure

In Figure B. 7, flow rate measurement is shown for the test performed at 140 bar load pressure over the pump. Change in the internal leakage for the motor speed profile in Figure 66 is shown in Figure B. 8.

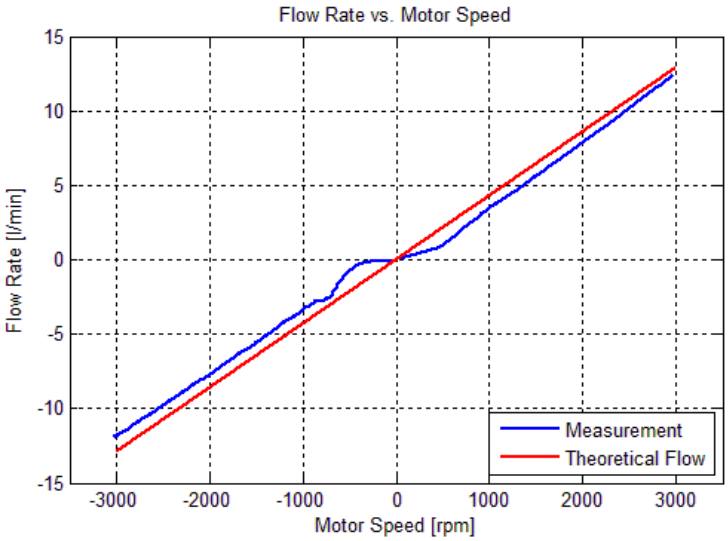

Figure B. 7: Flow Rate vs. Motor Speed at 140 bar Load Pressure

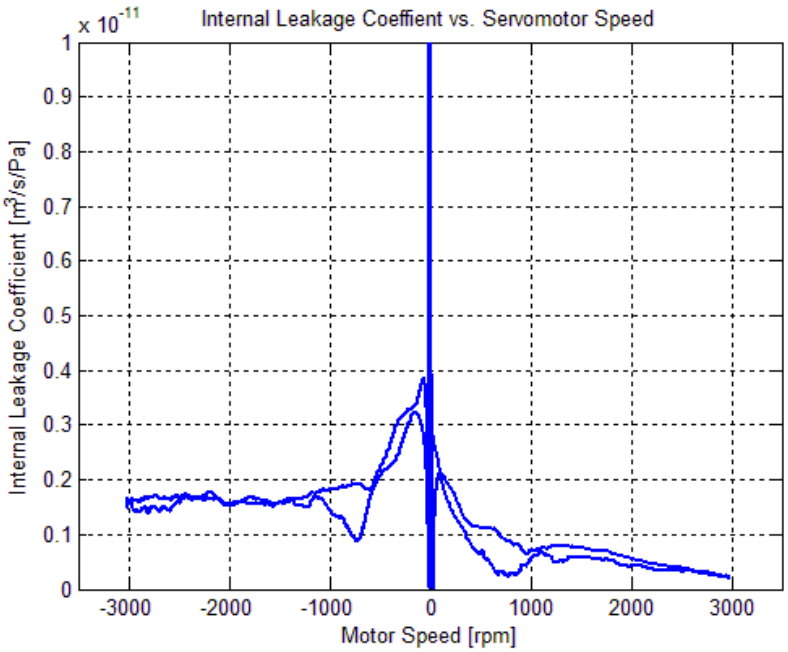

Figure B. 8: Internal Leakage Coefficient vs. Motor Speed for 140 bar Load Pressure

APPENDIX C

TEST SOFTWARE

The test software is built in the LabVIEW® software of National Instruments which has user-friendly graphical blocks on the frontend, eliminates complicated programming and coding process and easy in creating user interface in parallel.

The user interface of the test software is illustrated in Figure C. 1. There are two Tab parts in the interface one of is aligned horizontally, and the other one aligned vertically.

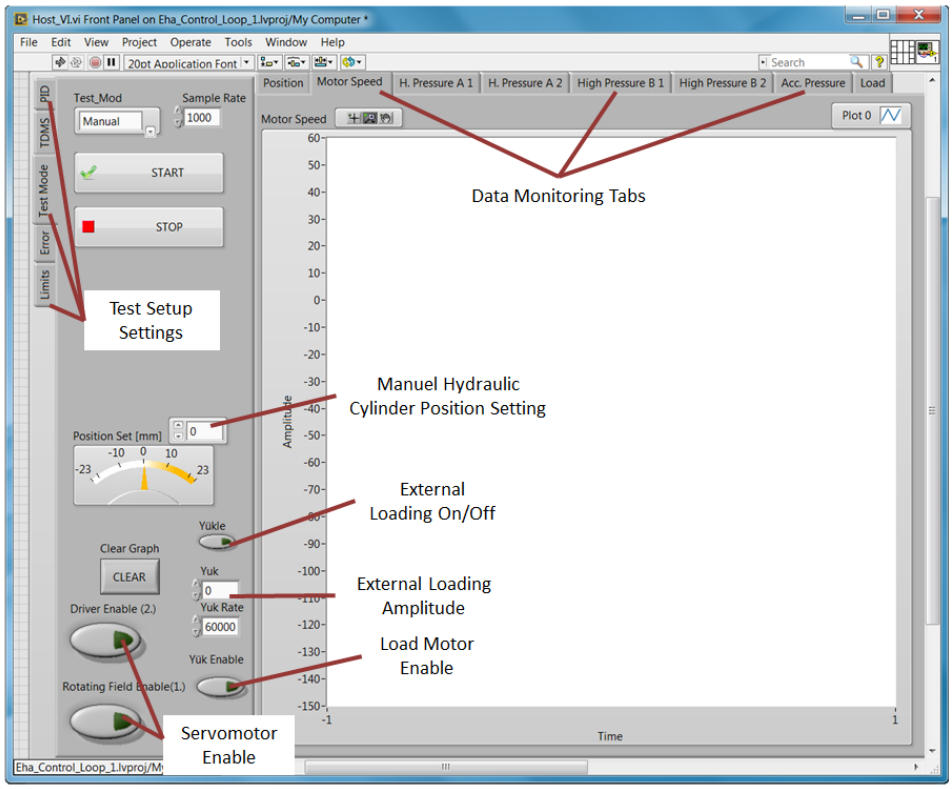

Figure C. 1: User Interface of the Test Software

At the horizontal tabs, the graphical demonstrations of the instantaneous data gathered such as, position of the cylinder, servomotor rotation speed, pressure values at the pump inlet & outlet, cylinder inlet & outlet and inner hydraulic circuit and load applied on the EHA prototype.

At the vertical tabs, there are settings and options for the test desired to conduct. The settings that can be done in this part are PID setting of the position controller, test mode selection, and the emergency stop conditions in the test. In Figure C. 2, the screenshots of these tabs are illustrated.

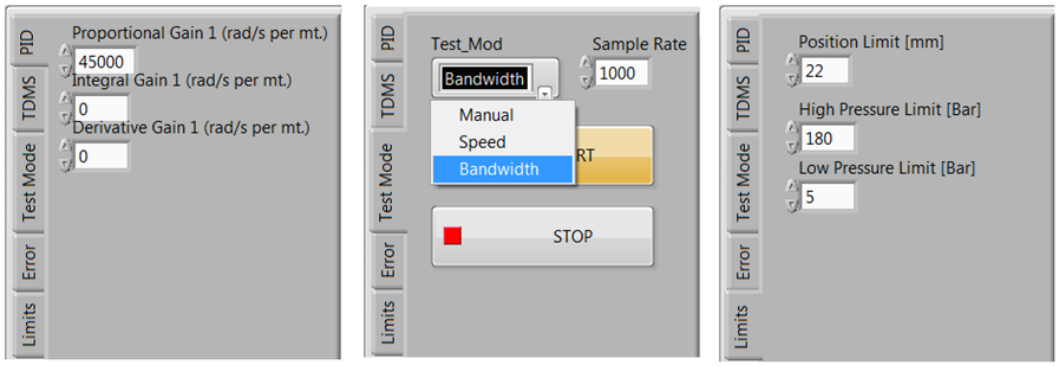

Figure C. 2: Tabs of Test Setup Settings

There is a block diagram of the software to execute the interface created. In Figure C. 3, the block diagram demonstration of the software written is shown.

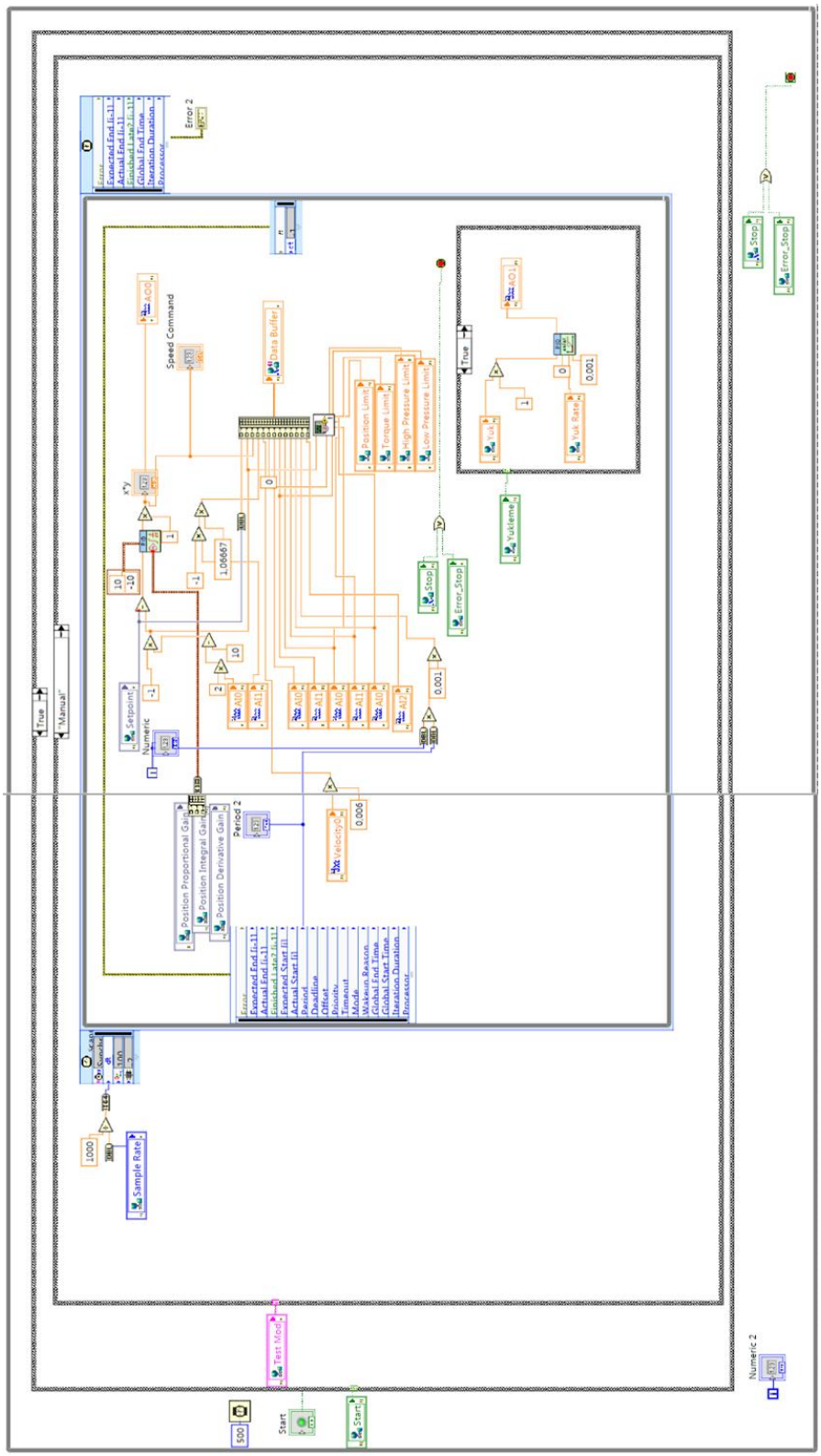

Figure C. 3: Block Diagram of the Test Software

APPENDIX D

EXTERNAL LOAD TEST

D.1 Test Setup

A test setup which is illustrated at Figure 89 is constructed to apply the necessary external load to the EHA prototype. A servomotor is used as a load generator and connected to a gear box to amplify the generated torque by the load motor to the EHA prototype. Moreover, between the transmission mechanism and the gearbox, the inertia is attached. The load motor is used in torque mode and desired torque value is applied to the EHA prototype.

As a load motor, Kollmorgen AKM 73Q is utilized as a DC motor with servo drive AKD-X02407. Their specifications are given in Appendix B.

Since the torque generated by the load motor is not sufficient to desired loading conditions, a gearbox from MS-Graessner GmbH, with the product name P210 is employed. Its gear ratio is 5:1 and it is demonstrated in Figure D. 1.

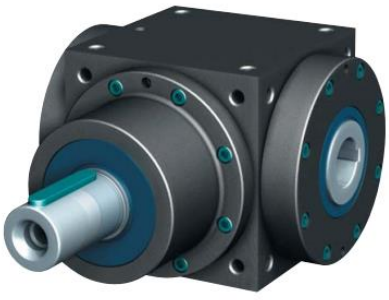

Figure D. 1: The Gear Box

D.2 Additional Results of The External Load Test

The external loading test is performed again with 90 Nm and the step response of 20 mm position command is demonstrated in Figure D. 2.

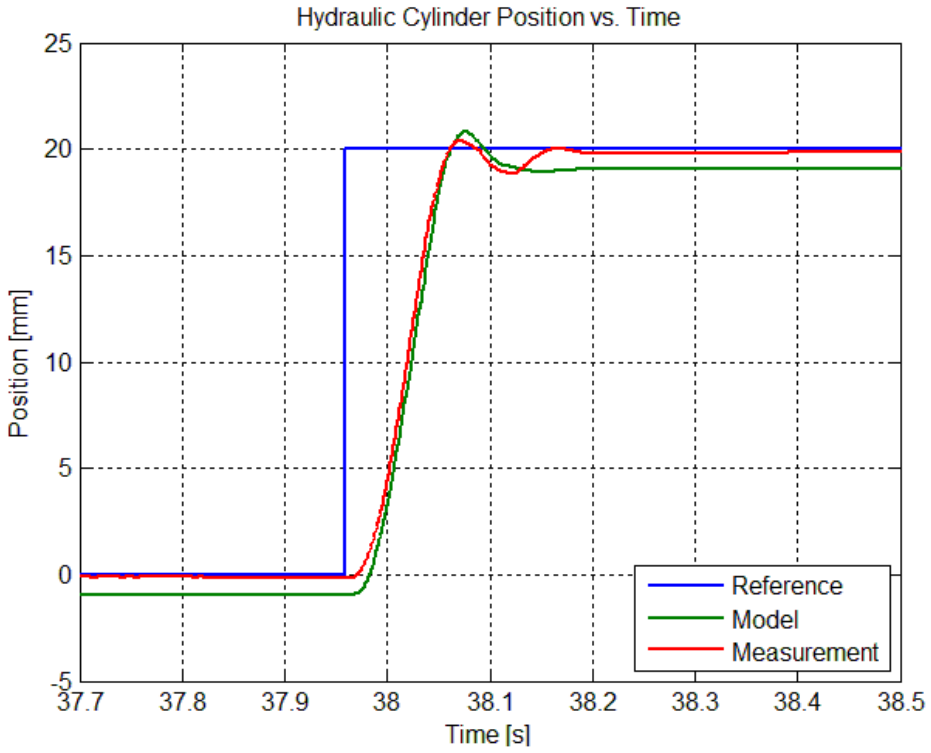

Figure D. 2: Step Response of the EHA Prototype under Inertial and 90 Nm External Load with K_p=45000 rad/s/m

The changes in the servomotor speed and the load pressure is shown in Figure D. 3 and Figure D. 4

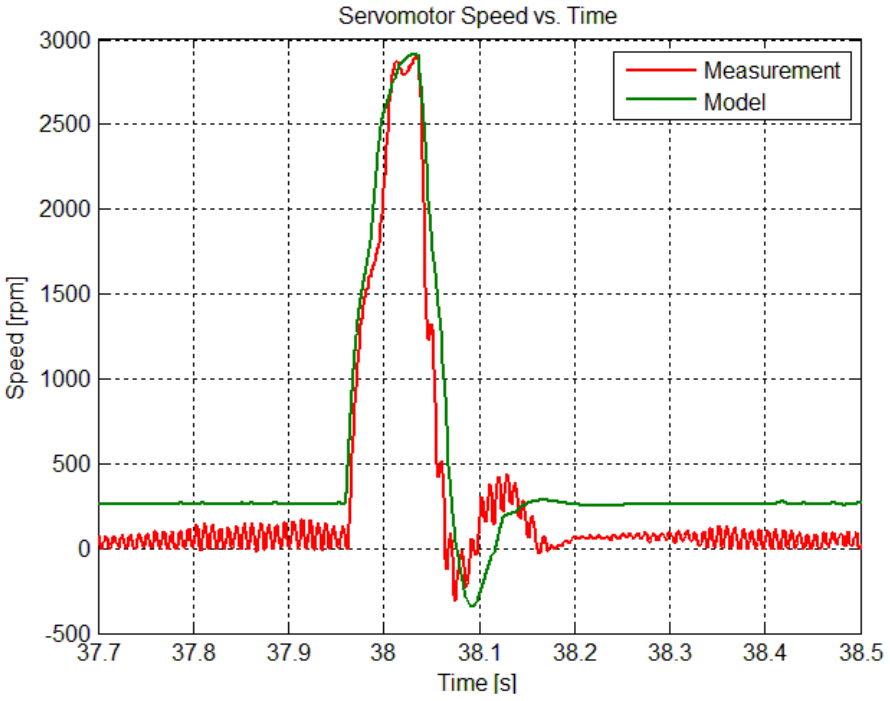

Figure D. 3: The Servomotor Speed at External Load Test with K_p=45000 rad/s/m

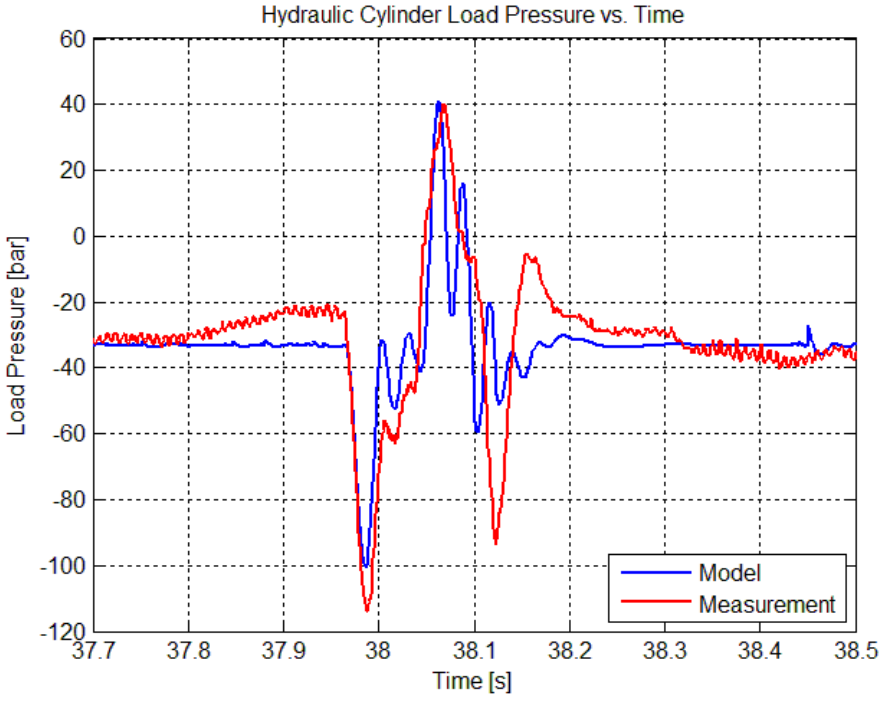

Figure D. 4: Load Pressure vs. Time for 90 Nm External Load Test